

DISSERTATION

Identifizierung von Substratproteinen von Mitogen-aktivierten Proteinkinasen durch Massenspektrometrie

angestrebter akademischer Grad

Doktor der Naturwissenschaften (Dr. rer.nat.)

Verfasser:	Alessandro Carreri
Matrikel-Nummer:	0648439
Dissertationsgebiet (lt. Studienblatt):	Moleculare-Biologie
Betreuer:	Univ.-Prof. Dr. Heribert Hirt
Wien, am 20. Jänner 2009	

DISSERTATION

Mass spectrometry-based screening for mitogen-activated protein kinase substrates

The work presented in this thesis was undertaken in the laboratory of Prof. Dr. Heribert Hirt from May 2005 until February 2009 at the Max F. Perutz laboratories Vienna Biocenter, Dr. Bohrgasse 9/4, 1030 Vienna, Austria.

Author:	Alessandro Carreri
Student number:	0648439
Department:	Plant molecular biology
Supervisor:	Univ.-Prof. Dr. Heribert Hirt
Wien, am 20. Jänner 2009	

TABLE OF CONTENTS

TABLE OF CONTENTS	3
1a. Zusammenfassung.....	5
1b. Abstract	7
II. INTRODUCTION	8
2.1. AIMS OF THE PROJECT	9
2.2. MAPK CASCADES ARE EVOLUTIONARILY CONSERVED MODULES IN ALL EUKARYOTES.....	10
2.3. RECOGNITION PATTERNS IN PLANT PATHOGEN RESISTANCE	13
2.4. MAPK CASCADES AND THEIR ROLE IN INNATE IMMUNE RESPONSES	15
2.4.1 A plant pathogen studied case: <i>Salmonella typhimurium</i> and its interaction with <i>A. thaliana</i>	17
2.5. NEW ADVENTURES IN PHOSPHOPROTEOMICS	18
2.5.1 Phosphopeptide enrichment strategies	20
2.5.2 Quantitative phosphoproteomics approaches	22
2.5.3 Phosphopeptide analysis by mass spectrometry	24
III. REFERENCES	26
IV. MANUSCRIPT	31
Mass spectrometry-based screening for mitogen-activated protein kinase substrates	32
4.1 Abstract.....	33
4.2 Introduction.....	35
4.3 Materials and Methods.....	37
4.4 Results.....	39
4.5 Discussion	45
4.6 Figure legends.....	51
4.7 Tables.....	54
4.8 Figures.....	55
4.9 Supplemental Data	64
4.10 References.....	75

V. Previous projects.....	78
VI. Curriculum Vitae.....	101
VII. Acknowledgments	102

1a. Zusammenfassung

Mitogen-aktivierte Proteinkinasen (MAPKs) sind in eukaryotischen Organismen vorkommende Proteine, die der Weiterleitung exogener Signale an entsprechende Effektoren dienen. Die von pflanzlichen Genomen kodierten MAPK-Familien sind besonders umfangreich; in *Arabidopsis thaliana*, beispielsweise, existieren 20 MAPK-Gene. Bis auf wenige Ausnahmen sind die von pflanzlichen MAPKs regulierten Zielproteine unbekannt. In der vorliegenden Arbeit wurden potentielle MAPK-Substratproteine analysiert. Diese waren in einer vorangegangenen Studie anhand des Auftretens von Phosphopeptiden, deren Sequenz dem von MAPKs erkannten Konsensusmotif entspricht, ausgewählt worden. Für acht potentielle Substratproteine wurden rekombinante Proteine aufgereinigt und auf Phosphorylierbarkeit durch die MAPKs MPK3, MPK4 und MPK6 in *in vitro*-Kinase-Experimenten getestet. Dabei zeigten die drei MAPKs deutliche Unterschiede hinsichtlich ihrer Spezifität für diese acht Substrate. Bei fünf der Kandidaten konnten die phosphorylierten Gruppen durch Flüssigchromatographie-Tandem-Massenspektrometrie (LC-MS/MS/MS) den entsprechenden Aminosäureresten zugeordnet werden. Dies sind die Proteine: Phosphoglucose-Isomerase 1 (PGI1), das putative Golgi SNARE protein GOS12, der mechanosensitive Ionenkanal MSL9, eine Histon-Deacetylase (HDT2/HD2b) sowie Phosphatidylinositol-4-phosphat-Kinase 4β1 (PI-4Kβ1). Die LC-MS/MS/MS-Analyse zeigte außerdem, dass jedes der untersuchten MAPK-Substratproteine mehrere phosphorylierte Reste enthielt. In *in vitro* Kinase-Experimenten wurde für fast alle der *in vivo*-identifizierten Phosphopeptide eine Modifizierung durch MAPKs beobachtet. Dies deutet darauf hin, dass die untersuchten Proteine potentielle *in vivo*-Substrate für MAPKs darstellen. Mit Hilfe von fluoreszierenden Fusionsproteinen an HDT2 und seiner an der phosphorylierbaren Aminosäure mutierten Derivate konnte gezeigt werden, dass Verlust der Phosphorylierung zur partiellen Exclusion des Proteins vom Nukleolus führt. Weiters wurde für GOS12 eine phosphorylierungsabhängige Lokalisation im Golgi-Apparat beobachtet und eine potentielle Rolle von GOS12 im Erhalt der Golgi-Struktur abgeleitet. Die Behandlung von Protoplasten mit dem bakteriellen Elicitor flg22 führte zur Relokalisierung von GOS12 aus Nukleus und Cytoplasma zum Golgi-Apparat. Zusammengefasst, konnten durch die auf MS-Daten basierende Herangehensweise MAPK Substrate ihren spezifischen MAPKs zugeordnet werden.

Eine potentielle Rolle von MAPKs in der Regulation des Vesikeltransports und der Histon-Deacetylierung in Pflanzen wurde aufgedeckt

1b. Abstract

Mitogen-activated protein kinases (MAPKs) transmit numerous incoming signals to downstream targets in animals and yeasts. Plant genomes encode the largest families of MAPKs in all eukaryotes, with 20 members in *Arabidopsis thaliana*. With a few exceptions, however, downstream targets have remained undiscovered. Here, we present a systematic screen for Arabidopsis MAPK substrates. Potential MAPK targets were selected on the basis of previously identified *in vivo* phosphorylation sites that match a MAPK motif. Eight candidates were purified and tested in *in vitro* kinase assays for phosphorylation by MPK3, -4, -6. These MAPKs clearly differed in their specificity towards these substrates. Phosphorylation sites were mapped by liquid chromatography-tandem mass spectrometry (LC-MS/MS/MS) in phosphoglucose isomerase 1 (PGI1), the putative Golgi SNARE protein GOS12, the mechanosensitive ion channel MSL9, the histone deacetylase HDT2/HD2B and phosphatidylinositol 4-phosphate kinase 4β1 (PI-4Kβ1). This analysis showed that MAPKs phosphorylate multiple residues in each substrate. Moreover, nearly all *in vivo* sites were phosphorylated *in vitro* by MAPKs, suggesting that these candidates could be *in vivo* targets. The phosphosite mapping and subsequent mutagenesis showed that several candidates were phosphorylated on multiple residues. The use of a fluorescent protein reporter showed that a phosphorylation site mutant of HDT2 excludes a subpool of the protein from the nucleolus. Moreover, the use of phosphosite mutants of GOS12 showed that phosphorylation of GOS12 likely mediates Golgi localization and that GOS12 is involved in maintaining Golgi morphology. Treatment of protoplasts with flg22 caused relocalization of GOS12 from the nucleus and cytosol to the Golgi, similar to the phosphomimicking mutant. This selective MS-based approach to connect MAPK isoforms with these MAPK substrates revealed a potential MAPK network regulating vesicular trafficking and histone deacetylation in plants.

II. INTRODUCTION

2.1. AIMS OF THE PROJECT

The main aim of the project was to screen for *Arabidopsis thaliana* mitogen activated protein kinase (MAPK) targets in order to define where these putative substrates are phosphorylated and to understand the effect of this post-translational modification on their biological function.

To achieve the aims described above, the following studies were performed:

- Mass-spectrometry analysis of *A. thaliana* cell suspension culture
- *In vitro* kinase assays for the validation of the putative MAPK targets
- *In vivo* transient expression of the MAPK targets in plant protoplasts
- Production and analysis of partial phosphomimicking and phosphoinactive version of some of the MAPK substrates

Among all the post-translational modifications, phosphorylation is one the most common ways to control the function of proteins. Animal and yeast research have shown that different kinases can selectively phosphorylate multiple sites in their substrates (Ubersax et al, 2007; Lindling et al, 2007) and thereby fine-tune the activity of a particular protein (Deshaies et al, 2001).

This project shows that MAPKs can discriminate and specifically phosphorylate different kinds of proteins and this can help to understand how the phosphorylation affects some characteristics in the behavior of previously unknown substrates.

2.2. MAPK CASCADES ARE EVOLUTIONARILY CONSERVED MODULES IN ALL EUKARYOTES

Plants undergo continuous exposure to various abiotic (such as cold, drought, heat, salinity, osmotic shock, ozone exposure, UV irradiation) and biotic (herbivores, pathogens) stresses in their natural environment. Plants differs from animals by their inability to escape the surrounding environment and, because of that, they developed numerous physical and biochemical strategies to cope with adverse conditions.

Much progress has been made in the identification and characterization of the mechanisms to perceive external signals and to manifest adaptive responses with proper physical changes. In the recent past many studies clarified how signal transduction pathways play a central role in different aspects of plants life enhancing phosphorylation/dephosphorylation of intracellular molecules, which enable rapid, reversible and precise cell responses.

The MAPK cascades are evolutionarily conserved signaling modules with essential regulatory functions in all eukaryotic organisms. The entire MAPK family, including yeast, plant and animal sequences has three major groups: ERK (extracellular signal-regulated protein kinase), p38/HOG1 and c-Jun NH₂-terminal kinase (JNK)/stress-activated protein kinase (SAPK) (*Takekawa et al., 1997*). The name of the family of MAP kinases reflects their identification as mitogen-activated protein kinases.

The basic assembly of a mitogen activated protein kinase (MAPK) cascades consists of three kinases grouped in this kind of module: MAPK Kinase Kinase (MAPKKK)-MAPK Kinase (MAPKK)-MAPK (**Figure 1**).

These three-level cascades are triggered by receptor-mediated activation of a MAPKKK that occur through physical interaction and/or phosphorylation by either the receptor itself, intermediate bridging factors or interlinking MAPKKKKs (*Nakagami et al, 2006*). MAPKKKs are serine/threonine kinases that activates MAPKKs through phosphorylation of two aminoacids in the (S/T)X₃₋₅(S/T) of the activation loop. In contrast, MAPKKs are dual-specificity kinases that activate a MAPK through dual phosphorylation of the TXY motif in the activation loop.

The last step leads finally to phosphorylation of the MAPK targets that triggers changes in cell phenotypes varying from growth to differentiation depending on cell type, to phosphorylation of signaling components enzymes or of cytoskeleton-

associated proteins that may directly influence the cell structure (Widmann *et al.*, 1999).

This three-level cascade prototype is common to all eukaryotes and is utilized for the majority of signal transduction pathways that originate from the cell surface.

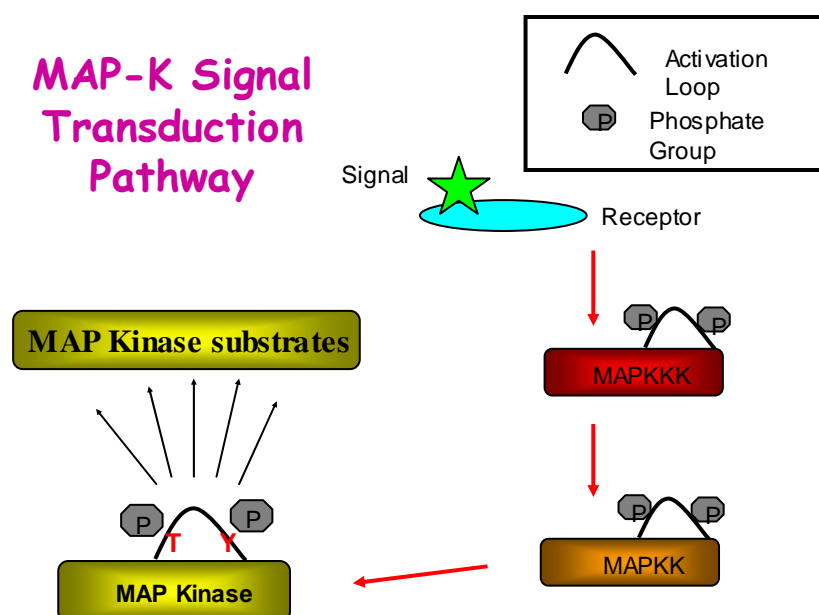


Figure 1: Three-kinase module of the MAPK pathways.

The environmental signal is transmitted from the receptor to the first member in the cascade, the MAPK kinase kinase that activates MAPKK by phosphorylation on serine and/or threonine residues. The second member in the cascade, MAPKK activates the MAPK by phosphorylation on tyrosine and threonine residues and consequently, the MAP kinase catalyses phosphorylation of its downstream targets.

Numerous signals can trigger these cascades and have different end effects in each eukaryotic organism, but many of the intermediate components are playing analogous roles (**Figure 2**). A similar scheme to the stress signaling MAPK cascade in *A. thaliana* (Asai *et al.*, 2002; Ichimura *et al.*, 2000; Kovtun *et al.*, 2000; Matsuoka *et al.*, 2002; Nakagami *et al.*, 2005) was found in various other eukaryotic organisms: in the pathway involved in eye development in the fly *Drosophila melanogaster* (Rawlings *et al.*, 2003), in the mating process in the yeast *Saccharomyces cerevisiae* (Hohmann, 2002), in the vulva developmental pathway in the worm *Caenorhabditis elegans* (Beitel *et al.*, 1995; Wu & Han, 1994), and in the response signal cascade for growth of mammalian cultured cells (Sorrentino *et al.*, 2001).

Conservation of innate immunity signaling pathways

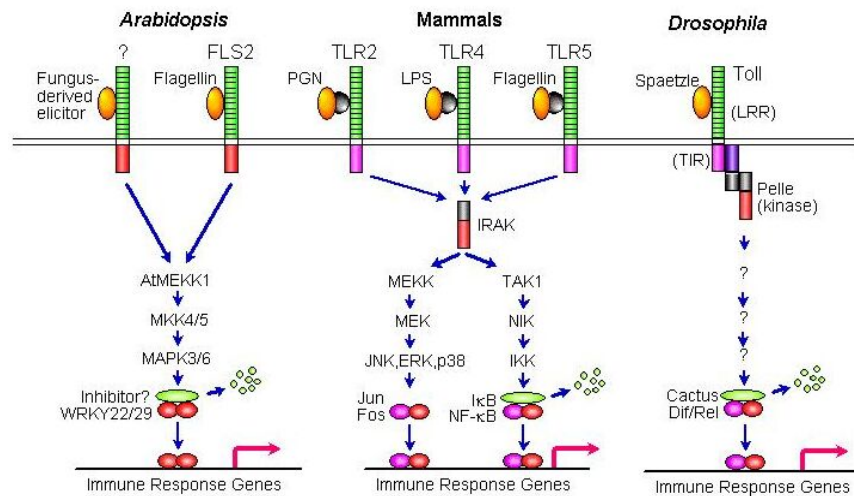


Figure 2: The MAPK signaling pathways are conserved through eukaryotic world (this picture is taken from Asai et al., 2002).

The components of a three-kinase module are termed differently, are activated by various stimuli and have different downstream targets, but still show strong sequence and structural conservation between all eukaryotic organisms. This figure shows a pattern of innate immunity mitogen-activated protein kinase signaling pathway in *Arabidopsis*, mammals and *Drosophila* as an example.

In *Arabidopsis* both bacterial and fungal pathogens activate the MAPK cascade (MEKK1-MKK4/MKK5-MPK3/MPK6) and WRKY22/WRKY29 transcription factors that switch on the transcription of the plant immune response genes (Asai et al., 2002).

In mammalian cells, the cascade is initiated as well by an activation of the receptor by a ligand. The signal is transferred via IRAK kinase to the MEKK, which activates the kinase MEK. MEK in turn activates the MAPKs. Finally, activated MAPKs phosphorylate transcription factors that turn on the transcription of the immune response genes (Crews & Erikson, 1993).

In *Drosophila* is the extracellular protein Spätzle required for activation of the Toll signaling pathway in the embryonic development and innate immune defense. Weber et al. (2003) showed that the mature form of Spätzle specifically binds to *Drosophila* cells and to Cos-7 cells expressing Toll receptor and triggers a Toll-dependent immune response after injection into the hemolymph of flies.

Signals are perceived by proteins located in the plasma membrane that can bind extracellular ligands and, through this interaction, become activated. The activation can lead to dimerization of two receptor subunits and the intracellular *trans*-autophosphorylation of other cytosolic proteins involved downstream in the specific signaling pathway.

The components of a three-kinase module are termed differently through all the model organisms and they can react to different stimuli, have different upstream activators and downstream targets, but they still show high sequence and structural conservation between all eukaryotic organisms: from yeast as the simplest to human as the most complex eukaryotic organism.

2.3. RECOGNITION PATTERNS IN PLANT PATHOGEN RESISTANCE

To prevent the constant attack by microorganisms and pathogens, plants are equipped with various defense structures like a wax cuticle. They also express different preformed antimicrobial compounds and use a variety of mechanisms that rely on the perception of pathogens and the subsequent induction of defense responses (Mészáros *et al*, 2006). These defense mechanisms of higher plants are referred as “innate immune system” which enables the plant to detect and rapidly respond to different pathogen aggressions.

The first line in this active plant defense relies on the recognition of pathogen-associated (or microbe-associated) molecular patterns (PAMPs) that are small molecules usually derived from abundant pathogen-derived structure such as structural proteins or cell-wall components that are shared by a large number of pathogen varieties (Colcombet *et al*, 2008).

The proteins involved in perception and recognition of PAMPs are the PRR-NBS-LRRs which trigger immune responses in within a few minutes after sensing the pathogen molecules leading to the so-called PAMP-triggered immunity (PTI). Immune responses include changes in gene transcription, rapid ion fluxes across the plasma membrane, MAP kinase activation and production of anti-microbial reagents like phytoalexins and active oxygen species (AOS).

On the other hand, successful pathogens have evolved mechanisms to infect host plants either by evading recognition or by suppressing the subsequent signaling steps (Zipfel, 2008).

To overcome their detection by plants, pathogens can inject effectors into the plant cells that are able to interfere with the PTI signaling cascades and thereby abolish basal defense responses. In some cases pathogen effectors can be recognized by plant resistance proteins (R proteins), inducing the so-called effector trigger immunity (ETI), a mechanism that activates a hypersensitive response (HR) causing local cell death and limiting the pathogen infection area (**Figure 3**).

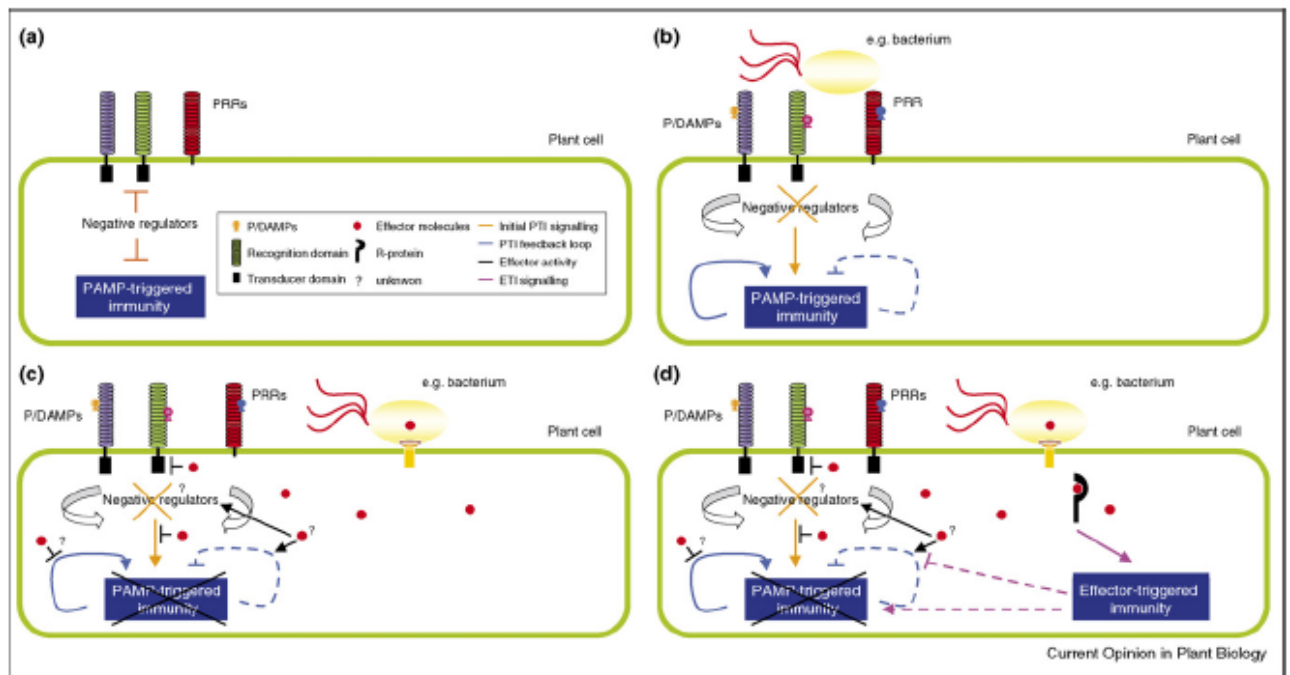


Figure 3: Mechanisms of plant innate immunity. (Picture taken from Schwessinger *et al*, 2008)

(A) Hypothetical constitutive negative regulation of PTI. Plants tightly regulate their defense responses in the absence of microbes by constitutive negative regulators. (B) PTI is activated by recognition of infectious-self and non-self. Plants recognize invading microbes (e.g. bacteria) by sensing PAMPs/MAMPs or DAMPs via PRRs. This triggers diminution of the negative regulation and consequently activation of downstream signaling cascades leading to PTI. This activation is in turn dampened and/or enhanced by negative and/or positive feedback loops, respectively. (C) Suppression of PTI by pathogen effectors. Pathogens can suppress PTI via effector molecules. This includes binding to and modification of PRRs and signaling components. Additionally, effectors could mimic or stabilise negative regulators. (D) Activation of ETI by recognition of pathogen effectors. Some plants recognize individual effector molecules leading to ETI. This leads to the activation of the HR responses that cause localized cell death preventing the spreading of the pathogen infection.

The HR response is a specific defense mechanism towards plant pathogens and involves the plant hormone salicylic acid (SA) but, among other factors, it is the regulation and the balance of all plant hormones that is necessary for a correct and effective long-term plant response to pathogens. The three hormones SA, ethylene (ET) and jasmonic acid (JA) are mainly involved in regulating distinct gene expression patterns.

Another level of defense that results in resistance, throughout the plant, to a broad spectrum of pathogens is called systemic acquired resistance (SAR). SAR is defined as a long-range process and involves priming against pathogen resistance in unaffected tissues (Colcombet *et al*, 2008).

2.4. MAPK CASCADES AND THEIR ROLE IN INNATE IMMUNE RESPONSES

Flg22 is a 22-amino-acid-long peptide derived from flagellin, the main structural protein of the eubacterium flagellum. The perception of this peptide by *A. thaliana* became one of the main models to study early signaling events upon pathogen recognition because it is acting as a PAMP inducing a wide range of defense-related responses.

The pattern-recognition receptor (PRR) responsible for triggering the flagellin cascade in *A. thaliana* is the leucine-rich repeat receptor-like kinase (LRR-RLK) FLAGELLIN-SENSING 2 (FLS2) (Chinchilla *et al*, 2006) together with BRI1-ASSOCIATED KINASE 1 (BAK1). The exact binding site for flg22 is still unknown but FLS2 shows direct interaction with this particular peptide. Functional orthologues of FLS2 have been recently identified in *Nicotiana benthamiana* and tomato, demonstrating the conservation and the importance of flagellin perception on plant-bacteria interactions.

Protoplasts, plant cells that without cell walls, played a major role in uncovering the signal transduction pathways downstream of the interaction between FLS2-BAK1 receptor complex and flagellin (**Figure 4**).

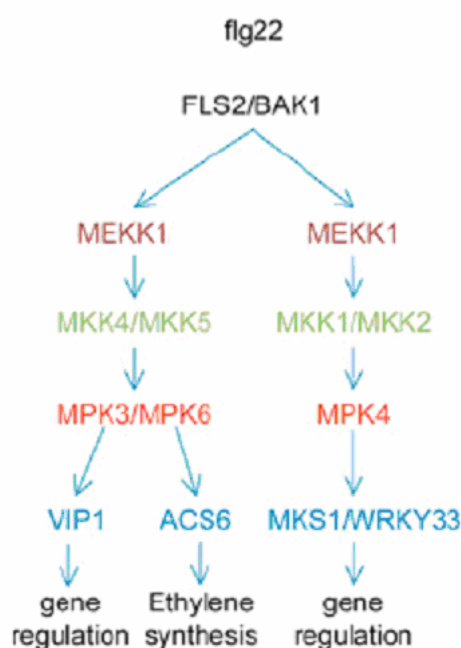


Figure 4: Model of flg22-induced MAPK signaling. (Picture taken from Colcombet *et al*, 2008) The perception from the FLS2 receptor or the presence of flg22 triggers the MEKK1-MKK1/2-MPK4 and the MEKK1-MKK4/5-MPK3/6 modules with the subsequent phosphorylation of the MAPK substrates.

The flagellin-activated cascade is a typical three-step kinase module that consists of the MAPKKK MEKK1, two MAPKKs MKK4/5 and two MAPKs MPK3/6. Once being activated, MPK3/6 induce the expression of the flg22 early responsive genes including WRKY DNA-BINDING PROTEIN (WRKY29), FLG22-INDUCED RECEPTOR KINASE 1 (FRK1), ACS6, a gene involved in ET production and VIP1, a bZIP transcription factor recently shown to re-localize from the cytoplasm to the nucleus after MPK3-mediated phosphorylation (*Djamei et al*, 2007).

The MEKK1-MKK4/5-MPK3/6 kinase cascade is not the only that is activated by flagellin. Infact a second cascade that increases the activity of the negative defense regulator MPK4 was uncovered. (Figure 4)

The activation of MPK4 is MEKK1-dependent and could be achieved in two different ways: either by MEKK1 phosphorylating MKK1/MKK2 which in turn will activate MPK4 or either by a direct physical interaction between MEKK1 and MPK4.

Extensive genetic and biochemical studies showed how MEKK1 and MPK4 are important elements of an flg22-induced signaling cascade involved in negative regulation of pathogen- or PAMP-induced cell death. The currently known targets of MPK4 are MPK4 substrate 1 (MKS1) and the two transcription factors, WRKY25 and WRKY33. Nevertheless, it was never demonstrated that these proteins are targets of MPK4 after its induction through the flg22-induced signaling pathway (*Colcombet et al*, 2008).

The common characteristic of the MAPK cascades described above is that both are triggered by the so far best studied PAMP: flg22. Although it is clear that the flg22 system has helped extensively to map these MAPK signaling pathways, this specific PAMP is not the only known one.

Recently elongation factor thermo-unstable (EF-Tu) was identified, a peptide from *Escherichia coli* that is sensed by a EF-Tu RECEPTOR (EFR), a RECEPTOR-LIKE KINASES (RLK) that belongs to the same family as FLS2 (*Kunze et al*, 2004). Notably, despite being sensed by independent receptors, flg22 and EF-Tu regulate a very similar set of genes, indicating that they use the same signaling pathways (*Zipfel et al*, 2006).

Very recently, it was also shown that chitin can be perceived by *Arabidopsis*, through the CHITIN ELICITOR RECEPTOR KINASE 1 (CERK1), and this PAMP activates MPK3/6 and a set of genes that overlap with those regulated by flg22 and EF-Tu (*Miya et al*, 2007).

These studies show how the perception of PAMPs organisms leads to the activation of similar signal transduction cascades that can regulate a common set of genes, indicating that already a single PAMP can saturate the pathways in order to prevent additive effects derived from the presence of more than one PAMP.

2.4.1 A plant pathogen studied case: *Salmonella typhimurium* and its interaction with *A. thaliana*

Salmonella enterica serovar *typhimurium* (*S. typhimurium*) is a facultative endopathogen that causes salmonellosis, which is the most frequent food-borne disease with around 1.5 billion yearly infections world wide.

Salmonella-contaminated vegetables and fruits were recently identified as a widespread source of human infection (Brandl, 2006). Although diverse plant species support growth of *Salmonella* (Jablasone et al, 2005), the underlying mechanism of the *Salmonella*-plant interaction is largely unknown.

In animal *Salmonella* can infect tissues after consumption of contaminated food or water. *Salmonella* infections mechanisms involve genes encoded by two pathogenicity island (SPI-1 and SPI2), DNA regions that carry genetic information for the assembly of the type III secretion system and effectors injected in the host cells, structure that are necessary for *Salmonella* proliferation within mammalian cells.

A recent publication has shown that *Salmonella typhimurium* can act as a common plant pathogen using *A. thaliana* as a plant organism.

It has been demonstrated that *Salmonella* can actively invade and proliferate in plant cells but lacks the ability to spread to non-exposed parts of the plant, suggesting that it cannot migrate via the xylem (root-to-shoot) nor via the phloem (leaf-to-leaf) system (Schikora et al, 2008).

To prove that *Salmonella* acts like a plant pathogen different experiments have been done in order to prove its interaction with the plant immune system.

It was shown that *Arabidopsis* can sense *Salmonella* flagellin (and others yet unknown PAMPs). After *Salmonella* recognition, MAPKs cascades are triggered in order to activate MPK3/6.

Extensive observations have been done to understand the role of phytohormones in the interaction process between *Arabidopsis* and *Salmonella*. The involvement of all the three principal phytohormones SA, JA and ET was demonstrated proving the transcriptional upregulation of some of defense marker genes like PDF1.2 (for JA and ET), PR2 and PR4 (for JA), PR1 (for SA) proving the activation of multiple defense pathways of the innate immune system (Schikora *et al*, 2008).

Analysis of *A. thaliana* mutants (*NahG*, *coi1-16*, *ein2-1*) blocked in their phytohormone signaling pathways demonstrated that the JA signaling is absolutely required to elicit activation of MPK6. Moreover *mkk3* mutant plants showed a total impairment of MPK6 activation after *Salmonella* infection, revealing a MKK3 and JA dependency for the activation of this MAPK pathway and the consequent induction of defense mechanisms against *Salmonella*.

2.5. NEW ADVENTURES IN PHOSPHOPROTEOMICS

The protein kinase family in plants counts more than 1000 members which is approximately twice the number found in mammals. Different studies suggest that at least 30% of all proteins are modified by phosphorylation (De la Fuente van Bentem *et al*, 2008). Despite the importance of this post-translational protein modification in regulating multiple processes like cell cycle, metabolism, differentiation or responses to stress and hormones the mapping of phosphorylated sites in proteins was, until very recently, difficult and tedious.

In order to bridge this gap of knowledge, new techniques have been developed and nowadays it is possible to perform excellent qualitative studies on phosphosites. More importantly, quantitative analysis of dynamic phosphorylation events that permit us to understand cell signaling pathways.

The core of these new techniques resides in the use of mass spectrometry (MS), a technology that can, in theory, identify each phosphopeptide and localize the exact position of the phosphate(s) group(s) in the peptide sequences.

The commonly used MS methods involve the enzymatic digestion of complex proteomes into peptide mixtures which are then separated by nanoscale liquid chromatography and analyzed by MS (**Figure 5**).

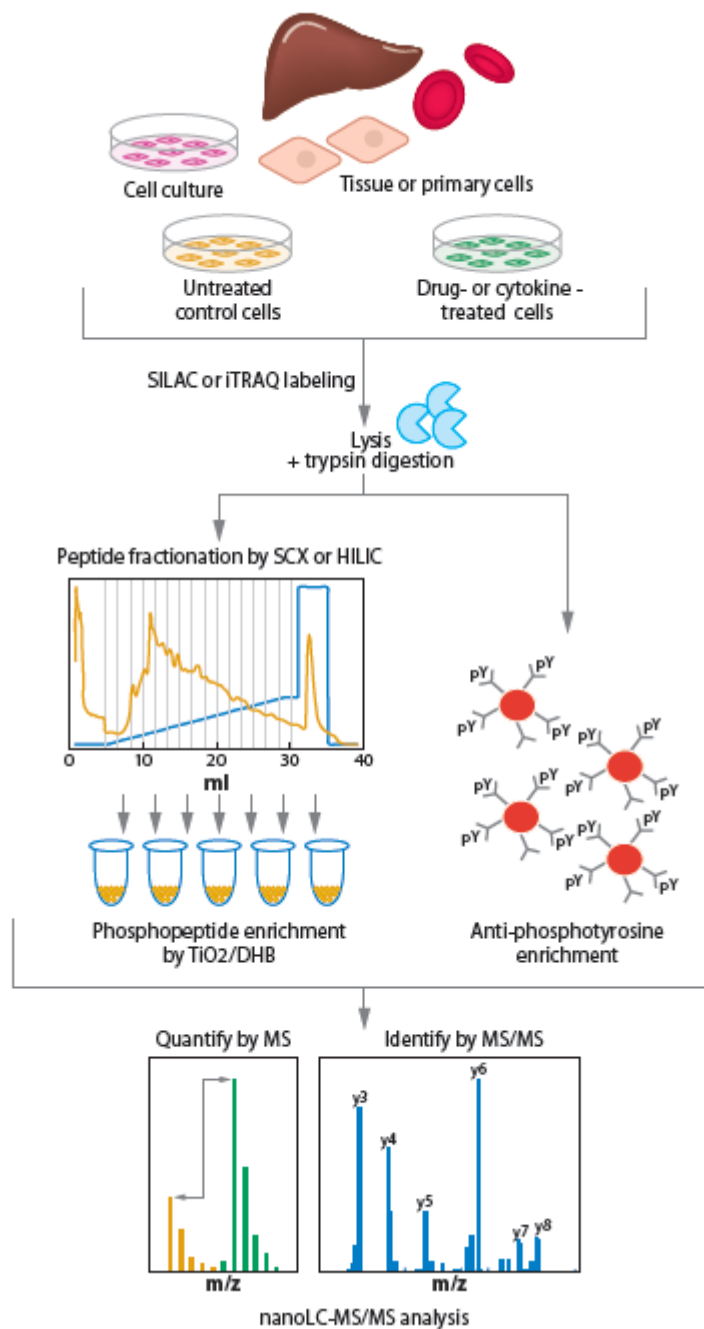


Figure 5: Typical quantitative phosphoproteomics workflow. (Picture taken from *Macek et al*, 2008)

Control and treated cells or tissues are differentially labeled by stable isotopes, lysed, and mixed together. Protein extracts are digested by trypsin, and phosphopeptides are enriched by a combination of strong cation exchange and TiO₂ chromatographies, or by immunoprecipitation with phospho-specific antibodies. Resulting enriched phosphopeptide mixtures are separated on nanoLC and directly measured in a mass spectrometer. Relative peptide quantitation is usually based on the first stage of mass spectrometry (MS), whereas peptide identification is achieved upon gas-phase fragmentation in the second stage of mass spectrometry (MS/MS).

After the enzymatic digestion step the analysis of the phosphosites has to counteract a problem due to the real low amount of the phosphopeptides present in the complete peptide mixtures in the cell lysate. To overcome these difficulties many different methods have been developed for the enrichment of phosphopeptides and phosphoproteins.

2.5.1 Phosphopeptide enrichment strategies

2.5.1.1 Immobilized Metal Affinity Chromatography (IMAC)

One of the most used enrichment phosphorylation technique is called “Immobilized Metal Affinity Chromatography” (IMAC), a strategy based on the high affinity of the phosphate groups for metal ions such as Fe^{3+} , Ga^{3+} , Al^{3+} and Zn^{2+} .

The concept of this method relies on the loading, and immobilization, of metal ions in a column packing material where phosphopeptides will be subsequently introduced permitting the formation of a complex. One of the main limitations of this strategy is the non-specific retention of non-phosphorylated peptides due either to the overloading of the column, or to the high coordination affinity for the ion metals of acidic peptides rich in glutamic and aspartic acid residues. However, elimination of non-specific binding is reached when samples are loaded with pH outside the 2.0-3.5 range or via additional chemistry steps like the conversion of carboxylate groups to esters.

2.5.1.2 Titanium Dioxide (TiO_2) Enrichment

Titanium dioxide (TiO_2) is a chemical showing high stability, rigidity and unique amphoteric ion-exchange properties (*Macek et al*, 2008). The first paper reported its usage in phosphopeptides separation is dated 1997 when *Ikeguchi et al* demonstrated the potentiality of this compound like a material permitting phosphopeptides enrichment.

Over the years the techniques based on TiO_2 have become more and more popular, compare to the IMAC ones, because of their shorter preparation time and increased affinity and selectivity.

Nevertheless, TiO₂ protocols suffer the same non-specific binding problems described above for the IMAC. To circumvent this difficulties samples are loaded in 2,5-dihydroxybenzoic acid (DHB), a compound that works as a competitive binder, permitting an improvement of phosphopeptides enrichment without chemical modification of the sample.

2.5.1.3 Strong Cation Exchange Chromatography (SCX)

Metal-ion based strategies are not the only enrichment methods that have been developed in the past few years. Alternatively to them it's possible to use an ion exchange chromatography strategy based on the difference in the solution charge states of phosphorylated and non-phosphorylated peptides.

In fact if sample loading is done at pH 2.7 a common tryptic peptide shows a net charge of +2; conversely if the same peptide would have been phosphorylate its net charge would diminish to +1, permitting an easy separation, using a linear salt gradient, by SCX chromatography due to its lower affinity with the SCX resin.

This protocol allows us a semi-selective enrichment of only singly-phosphorylate peptides 'cause peptides presenting double or multiple phosphorylation sites are not retained by the column, due to their net zero or negative charge.

For this reason, an because SCX technique needs a large amount of starting material, ion exchange chromatography methods are used as a first enrichment step usually followed by IMAC or TiO₂.

2.5.1.4 Antibody-Based Enrichment

The use of specific antibodies as enrichment strategies is well established since almost ten years (*De Corte et al*, 1999).

The immunoprecipitation (IP) of proteins and peptides phosphorylated on their tyrosine residues gives good yields and permits an easy and direct mapping of Tyr phosphosites.

Many commercial anti-phosphotyrosine antibodies are available and each one presents a certain preference towards phosphosites surrounded by determine

aminoacid sequences. Therefore performing the IP with multiple antibodies may increase coverage of the tyrosine phosphorylated proteome (*Nita-Lazar et al*, 2008). The improvements of the antibody-based enrichment method were demonstrated by two recent papers from *Rush et al* and *Rikova et al* where they map thousands of phosphosites in different cancer cell lines.

The enrichment strategies described above show diverse working logics and preferences towards specific groups of phosphopeptides. Therefore, the combination of two or more enrichment methods is to consider as the best option for reaching the widest level of phosphosites coverage when we deal with complex biological samples.

2.5.2 Quantitative phosphoproteomics approaches

Most of the techniques developed in the phosphoproteomics field focused on the creation of lists where the phosphopeptides and their phospho-residues were merely annotated. This huge amount of data can be possibly useful for people working on specific selected phosphorylated proteins, but is difficult to link to large-scale phosphorylation cascades that regulate different cell processes.

To understand the biological responses of a cell to specific signal(s) researchers moved their attention to different, more functional, approaches that will enable us to quantify changes in the phosphoproteome.

2.5.2.1 Stable Isotope Labeling by Amino acids in Cell culture (SILAC)

The stable isotope labeling by amino acids in cell culture (SILAC) is an *in vivo* labeling method in which cell cultures are growing in a medium where the natural form of some aminoacids is replaced with a stable isotope form like $^{13}\text{C}_6$ -Arg or -Lys. In this way cells grown in the medium containing the heavier form of the aminoacids are incorporating the stable isotope form altering, in this way, the molecular mass of their protein, permitting the detection of this modification by subsequent MS analysis.

This strategy, with the additional use of isotopes like $^{13}\text{C}_6$ - $^{15}\text{N}_4$ -Arg or -Lys, gives us the possibility to compare a maximum of three different samples in a single analysis. Moreover, although it was thought to be possibly used only for dividing cells, recently new methods have been established for the usage of SILAC for differentiated cells (Spellman *et al*, 2008) and for the analysis of *in vivo* metabolic labeling in whole organisms like *Drosophila* or *Arabidopsis* (Gruhler *et al*, 2005). Although SILAC methods have provided a very large amount of data in the past few years, these protocols are anyway presenting some disadvantages like the conversion of the arginine to proline, that requires a constant monitoring of the cell culture conditions, or it's demanding many MS analyses.

2.5.2.2 iTRAQTM Reagent

Like described above SILAC methods label proteins *in vivo* during cell growth, nevertheless there are *in vitro* techniques for the protein labeling at the final stage before mass spectrometry analysis for instance iTRAQ (Figure 6).

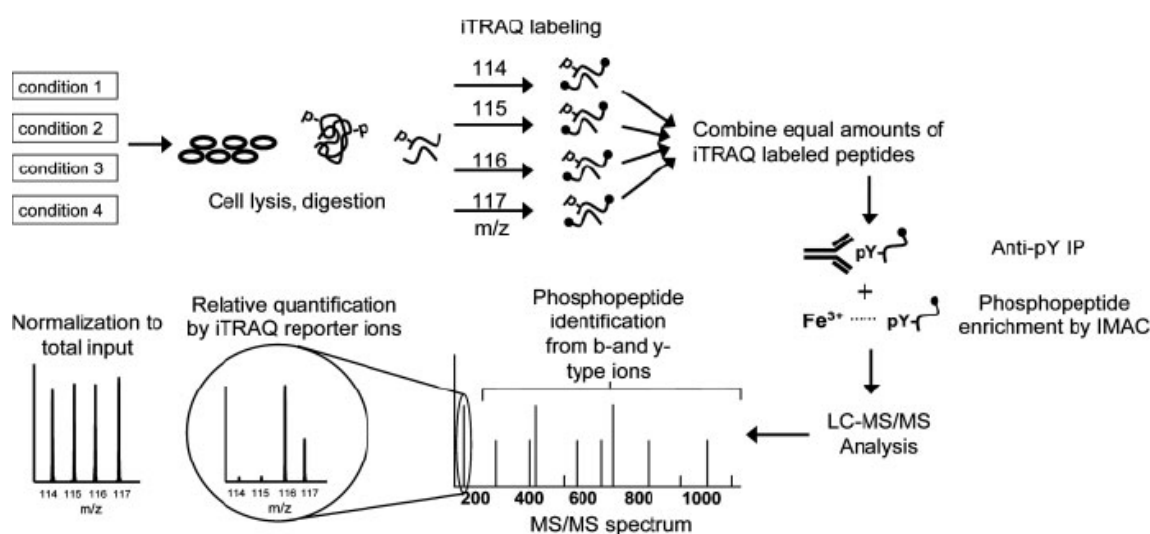


Figure 6. Example workflow of the quantitative phosphotyrosine analysis experiment using iTRAQ labeling.

Proteins are extracted from four biological samples (cell lines, stimulation time points, tissue samples), modified and digested. For quantification, the resulting peptides are labeled with iTRAQ reagent and combined. The mixture is then subjected to two steps of enrichment for tyrosine phosphorylated peptides: IP with antiphosphotyrosine antibodies and IMAC. Phosphorylated peptides eluted from the IMAC column are analyzed by LCMS/ MS, typically on a quadrupole TOF mass spectrometer. Each MS/MS spectrum contains both sequence-specific fragmentation events for identification of the peptide and phosphorylation site as well as the low-mass iTRAQ marker ions to quantify phosphorylation across the four samples. iTRAQ quantification is normalized to the supernatant to eliminate variation resulting from the preparation process.

This method is based on isobaric tags which react with primary amines permitting the quantitative and parallel comparison of four different protein samples. The isobaric tags, in the iTRAQ method, react with primary amines of intact proteins and of peptides resulting from proteolytic digestion allowing the quantification, in the MS/MS, of a certain determined peptide. Since each tag is isobaric, the quantification is performed by comparing the peak areas of the marker ions resulting from the fragmentation of the iTRAQ tags.

Recently an upgrade of the iTRAQ reagent has been introduced enabling the simultaneous proteome analysis of eight cell culture conditions but this new method it has not been tested yet for the quantification of protein phosphorylation (*Choe et al*, 2007).

2.5.3 Phosphopeptide analysis by mass spectrometry

The final aim of the complete set of methods described above is to sequence the entire protein extracts of a biological sample in order to localize on which residues of which peptides the phosphate groups are located.

The phosphopeptides are usually first separated on nanoLC column and then electrosprayed for the analysis in high-resolution mass spectrometry, providing us information about the mass-to-charge (m/z) ratio and the intensity of each detected phosphopeptide present in the protein extract. At the same time the phosphopeptides undergo a dissociation treatment by the mass spectrometer that simultaneously detects the resulting fragment ions in a so-called tandem mass spectrum (MS^2 spectrum) (*Aebersold et al*, 2003). The most common dissociation treatment increases the internal energy of ions to induce their fragmentation. This mechanism leads to the loss of phosphoric acid from the precursor (phosphopeptide) ion providing MS^2 spectra that, usually, do not contain the entire set of information that is needed to complete the peptide sequence or to map the exact position of the phosphate group. These problems have been solved with the introduction of the MS/MS/MS (MS^3) process, a method where the neutral loss precursor is further isolated, fragmented and the extrapolated data from this set of experiments analyzed again.

In the past few years new techniques have been developed allowing high throughput identification of potential phosphorylation substrates using quantitative phosphoproteomics and peptide or protein microarrays (*Benschop et al*, 2007; *Nühse et al*, 2007; *Feilner et al*, 2005).

Using different phosphoproteomic approaches two distinct groups showed the possibilities to understand the dynamics of the phosphorylation events after the perception by the plants of flg22 and, despite the differences in experimental setup and analysis, the published data were mostly overlapping.

Once it is known that a protein is phosphorylated, it is necessary to find out which kinases are involved in the phosphorylation step. *Feilner et al* (2005) developed a method that combines the use of peptide and protein microarrays. With this approach they were able to compare the substrate specificity of the closely related AtMPK3 and AtMPK6 showing a large overlap but also distinct sets of substrates.

The development of the MS³ and the new method of analysis described above have increased the chance to determine, with almost 100% confidence, the position of a phosphate group(s) on a protein revealing a very large group of putative kinases substrates. Nevertheless, this kind of knowledge will remain sterile until the function of the phosphorylation, and then the biological function of a kinase substrate, will be determined.

In this thesis I describe an approach for the discovery and validation of new potential MAPKs substrates in Arabidopsis that utilizes data collected with mass-spectrometry and molecular biology experiments, with the aim of unraveling previously unidentified phosphosites and the functional analysis of some of the observed phosphorylation events.

III. REFERENCES

1. Aebersold R, Mann M: **Mass spectrometry-based proteomics**. *Nature* 2003, **422**:198–207.
2. Asai T, Tena G, Plotnikova J, Willmann M, Chiu WL, Gomez-Gomez L, Boller T, Ausubel FM, Sheen J: **MAP kinase signaling cascade in Arabidopsis innate immunity**. *Nature* 2002, **415**: 977-983.
3. Beitel GJ, Tuck S, Greenwald I, Horvitz HR: **The Caenorhabditis elegans gene lin-1 encodes an ETS-domain protein and defines a branch of the vulval induction pathway**. *Genes & Development* 1995, **9**: 3149-3162.
4. Benschop JJ, Mohammed S, O'Flaherty M, Heck AJ: **Quantitative phosphoproteomics of early elicitor signaling in Arabidopsis**. *Mol. Cell. Proteomics* 2007, **6**: 1198–1214.
5. Brandl MT: **Fitness of Human Enteric Pathogens on Plants and Implications for Food Safety** doi:10.1146/annurev.phyto.44.070505.143359. *Annual Review of Phytopathology* 2006, **44**: 367–392.
6. Colcombet J, Hirt H: **Arabidopsis MAPKs: a complex signaling network involved in multiple biological processes**. *Biochem. J.* 2008, **413**: 217-226.
7. Chinchilla D, Bauer Z, Regenass M, Boller T, Felix G: **The Arabidopsis receptor kinase FLS2 binds flg22 and determines the specificity of flagellin perception**. *Plant Cell* 2006, **18**: 465-476.
8. Choe L, D'Ascenzo M, Relkin NR, Pappin D: **8-plex quantitation of changes in cerebrospinal fluid protein expression in subjects undergoing intravenous immunoglobulin treatment for Alzheimer's disease**. *Proteomics* 2007, **7**, 3651–3660.
9. De Corte V, Demol H, Goethals M, Van Damme J, Gettemans J, Vandekerckhove J: **Identification of Tyr438 as the major in vitro c-Src phosphorylation site in human gelsolin: a mass spectrometric approach**. *Protein Sci.* 1999, **8**: 234–41.
10. De la Fuente van Bentem S, Hirt H: **Using phosphoproteomics to reveal signalling dynamics in plants**. *Trends Plant Sci.* 2007, **9**: 404-411.
11. Deshaies RJ, Ferrel JE Jr: **Multisite Phosphorylation Minireview and the Countdown to S Phase**. *Cell* 2001, **107**: 819–822.
12. Djamei A, Pitzschke A, Nakagami H, Rajh I, Hirt H: **Trojan horse strategy in Agrobacterium transformation: abusing MAPK defense signaling**. *Science* 2007, **318**: 453–456.

13. Feilner T, Hultschig C, Lee J, Meyer S, Immink RGH, Koenig A, Possling A, Seitz H, Beveridge A, Scheel D, Cahill DJ, Lehrach H, Kreutzberger J, Kersten B: **High Throughput Identification of Potential Arabidopsis Mitogen-activated Protein Kinases Substrates.** *Mol. Cell. Proteomics* 2005, **4**: 1558-1568.
14. Gruhler A, Schulze WX, Matthiesen R, Mann M, Jensen ON: **Stable isotope labeling of Arabidopsis thaliana and quantitative proteomics by mass spectrometry.** *Mol. Cell. Proteomics* 2005, **4**: 1697-1709.
15. Hohmann S: **Osmotic stress signaling and osmoadaptation in yeasts.** *Microbiology and Molecular Biology Reviews* 2002; 300-372.
16. Ichimura K, Miziguchi T, Irie K, Morris P, Giraudat J, Matsumoto K, Shinozaki K: **Isolation of ATMEKK1 (a MAP kinase kinase kinase)-interacting proteins and analysis of a MAP kinase cascade in Arabidopsis.** *Biochemical and Biophysical Research Communications* 1998, **253**: 532-543.
17. Ikeguchi Y, Nakamura H: **Determination of organic phosphates by column-switching high performance anion-exchange chromatography using on-line preconcentration on titania.** *Anal. Sci.* 1997, **13**: 479-85.
18. Jablasone J, Warriner K, Griffiths M: **Interactions of Escherichia coli O157:H7, Salmonella typhimurium and Listeria monocytogenes plants cultivated in a gnotobiotic system.** *International Journal of Food Microbiology* 2005, **99**: 7-18.
19. Kovtun Y, Chiu WL, Zeng W, Sheen J: **Suppression of auxin signal transduction by a MAPK cascade in higher plants.** *Nature* 1998, **395** (6703): 716-20.
20. Kunze G, Zipfel C, Robatzek S, Niehaus K, Boller T, Felix G: **The N terminus of bacterial elongation factor Tu elicits innate immunity in Arabidopsis plants.** *Plant Cell* **2004**, **16**: 3496-3507.
21. Linding R, Jensen LJ, Ostheimer GJ, van Vugt, MA *Et al.*: **Systematic discovery of *in vivo* phosphorylation networks.** *Cell* 2007, **129**: 1415-1426.
22. Macek B, Mann M, Olsen JV: **Global and Site-Specific Quantitative Phosphoproteomics: Principles and Applications.** *Annu. Rev. Pharmacol. Toxicol* 2009, **49**: 199-221.
23. Matsuoka D, Nanmori T, Sato K, Fukami Y, Kikkawa U, Yasuda T: **Activation of AtMEK1, an Arabidopsis mitogen-activated protein kinase kinase, in vitro and in vivo: analysis of active mutants expressed in E.coli and generation of the active form in stress response in seedlings.** *The Plant Journal* 2002, **29**: 637-647.

24. Meszaros T, Helfer A, Hatzimasoura E, Magyar Z, Serazetdinova L, Rios G, Bardozy V, Teige M, Koncz C, Peck S et al.: **The *Arabidopsis* MAP kinase kinase MKK1 participates in defense responses to the bacterial elicitor flagellin.** *Plant J* 2006, **48**: 485-498.
25. Miya A, Albert P, Shinya T, Desaki Y, Ichimura K, Shirasu K, Narusaka Y, Kawakami N, Kaku H, Shibuya N: **CERK1, a LysM receptor kinase, is essential for chitin elicitor signaling in *Arabidopsis*.** *Proc. Natl. Acad. Sci. U.S.A.* 2007, **104**:19613–19618.
26. Nakagami H, Pitzschke A, Hirt H: **Emerging MAP kinase pathways in plant stress signaling.** *Trends in Plant Science* 2005, **10** (7): 339-346.
27. Nakagami H, Soukupova H, Schikora A, Zarsky V, Hirt H: **A mitogen-activated protein kinase kinase kinase mediates reactive oxigens species homeostasis in *Arabidopsis*.** *J. Biol. Chem.* 2006, **281**, 38697-38704.
28. Nita-Lazar A, Saito-Banz H, White FM: **Quantitative phosphoproteomics by mass spectrometry: Past, present and future.** *Proteomics*, 2008, **8**: 4433-4443.
29. Nühse TS, Bottrill AR, Jones AM, Peck SC: **Quantitative phosphoproteomic analysis of plasma membrane proteins reveals regulatory mechanisms of plant innate immune responses.** *Plant J.* 2007, **51**: 931–940.
30. Rawlins EL, White NM, Jarman AP: **Echinoid limits R8 photoreceptor specification by inhibiting inappropriate EGF receptor signaling within R8 equivalence groups.** *Development* 2006, **130** (16): 3715-3724.
31. Rikova K, Guo A, Zeng Q, Possemato A, Yu J: **Global survey of phosphotyrosine signaling identifies oncogenic kinases in lung cancer.** *Cell* 2007, **131**: 1190–203.
32. Rush J, Moritz A, Lee KA, Guo A, Goss VL: **Immunoaffinity profiling of tyrosine phosphorylation in cancer cells.** *Nat. Biotechnol.* 2005, **23**: 94–101.
33. Schikora A, Carreri A, Charpentier E, Hirt H: **The Dark Side of the Salad: *Salmonella typhimurium* Overcomes the Innate Immune Response of *Arabidopsis thaliana* and Shows an Endopathogenic Lifestyle.** *PloS ONE* 2008, **3** (5): e2279.
34. Schwessinger B, Zipfel C: **News from the frontline: recent insights into PAMP-triggered immunity in plants.** *Current Opinion in Plant Biology* 2008, **11**: 389-395.
35. Sorrentino R, Porcellini A, Spalletti-Cernia D, Lombardi V, Vecchio G, Laccetti P: **Inhibition of MAPK activity, cell proliferation, and anchorage-independent growth by N-Ras antisense in an N-ras-transformed human cell line.** *Antisense Nucleic Acid Drug Development* 2001, **11** (6): 349-358.

36. Spellman DS, Deinhardt K, Darie CC, Chao MV, Neubert TA: **Stable isotopic labeling of amino acids in cultured primary neurons: Application to BDNF-dependent phosphotyrosine-associated signaling.** *Mol. Cell. Proteomics* 2008, **7**: 1067–1076.
37. Takekawa M, Posas F, Saito, H: **A human homolog of the yeast Ssk2/Ssk22 MAP kinase kinase kinases, MTK1, mediates stress-induced activation of the p38 and JNK pathways.** *The EMBO Journal* 1997, **16**: 4973-4982.
38. Ubersax JA, Ferrell JE Jr: **Mechanisms of specificity in protein phosphorylation.** *Nat. Rev. Mol. Cell. Biol.* 2007, **8**:530–541.
39. Widmann C, Gibson S, Jarpe MB, Johnson GL: **Mitogen-activated protein kinase: conservation of a three-kinase module from yeast to human.** *Physiological Reviews* 1999, **79** (1): 143-180.
40. Wu Y, Han M: **Suppression of activated Let-60 ras protein defines a role of *Caenorhabditis elegans* Sur-1 MAP kinase in vulval differentiation.** *Genes & Development* 1994, **8**: 147-159.
41. Zipfel C, Kunze G, Chinchilla D, Caniard A, Jones JD, Boller T, Felix G: **Perception of the bacterial PAMP EF-Tu by the receptor EFR restricts *Agrobacterium*-mediated transformation.** *Cell* 2006, **125**: 749–760
42. Zipfel C: **Pattern-recognition receptors in plant innate immunity.** *Current opinion in Immunology* 2008, **20**: 10-16.

IV. MANUSCRIPT

Mass spectrometry-based screening for mitogen-activated protein kinase substrates

Alessandro Carreri^{1,*}, Aladár Pettkó-Szandtner^{1,*}, Sergio de la Fuente van Bentem^{1,*}, Ilse Dohnal², Dorothea Anrather², Sonja Kolar², Jean Bigeard³, Delphine Pflieger³, Gustav Ammerer² and Heribert Hirt^{1,3,4}

¹Department of Plant Molecular Biology, Max F. Perutz Laboratories, University of Vienna, Dr. Bohr-Gasse 9, 1030 Vienna, Austria

²Department of Biochemistry, Max F. Perutz Laboratories, University of Vienna, Dr. Bohr-Gasse xxx, 1030 Vienna, Austria

³URGV Plant Genomics, 2 rue Gaston Cremieux, 91057 Evry, France

⁴Corresponding author; Telephone: +43-1427754612/+33-160874508; Fax: +43-142779546; E-mail address: heribert.hirt@univie.ac.at/hirt@evry.inra.fr

*These authors contributed equally

Abbreviations:

MAPK mitogen-activated protein kinase

MS Mass spectrometry

Keywords:

MAPK, kinase substrate, mass spectrometry, phosphosite mapping, signalling network

4.1 Abstract

Mitogen-activated protein kinases (MAPKs) transmit numerous incoming signals to downstream targets in animals and yeasts. Plant genomes encode the largest families of MAPKs in all eukaryotes, with 20 members in *Arabidopsis thaliana*. With a few exceptions, however, downstream targets have remained undiscovered. Here, we present a systematic screen for Arabidopsis MAPK substrates. Potential MAPK targets were selected on the basis of previously identified *in vivo* phosphorylation sites that match a MAPK motif. Eight candidates were purified and tested in *in vitro* kinase assays for phosphorylation by MPK3, -4, -6. These MAPKs clearly differed in their specificity towards these substrates. Phosphorylation sites were mapped by liquid chromatography-tandem mass spectrometry (LC-MS/MS/MS) in phosphoglucose isomerase 1 (PGI1), the putative Golgi SNARE protein GOS12, the mechanosensitive ion channel MSL9, the histone deacetylase HDT2/HD2B and phosphatidylinositol 4-phosphate kinase 4β1 (PI-4KB1). This analysis showed that MAPKs phosphorylate multiple residues in each substrate. Moreover, nearly all *in vivo* sites were phosphorylated *in vitro* by MAPKs, suggesting that these candidates could be *in vivo* targets. The phosphosite mapping and subsequent mutagenesis showed that several candidates were phosphorylated on multiple residues. The use of a fluorescent protein reporter showed that a phosphorylation site mutant of HDT2 excludes a subpool of the protein from the nucleolus. Moreover, the use of phosphosite mutants of GOS12 showed that phosphorylation of GOS12 likely mediates Golgi localization and that GOS12 is involved in maintaining Golgi morphology. Treatment of protoplasts with flg22 caused relocalization of GOS12 from the nucleus and cytosol to the Golgi, similar to the phosphomimicking mutant.

This selective MS-based approach to connect MAPK isoforms with these MAPK substrates revealed a potential MAPK network regulating vesicular trafficking and histone deacetylation in plants.

4.2 Introduction

MAPKs are involved in signalling cascades regulating ethylene responses and biosynthesis, pollen development and pathogen resistance. The exact mechanisms behind their regulatory roles have mostly remained enigmatic, since only few *in vivo* MAPK targets have been identified. Among these are ACC synthase 6 (ACS6) and PHOS32 that have been identified as MPK6 substrates, MKS1 as an MPK4 substrate, and VIP1 as an MPK3 substrate (Djamei et al., 2007; Merkourpoulis et al., 2008). Recently it was shown that phosphorylation of substrates by MAPKs affect stability (Joo et al., 2008) or subcellular localization (Djamei et al., 2007).

In animal and yeast systems, dozens of MAPK substrates have been identified (Menges et al, 2003). The little knowledge on plant MAPK substrates could be expanded by the use of more high-throughput approaches, which provide good candidates for further *in vivo* verification. High-throughput *in vivo* screening for protein kinase targets is, even in the human field, still a daunting task. Promising approaches include antibody-based purification of protein kinase targets on the basis of phosphorylation motifs, and their identification by mass spectrometry (Matsuoka et al., 2007; Stokes et al., 2007). An alternative high-throughput method for kinase target screening, protein arrays, has been used for discovering MAPK substrates (Feilner et al., 2005). The strength of this method is that it comes up with many potential candidates. Its main drawbacks are that it is an *in vitro* method and that no phosphorylation sites are identified.

With the current discovery of *in vivo* phosphorylation sites by mass spectrometry-based approaches, a rich pool of protein kinase target sites has become available. However, although several thousands of phosphorylation sites of *A. thaliana* proteins have been described (Benschop et al., 2007, Nuhse et al., 2004,

2007, De la Fuente van Bentem et al., 2006, 2008), for nearly all sites the responsible protein kinases are unknown. The challenge is now to couple protein kinases to all their downstream sites, which potentially can reach more than a thousand for individual, broad-spectrum kinases (Linding et al., 2007). A recently developed approach uses contextual information (for instance, knowledge on protein-protein interaction, gene expression patterns, protein kinase phosphorylation motifs) to computationally link protein kinases to their *in vivo* substrate sites (Linding et al., 2007). This NetworKIN algorithm is about 60% accurate in predicting links between human protein kinases and their targets, based on a validated set of known interactions. With more contextual information becoming available, and further training of the NetworKIN program, it might be possible to predict *in vivo* connections between kinases and substrates. In case of plants, however, little data is available to train a plant NetworKIN algorithm, and contextual data are limited. Plant researchers therefore rely, at least for gathering *in vivo* data, on low throughput methods for finding connections between kinases and their targets.

Here, we show a small-scale approach to mine a data set of *in vivo* phosphorylation sites of *A. thaliana* proteins for potential MAPK targets. A selection of potential candidates with *in vivo* phosphoserine/phosphothreonine-proline (pSP or pTP) sites, which are potential MAPK sites, was cloned and tested for phosphorylation by MPK3, -4 and -6. The most promising substrates were used for phosphosite mapping and subsequent mutational analysis of the identified sites, analysis of subcellular localization in plant cells and functional analysis of the observed phosphorylation events.

4.3 Materials and Methods

Cloning of MAPK substrates and purification

Full-length *PVA11* (At3g60600.1), *HDT2/HD2B* (At5g22650.1), *NOVA-LIKE RNA BINDING PROTEIN (NEO1)* (At5g04430.2), Golgi SNAP receptor complex member 1-2 (*GOS12*; At2g45200.1), *SCARFACE (SCF)* (At5g13300) and *PGII* (At4g24620.1), and partial cDNAs of *PI-4K β 1* (At5g64070) and *MSCS-LIKE 9 (MSL9)* (At5g19520.1) were amplified and cloned into pGEX4T-1. Primers used for each cloning are provided in Table 1. GST protein expression was induced for 4 hours at 37°C with 1 mM IPTG, and purified according to the manufacturer's protocol.

Kinase assays

Radioactive kinase assays were performed with MPK3, -4 and -6 immunoprecipitated from extracts of *A. thaliana* cell cultures that were treated for 10 minutes with 1 μ M flg22. Non-radioactive kinase assays for phosphosite mapping were performed the same for 45 minutes at 30°C.

Phosphosite mapping by liquid chromatography-tandem mass spectrometry

After the kinase assay, proteins were boiled in 1 x SDS buffer and subjected to SDS-PAGE. Gels were stained with either silver (Shevchenko et al., 1997) or coomassie brilliant blue (CBB). Proteins were cut out of gels with a scalpel, digested in-gel with trypsin and prepared for LC-MS³ as described before.

Mutagenesis of MAPK substrates

For mutagenesis, PCR was performed on plasmids with Pfu Ultra. PCR mixtures were digested for 2 hours with *DpnI* and transformed into *Escherichia coli*. Different clones were sequenced and one for each mutation was transformed into *E. coli* BL21 for protein purification as described above. The following mutations were made:

Table 1. Primers used for mutagenesis of phosphorylation sites				
Protein	Identifier	Forward primer	Reverse primer	Mutation
HDT2	At5g22650	GCAGCACCAGCTTCT GA ACCTCAGAAGACA ¹	TGTCTTCTGAGG TC CAGAAGCTGGTGCTGC	T234E
		GGAGGACACACCGCC GA ACCACACCCAGCT	AGCTGGGTGTGGT TC GGCGGTGTGCTCTCC	T249E
		GTGAATGCTAACCAGG AC CCCAAGTCTGGA	TCCAGACTTGGGG TC TGGTTAGCATTAC	S266D
MSL9	At5g19520	AAAGATCCAAGAGCAGCTCCTTCTTTCAAT	ATTGAAAGAAGGAGCTGCTTGGATCTTT	S28A
		AAAGATCCAAGAGCAG A TCCTTCTTTCAAT	ATTGAAAGAAGG A CTGCTCTTGGATCTTT	S28D
		TTCAATCCATTGGCT G CACCAGACTCCGAT	ATCGGAGTCTGGT G CAGCCAATGGATTGAA	S36A
		TTCAATCCATTGGCT GAT CCAGACTCCGAT	ATCGGAGTCTGGAT TC AGCCAATGGATTGAA	S36D
		CCACCTAAAATTCAG CT CCTGAAGGTCTA	TAGACCTTCAGGAG CT TGGAATTTTAGGTGG	S74A
		CCACCTAAAATTCAG AT CTCTGAAGGTCTA	TAGACCTTCAGGAT CT TGGAATTTTAGGTGG	S74D
		TCTTTTGACAGGGCTGCTCTAATAACAAA	TTTGTTATTAGGAGCAGCCGTGTCAAAAGA	S134A
		TCTTTTGACAGGGCT GAT CTAATAACAAA	TTTGTTATTAGGAT TC AGCCCTGTCAAAAGA	S134D
GOS12	At2g45200	TATGTTGACACTGGGGCTCCAACCGTTGGA	TCCAACGGTTGGAGCCCCAGTGTCAACATA	S51A
		TATGTTGACACTGGGG AT TCCAACCGTTGGA	TCCAACGGTTGGAT CCCC AGTGTCAACATA	S51D
		GCTTCTGGTAGTAT G CACCAAGGTGTGCAA	TTGCACACCTGGTGC CTA CTACCAGAAGC	S146A
		GCTTCTGGTAGTAT GAT CCAGGTGTGCAA	TTGCACACCTGGAT TC CATACTACCAGAAGC	S146D
PGII	At4g24620	GGAAACTGTGGAGCGCCACGAAGTATCAAA	TTTGATACTTCGTGGCG CT CCACAGTTTCC	S595A
		GGAAACTGTGGAG GA CCCACGAAGTATCAAA	TTTGATACTTCGTGGG TC TCCACAGTTTCC	S595D
¹ Mutated residues are in bold				

Localization of MAPK substrates in protoplasts

Full-length *GOS12* and *HDT2* and their phosphosite mutants were cloned in a pGreen plasmid behind a *yellow fluorescent protein (YFP)* gene driven by a 35S promoter. Plasmids were transformed into protoplasts as described (Cardinale et al., 2000). One day after transformation localization was checked by fluorescence and confocal microscopy.

4.4 Results

Selection of candidate MAPK substrates from a phosphoproteomic approach

A previous phosphoproteomic approach identified 303 *in vivo* phosphorylation sites in proteins isolated from Arabidopsis root cell suspension (De la Fuente van Bentem et al., 2008). Of these sites, 91 matched the proline-directed motifs pSP and pTP (Figure 1). We were interested in finding MAPK targets among the 73 proteins that contained *in vivo* pSP/pTP sites. However, other protein kinases like cyclin-dependent kinases (CDKs) also target this motif. Therefore we additionally searched in these candidates for a MAPK docking domain or D-domain, which is required for interaction with MAPKs in yeast, animal and plant proteins. For instance, MAPKKs and MAPK phosphatases contain such domains, and the D-domain of the plant phosphatase P2C1 is required for MAPK interaction (Schweighofer et al., 2007). We screened for the presence of a ‘classical’ D-domain, which had to (1) consist of the sequence $(R/K)_{2-3}-X_{2-6}-\phi-X-\phi_n$ and (2) be positioned between 15-150 amino acids N-terminally of the phosphorylation site. These conserved criteria were chosen as most of the D-domains meet these requirements. It is important to note, however, that some *bona fide* D-domains in yeast and animal systems deviate from one of these criteria. Out of the 73 proteins that we inspected, 12 contained the D-domain (Figure 1 and Supplemental Table 1). Interestingly, a high occurrence of proteins with D-domains and pSP/pTP sites was observed among proteins predicted to be involved in protein/vesicular trafficking. Moreover, two of these proteins are GTPase exchange factors and four others are SNARE or SNARE-associated proteins (Supplemental Table 1).

Specificity of phosphorylation of candidate substrates by MAPKs

To verify whether candidates with D-domains are indeed preferential MAPK targets, we selected four candidates out of the 12 that contain a D-domain, and four out of the 61 lacking a D-domain (Figure 1). These eight other candidate substrates were tested for phosphorylation by endogenous, flg22-activated MPK3, -4 and -6 that were immunopurified from root cell culture extract. MBP and GST served as positive and negative controls, respectively (Figure 2). Whereas NEO1 and SCF were weakly phosphorylated by all three MAPKs, MPK6 showed highest activity towards MSL9, Golgi SNAP receptor complex member 1-2 (GOS12), PVA11 and PGI1. MPK3 showed highest activity towards PI-4K β 1 and HDT2 (Figure 2). Although MPK4 also phosphorylated several proteins, none of the substrates displayed MPK4 preference (Figure 2), in contrast to the splicing factor SCL30 (De la Fuente van Bentem *et al.*, 2008).

Mapping of phosphorylation sites in candidate MAPK substrates by mass spectrometry

To determine whether the observed phosphorylation events occurred on the known *in vivo* sites, we mapped phosphorylation sites of recombinant HDT2, GOS12, MSL9, PGI1 and PI-4K β 1 by mass spectrometry. Mass spectra of *in vitro* phosphorylated proteins revealed many phosphopeptides (Supplemental Figure 1). An overview of identified phosphopeptides is given in Table 2. Except for two sites, one in HDT2 and one in PI-4K β 1, all *in vivo* sites in these substrates are targeted by the MAPKs *in vitro* (Table 3). In addition to the *in vivo* sites, also several other sites in MSL9, GOS12 and HDT2 were phosphorylated. We note that if a site is not detected by MS this does not mean that the site is not phosphorylated. It can be that in fact more sites in these

substrates were phosphorylated but not detected. In conclusion, the findings that *in vivo* sites are targeted by MAPKs *in vitro*, suggest that these kinases could be responsible for the phosphorylation event *in vivo*.

For positive candidates, we checked whether the *in vivo* phosphosites are conserved in other plant homologues and orthologues. GOS12 sites are not conserved in GOS11. MSL9 sites are not conserved in orthologues, but MSL6 and MSL10 have shown to be phosphorylated *in vivo*. PGI1 site is conserved among orthologues (Supplemental Figure 2). Some sites of HDT2 are conserved in HDT1.

Mutagenesis of phosphorylation sites in candidate MAPK substrates

We then determined the contribution of individual phosphorylation sites to phosphorylation by MAPKs. As described above, GOS12 was phosphorylated on two sites by MPK6. There are no other potential MAPK sites in GOS12, and mutational analysis showed that GOS12^{S51D} is less phosphorylated by MPK6 and GOS12^{S51D/S146D} is not phosphorylated, showing that these are the only two MAPK substrate sites (Figure 3A).

Phosphorylation of MSL9 and MSL9 mutants by MPK6 gradually decreases along with the number of mutations (Figure 3). Because the GST-MSL9¹⁻¹⁸⁰ protein runs at the same position as the MPK6 autophosphorylation band (Figure 2), it is difficult to judge whether the quadruple MSL9^{S28A/S36A/S74A/S134A} mutant is slightly phosphorylated or not at all (Figure 3B). There is a TP motif in this region of MSL9 that was not detected in the MS analysis. In any case, that site likely represents a minor MAPK site.

The two identified *in vitro* MPK3 sites (T249 and S266) and the *in vivo* sites (potentially T234 and S266) in HDT2 were mutated. Successive mutation of these two sites decreased overall phosphorylation (Figure 3C).

Determinants of phosphorylation specificity in HDT2 and MSL9

Since HDT2 and MSL9 showed the highest degree of MAPK specificity (Figure 2), we sought to identify potential regions of specificity in these proteins. *A. thaliana* contains a family of 19 histone deacetylases, and HDT2 belongs to a plant-specific HD2 subfamily that comprises four members (Pandey et al., 2002). Truncated versions of HDT2 were tested to further localize phosphorylation sites and determinants that contribute to phosphorylation strength and specificity. In contrast to MPK3, MPK6 targets these truncated versions with similar activity to the full-length HDT2 protein (Figure 4A). These data suggest that MPK3 specificity in HDT2 is localized in the N-terminal 198 amino acids and, without this region, the C-terminal residues cannot be targeted any more.

MscS-like 9 (MSL9) is one out of 10 *A. thaliana* MscS-like mechanosensitive ion channels. We deleted the N-terminal D-domain to test its importance for phosphorylation by MPK6. Unexpectedly, the docking domain seems to be dispensable (Figure 4B).

MPK3 interacts *in vivo* with HDT2

Given the results described above we tested whether the specificity of the phosphorylation of MPK3 towards HDT2 is due to a true *in vivo* interaction between the two proteins.

For reaching this purpose we expressed MPK3-HA construct and HDT2-Myc under the control of the constitutive promoter 35S in *A. thaliana* root cells protoplasts. The cells had been then subjected to co-immunoprecipitation (Co-IP) experiment.

As shown in Figure 5A, when the two proteins are expressed in the protoplasts system it's possible to verified their interaction through the immunoprecipitation of HDT2 using Myc antibody.

It was also demonstrated that when HDT2 is co-expressed with another MAPK, MPK6 tagged with the HA epitope, it's not possible to co-immunoprecipitate MPK6 together with HDT2 (Figure 5B), proving that the interaction between HDT2 and MPK3 is specific.

Localization of MAPK substrates in plant cells

As published before, YFP-HDT2 localizes in the nucleolus (Figure 7A). To investigate whether the localization is affected by phosphorylation, we introduced phosphomimicking mutations (i.e. mutations that mimic a constitutively-phosphorylated state) at the positions of the three *in vitro* or *in vivo* sites (Table 3). We found that YFP-HDT2^{T234E/T249E/S266D} was localized in nucleoli as well. In addition, however, this fusion protein was localized in the nucleoplasm and cytosol as well (Figure 7B). YFP-HDT2 expressing protoplasts were also treated with flg22 in order to activate MPK3 and test the effect of the phosphorylation on HDT2 localization. We notice (figure 7D) that the distribution of HDT2 in the cell changes

and the protein, that in untreated cells is strictly localized in the nucleoli, it's moving out showing a very similar distribution to the one detected with the YFP-HDT2^{T234E/T249E/S266D} version. We were able to detect the same kind of effect in the diffusion inside the cells of YFP-HDT2 also when the fusion protein was co-expressed together with MPK3. Unfortunately, we failed to clone the HDT2^{T234A/T249A/S266A} mutant.

Gene ontology predicts that GOS12 is a putative orthologue of yeast Gos1p and human GOSR1/GOS-28/GS28. The GOS12 phosphorylation sites are not conserved in the closest Arabidopsis homologue GOS11. As GOS12 is a predicted Golgi SNARE, we investigated the localization of the protein in Arabidopsis protoplasts. YFP-GOS12 localizes in distinct, punctuated structures in the cytoplasm, but also displays diffuse nuclear and cytosolic localization (Figure 6). To determine the effect of phosphoinactive or phosphomimicking mutations on GOS12 localization, we expressed YFP-GOS12^{S51A/S146A} and YFP-GOS12^{S51D/S146D} in protoplasts.

Context-based approach to couple MAPKs to candidate substrates

A simple NetworKIN version was developed to couple the here-identified MAPK candidate substrates to individual MAPK isoforms. Expression analysis revealed that 9 out of the 20 MAPK isoforms are expressed in cell culture (Menges et al, 2003), our working system.

A potential MAPK network was built on the basis of the context-based approach (Figure 8). This network allows experimental validation of the MAPK model.

4.5 Discussion

In an attempt to discover novel MAPK targets, we carried out a simple approach to screen for targets from *in vivo* phosphorylation sites. The screen is based on mining a list of *in vivo* pSP/pTP sites, which are potential MAPK substrates, and additionally a D-domain for MAPK docking. Our approach is generally applicable, although it remains difficult for most plant kinases that target unknown motifs and dock to unknown domains. Motif discovery by approaches such as described by Stulemeijer et al. (2007) is therefore crucial to make such a screen successful. Merkouroupoulis et al., (2008) recently identified two Arabidopsis MAPK substrates by a gel-based approach. The MAPK phosphorylation site in PHOS32 was also identified in our phosphoproteomic approach, showing that this site is phosphorylated *in vivo* (De la Fuente van Bentem et al., 2008). Large-scale protein array-based approaches have revealed many potential CKII and MPK3 and -6 targets (Feilner et al., 2005; Kramer et al., 2004). However, for most of these targets no *in vivo* phosphorylation sites have been described. With more data becoming available, it can be envisaged that combining information from MS-based phosphoproteomic screens (Benschop et al., 2007; De la Fuente van Bentem et al., 2007, 2008; Sugiyama et al, 2008; Nuhse et al., 2004, 2007) and protein chip experiments enables the selection of good candidates for *in vivo* validation. Experiments as exemplified by our approach could be included in this validation: *in vitro* kinase assays followed by phosphosite mapping by MS and analysis of the effect of phosphorylation on protein localization, stability and activity.

Function of MAPK D-domains in substrates

MAPKs have D-domain-dependent and –independent interactions (Mayor et al., 2007). The D-domain of MAPK substrates and the docking (Chang et al., 2002 Mol Cell) domain of MAPKs can be phosphorylated. Phosphorylation of the CD domain causes preferential targeting of substrates that do not dock through their D-domains (Mayor et al., 2007). MPK6 has several potential phosphorylation sites in its CD domain, but MPK3 lacks these.

Our screen was based on the assumption that MAPK substrates need a D-domain to recruit the MAPK. The puzzling result that the D-domain of MSL9 is dispensable suggests that MPK6 does not require docking. However, all four selected candidates with a D-domain are best phosphorylated by MPK6 in our assay (Figure 2), suggesting that the D-domain might be a critical specificity determinant. The MSL9⁵⁶⁻¹⁸⁰ and MSL9¹⁻⁵⁵ truncations are both weakly phosphorylated by MPK6, at least not enough to equal phosphorylation of MSL9¹⁻¹⁸⁰ (Figure 4). This suggests that there might be a second docking region around residue 55. Of the four candidates without a D-domain, two were poor MPK3, -4 and -6 targets (NEO1 and SCF), and two were best targeted by MPK3 (Figure 2). Remarkable specificity of *in vitro* reactions is displayed by HDT2 and MSL9, which show a clear preference for MPK3 and MPK6, respectively. This suggests that even substrates for specific MAPK isoforms can be isolated in our approach. In conclusion, although the mechanism is still unclear, looking for classical D-domains in close vicinity of pSP/pTP sites can enable MPK6 target selection. Whether the docking domain of MPK3 and -4 is a D-domain variant or completely different remains to be investigated.

Phosphorylation of mechanosensitive ion channels

We found two putative MAPK sites in MSL10 (S131 and T136), which is the most closely related mechanosensitive ion channel to MSL9 (data not shown). These sites were also found in the plasma membrane phosphoproteome (Benschop et al., 2007; Nuhse et al., 2004). MAPKs might therefore target different mechanosensitive ion channel isoforms. In plasma membrane extracts, two MSLs were found to be phosphorylated, MSL6 and MSL10. MSL6 was phosphorylated on sites that do not confirm MAPK motifs. All sites were in the N-terminal extension, suggesting that this region in MSLs have a regulatory role.

Extramembrane regions of mechanosensitive ion channels might restrict ions that pass through the channel or affect docking interactions with proteins that regulate channel properties (Bass et al., 2002 Science). Hence, phosphorylation might regulate one or both these processes. Mechanosensitive ion channels are expected to function in osmotic stress-related changes in membrane tension. MSL9 was recently shown to act as a mechanosensitive ion channel (Haswell et al., 2008).

The potential function of HDT2 phosphorylation by MPK3

HDT2 is a preferential MPK3 target, the N-terminal region contains the catalytic domain and a charged region might contain a binding domain, as truncations lacking this region cannot be phosphorylated by MPK3 (Figure 4). Attempts to measure histone deacetylase activity of HDT2 *in vitro*, using either recombinant HDT2 or HDT2 immunopurified from large amounts of transfected protoplasts, were unsuccessful (C. Seiser, A. Carreri, H. Hirt, unpublished). Therefore we could not test the effect of phosphorylation on HDT2 activity. Expression of HDT2 and phosphorylation site mutants in protoplasts showed a clear difference in subcellular

localization. HDT2 was localized mainly in nucleoli, as shown before (Zhou et al., 2004), but a phosphomimicking form also localized to the nucleoplasm and the cytosol (Figure 7A). This protein distribution it was also noticed when protoplast expressing YFP-HDT2 were treated for 15 minutes with flagellin (Figure 7D). Moreover, co-expression of MPK3-HA with its putative target YFP-HDT2 leads to a redistribution of HDT2 between the nuclear and the cytoplasmic region. This finding suggests that HDT2 might be released from the nucleolus upon phosphorylation by MPK3.

HDT2 functions redundantly with HDT1 in controlling levels and/or patterns of miR165/166 distribution that regulates the establishment of adaxial-abaxial leaf polarity (Ueno et al., 2007). HDT2 is also required for *Agrobacterium tumefaciens*-mediated transformation of *A. thaliana*, potentially by affecting T-DNA integration (Crane and Gelvin, 2007). Importantly, MPK3 is activated by *A. tumefaciens* infection and subsequently phosphorylates VIP1, a protein that is required for transport of *A. tumefaciens* T-DNA from the cytosol into the nucleus (Djamei et al., 2007). Thus, we speculate that *A. tumefaciens* might exploit the phosphorylation of HDT2 in addition to VIP1 for efficient host transformation. We speculate that HDT2 is either released from nucleoli upon phosphorylation by MPK3, or retained out of the nucleolus by phosphorylation in the cytosol and/or nucleoplasm. As the phosphorylation form of HDT2 is localized in the nucleoplasm and cytosol, this form might affect T-DNA integration rather than the unphosphorylated, nucleolar form.

Do MAPKs regulate vesicular trafficking?

One of the potential MAPK targets identified in this study, GOS12, is predicted to function as a Q_b SNARE protein (Pratelli et al, 2004). Just as its yeast counterpart Gos1p (McNew JA et al., 1998), GOS12 is localized in the Golgi compartment (Uemura et al., 2004). With a SNARE domain and a C-terminal TM region, it is predicted to mediate membrane fusion. Our *in vivo* localization studies suggested that a pool of GOS12 protein is localized in the Golgi, whereas most was found to localize diffusely in the nucleus and cytoplasm. Interestingly, more of the GOS12 protein localized in the Golgi after cells were challenged with flg22. In agreement with this observation, the phosphomimicking version GOS12^{S51D/S146D} was found to localize primarily in the Golgi. Strangely, the GOS12^{S51A/S146A} protein is localized in a large membrane compartment, which can potentially be aggregated Golgi stacks. Such aggregates are also observed in yeast *gos1p* knock-out strains (McNew JA et al., 1998). If this hypothesis is right, GOS12 phosphorylation might affect interaction with other SNARE components on the Golgi compartment. Correct interaction with other components might be required for proper membrane fusion within the Golgi compartment. In animal cells, trafficking through the Golgi is regulated by a phosphorylation cascade (Pulvirenti et al., 2008).

Another potential MAPK target, PI-4KB1, specifically interacts with the GTP-bound form of RabA4b, a protein that localizes in a trans-Golgi compartment and is proposed to regulate membrane trafficking involved in the secretion of cell wall components at the tip of root hairs (Preuss et al., 2004). PI-4KB1 colocalizes with RabA4b on tip-localized membranes in growing root hairs (Preuss et al., 2006). PI-4KB1 acts redundantly with PI-4KB2, and double mutants in these genes display root hair abnormalities (Preuss et al., 2006). PI-4KB1 also interacts with the Ca²⁺-sensor

CBL1, and therefore PI-4K β 1 has been proposed to mediate Ca²⁺-dependent generation of phosphoinositol-4-phosphate (PI-4P) (Preuss et al., 2006). Interestingly, the *Medicago sativa* MAPK SIMK (the orthologue of *A. thaliana* MPK6) is involved in root hair tip growth (Samaj et al., 2002). The exact mechanism is unclear, although the actin cytoskeleton is involved in this process (Samaj et al., 2003). Active SIMK accumulates in spot-like structures at the root hair tip, and MAPK signalling is required for vesicle formation at and growth of the root tip (Samaj et al., 2002). We speculate that MAPK phosphorylation of PI-4K β 1 and vesicle trafficking components like PVA11 and GOS12 might be required. Moreover, SPIKE1 (SPK1) is an ARF-GEF that controls actin polymerisation and is phosphorylated *in vivo* on an SP site and has a neighbouring D-domain (Supplemental Table 1). We therefore speculate that a MAPK signalling subnetwork potentially mediates root hair tip growth (Figure 8). Interestingly, several sites in human PI-4KII are phosphorylated *in vivo* (Phospho.ELM; Olsen JV et al., 2006) and predicted by NetworKIN (Linding et al., 2007) to be phosphorylated by MAPKs. This suggests that PI-4K targeting by MAPKs might also take place in mammalian species.

Acknowledgements

We thank Andriy Belokurov for technical assistance and Christian Seiser for helpful discussions on histone deacetylases. Work in our laboratory is supported by the Austrian Science Foundation, the Vienna Science and Technology Fund and the European Union.

4.6 Figure legends

Figure 1. Selection and screening of candidate MAPK substrates.

91 previously identified *in vivo* phosphorylation sites matched a minimal MAPK consensus motif (SP or TP). Of the 73 proteins, 12 contained a D-domain for MAPK docking. Eight candidates were tested for phosphorylation by three MAPKs, and several of them were subjected to further experimenting.

Figure 2. *In vitro* phosphorylation of candidate MAPK substrates.

Immunocomplex kinase reactions were performed with MPK3, -4 and -6 on the negative GST and positive MBP controls. Arrows indicate full-length forms of all substrate proteins. Asterisks indicate an unknown phosphoprotein in the MPK4 lanes (not always observed), or MPK6 autophosphorylation in the MPK6 lanes.

Figure 3. Mutagenesis of phosphosites within MAPK substrates.

Phosphorylation of (A) GOS12 mutants by MPK6, (B) MSL9 mutants by MPK6, (C) PGI1 mutants by MPK6 and (D) HDT2 mutants by MPK3. The asterisk in panel (B) indicates the position of the MPK6 autophosphorylation band.

Figure 4. Phosphorylation of HDT2 and MSL9 truncations.

(A) HDT2 truncations were phosphorylated by MPK3 and -6. (B) Phosphorylation of MSL9 truncations by MPK3 and -6. Asterisks indicate MPK6 autophosphorylation signals.

Figure 5. Co-immunoprecipitation of HDT2 with MPK3.

Figure 6. Localization of fluorescently labelled GOS12 and its phospho mutants in protoplasts.

Yellow fluorescent protein fusions were expressed in root protoplasts. Upper panel: YFP fluorescence of a protoplast expressing YFP-GOS12; YFP-GPS12^{AA}; YFP-GOS12^{DD}; YFP-GOS12 co-express with MPK6-HA; YFP-GOS12 co-express with MPK6-HA in protoplasts treated with flg22. Bottom panel: corresponding bright field images.

Figure 7. Different localization of HDT2

(A) Yellow fluorescent protein fusions were expressed in seedlings protoplasts. Bright field image and fluorescent picture showing the nucleoli localization of YFP-HDT2.

In the bottom panel is showed the diffuse localization of the YFP-HDT2^{T234E/T249E/S266D} mutant in the nucleolus, in the nucleus and in the cytoplasm.

(B) Subcellular fractionation of Myc-HDT2 and Myc-HDT2^{T234E/T249E/S266D}.

HDT2 and HDT2^{EED} (HDT2^{T234E/T249E/S266D}) were expressed as Myc fusion proteins in Arabidopsis protoplasts. Western blotting with anti-Myc antibodies was performed on different subcellular fractions. T, total extract; P, nuclear pellet; S, soluble fraction.

(C) Confocal image of the localization of YFP-HDT2 in seedling protoplasts.

(D) Confocal image of the localization of YFP-HDT2 after 15 minutes of flg22.

(E) Confocal image of the localization of YFP-HDT2 co-express with MPK3-HA in seedling protoplasts.

Figure 8. A potential MAPK network in *A. thaliana*.

A subnetwork that mediates root hair tip growth. PI-4K β 1 and SPK1 are *in vivo* phosphorylated. PI-4K β 1 is *in vitro* phosphorylated by MPK3, -4 and -6.

Supplemental data

Supplemental Figure 1. MS/MS spectra of phosphopeptides derived from substrates that were phosphorylated *in vitro* by MAPKs

Supplemental Figure 2. Conservation of MAPK phosphorylation sites in plant homologues and orthologues

Supplemental Table 1. Summary list of *in vivo* phosphorylation sites of *A. thaliana* cell culture proteins

4.7 Tables

Table 2. Phosphopeptides of MAPK substrates identified by MS/MS									
Substrate	Kinase used	Phosphopeptide	MH+	deltaM	z	Ppep	XCorr	deltaCn	Site(s)
HDT2	GST-MPK3	K.SPVNANQS#PK.S ¹	1121.50	-0.45	2	1.94E-02	3.66	0.82	S266
		K.SPVNANQS@PK.S ²	1023.53	-0.11	2	3.07E-05	3.03	0.60	
		K.GGHTAT#PHPAK.K	1153.51	0.16	2	3.77E-02	3.10	0.22	T249
		K.GGHTATPHPAK.K	1073.55	0.24	2	5.92E-02	2.63	0.67	
		K.KGGHTAT#PHPAK.K	1281.61	0.29	2	1.00E+00	2.57	0.07	T249
MSL9	IP-MPK6	K.KKGGHTAT#PHPAK.K	1409.70	0.18	2	1.18E-01	2.17	0.03	T249
		R.ASPSFNPLAS#PDS DAGIEK.S	1982.87	0.65	2	1.53E-06	5.25	0.07	S28
		R.ASPSFNPLAS@PDS DAGIEK.S	1884.91	0.07	2	8.17E-09	3.84	0.09	
		R.AS#PSFNPLAS#PDS DAGIEK.S	2062.84	-0.11	2	1.55E-05	4.22	0.02	S28, S36
		K.IPS#PEGLVR.R	1047.52	0.03	2	6.37E-07	3.21	0.66	S74
		K.IPS@PEGLVR.R	949.56	-0.17	2	5.72E-06	2.50	0.61	
		R.GSFDRAS#PNNK.S	1272.54	-0.11	2	7.47E-02	2.91	0.25	S134
		R.GSFDRAS@PNNK.S	1174.57	-0.11	2	6.64E-06	2.56	0.35	
		R.FTQGGYVDTGS#PTVGSGR.S	1865.81	0.08	2	1.72E-06	6.04	0.08	S51
		R.FTQGGYVDTGS@PTVGSGR.S	1767.84	0.11	2	1.26E-05	5.59	0.04	
GOS12	IP-MPK6	K.ASGSMS#PGVQVLR.E	1368.63	-0.22	2	8.35E-04	4.38	0.21	S146
		K.ASGSMS@PGVQVLR.E	1270.67	0.26	2	3.42E-08	3.49	0.14	
PGI1	IP-MPK6	R.VLIAEGNCGS#PR.S							S595
PI-4KB1									S449

¹#, phosphorylated residue. ²@, dehydroalanine (serine that lost water)

Table 3. Overview mapping of phosphosites targeted <i>in vitro</i> by MAPKs					
Protein	Identifier	Function	Phosphorylation	<i>In vivo</i> sites	<i>In vitro</i> sites
HDT2	At5g22650	Transcriptional regulation	MPK3>MPK4=MPK6	S233 or T234, S266	T249 ¹ , S266 ¹
MSL9	At5g19520	Ion transport	MPK6>MPK3=MPK4	S28, S36, S134	S28, S36, S74, S134
GOS12	At2g45200	Vesicular trafficking	MPK6>MPK4>MPK3	S51	S51, S146
PGI1	At4g24620	Glucose metabolism	MPK6>MPK4>MPK3	S595	S595
PI-4KB1	At5g64070	Vesicular trafficking	MPK3> MPK6>MPK4	S449 ² , S454	S449 ²

¹by GST-MPK3; ²putative CKII motif

4.8 Figures

Figure 1

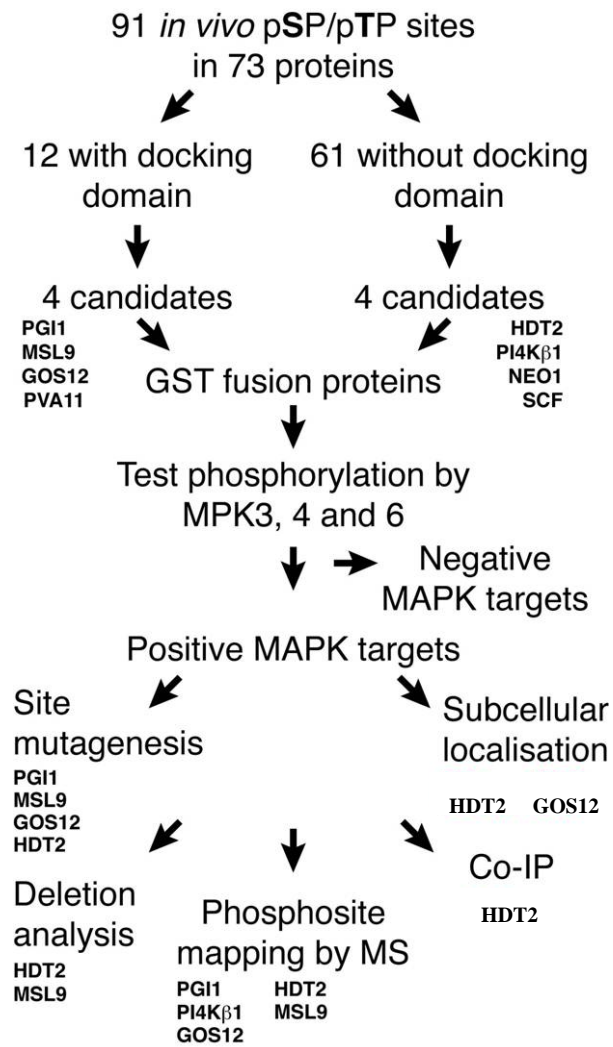


Figure 2

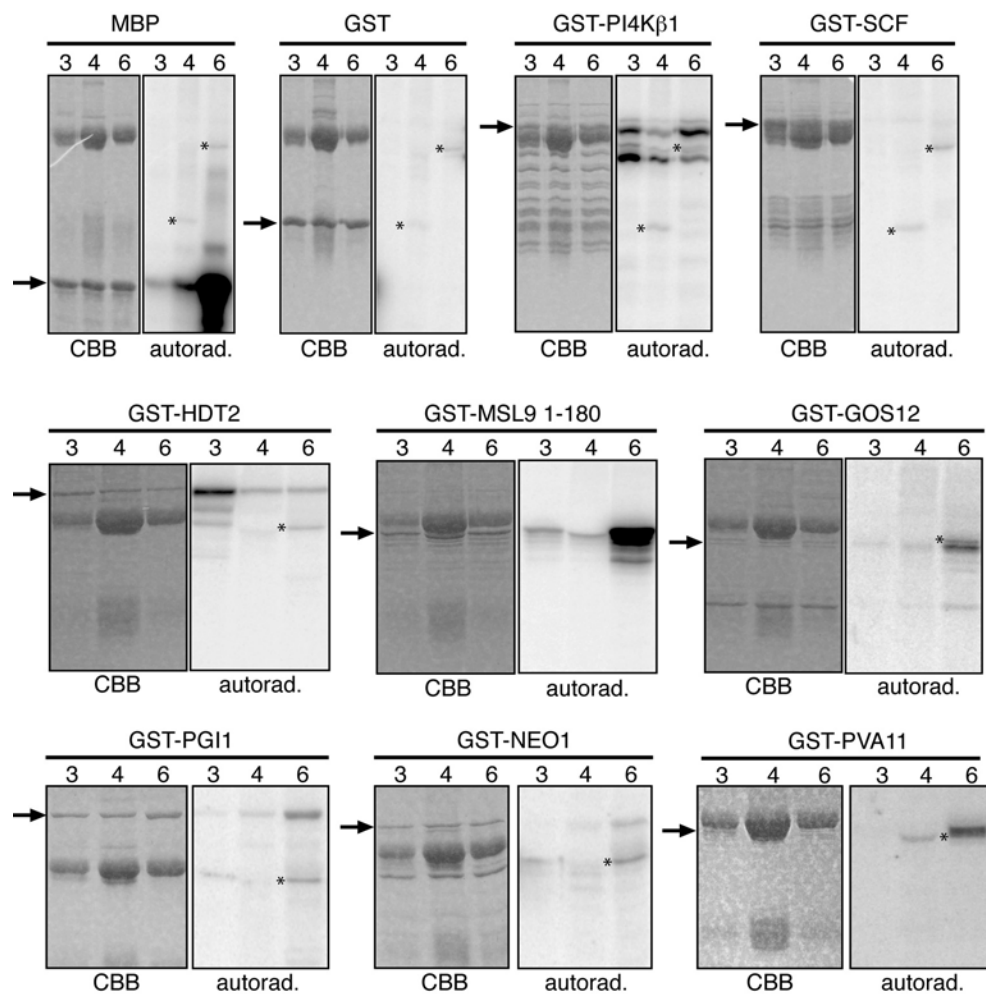


Figure 3

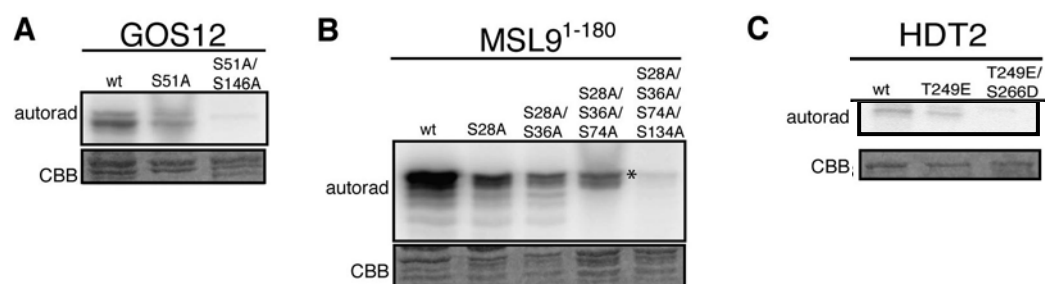


Figure 4

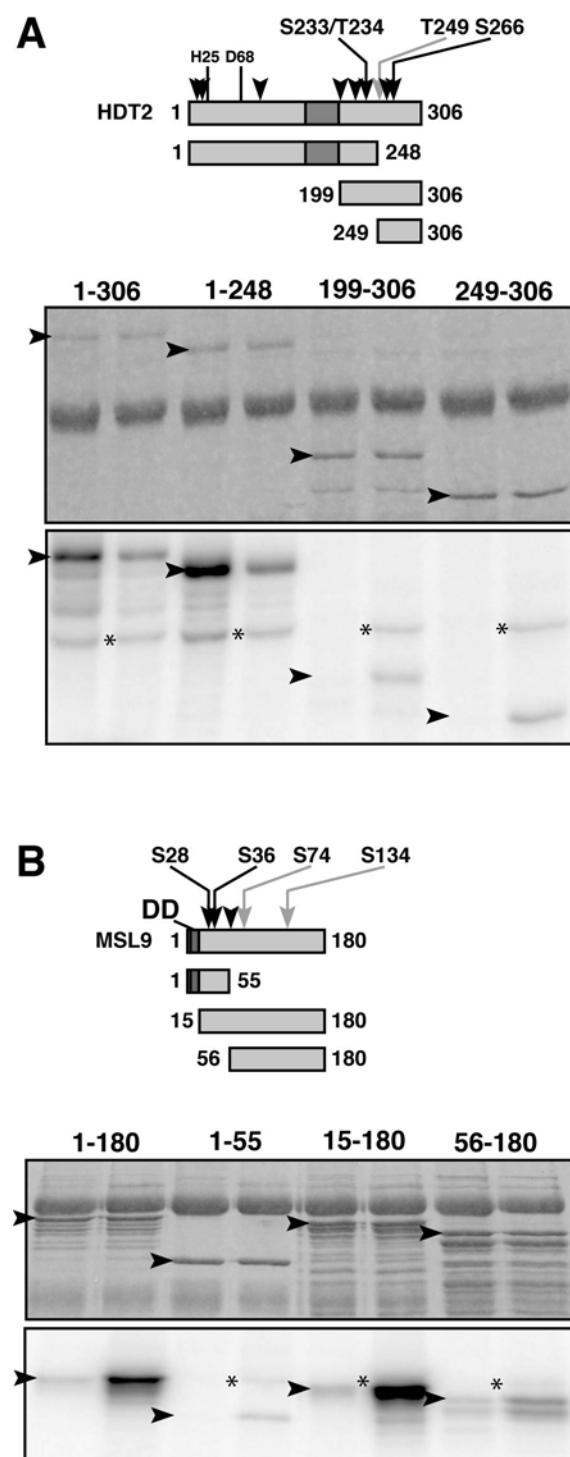
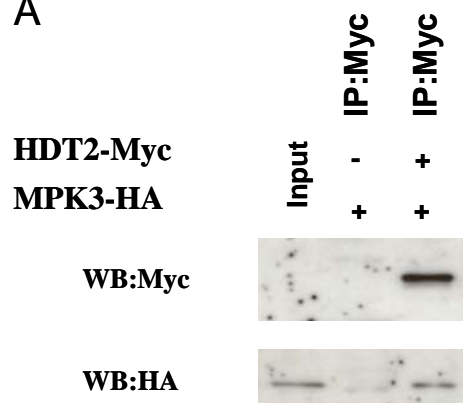


Figure 5

A



B

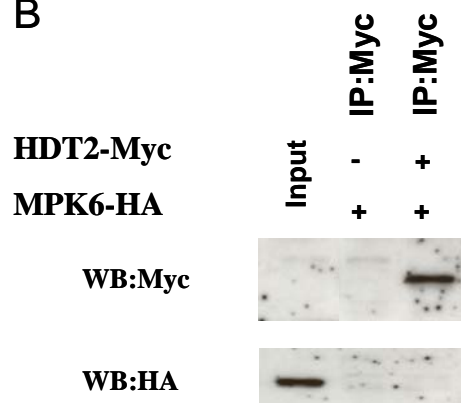


Figure 6

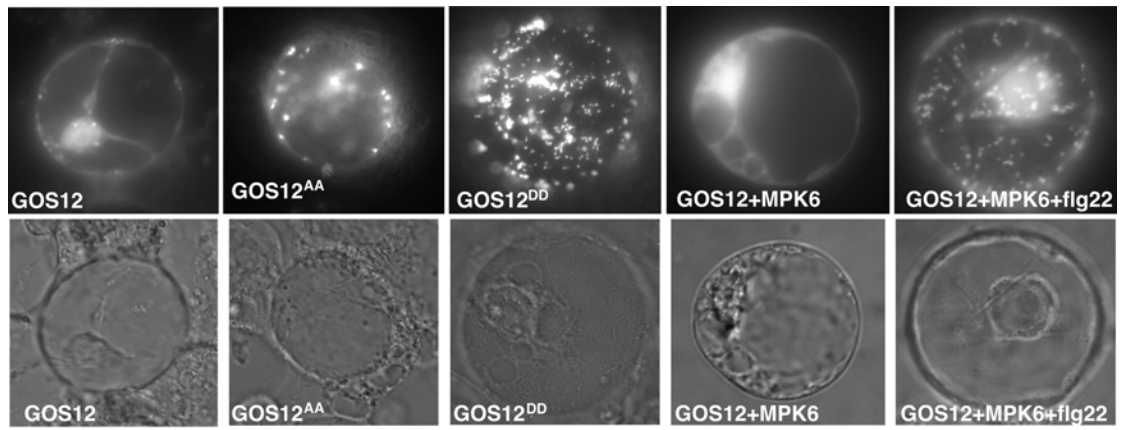
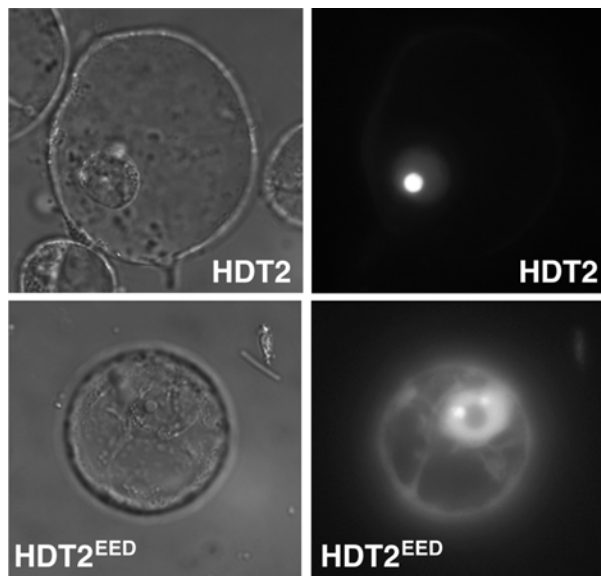


Figure 7

A



B

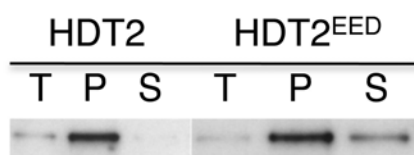


Figure 7

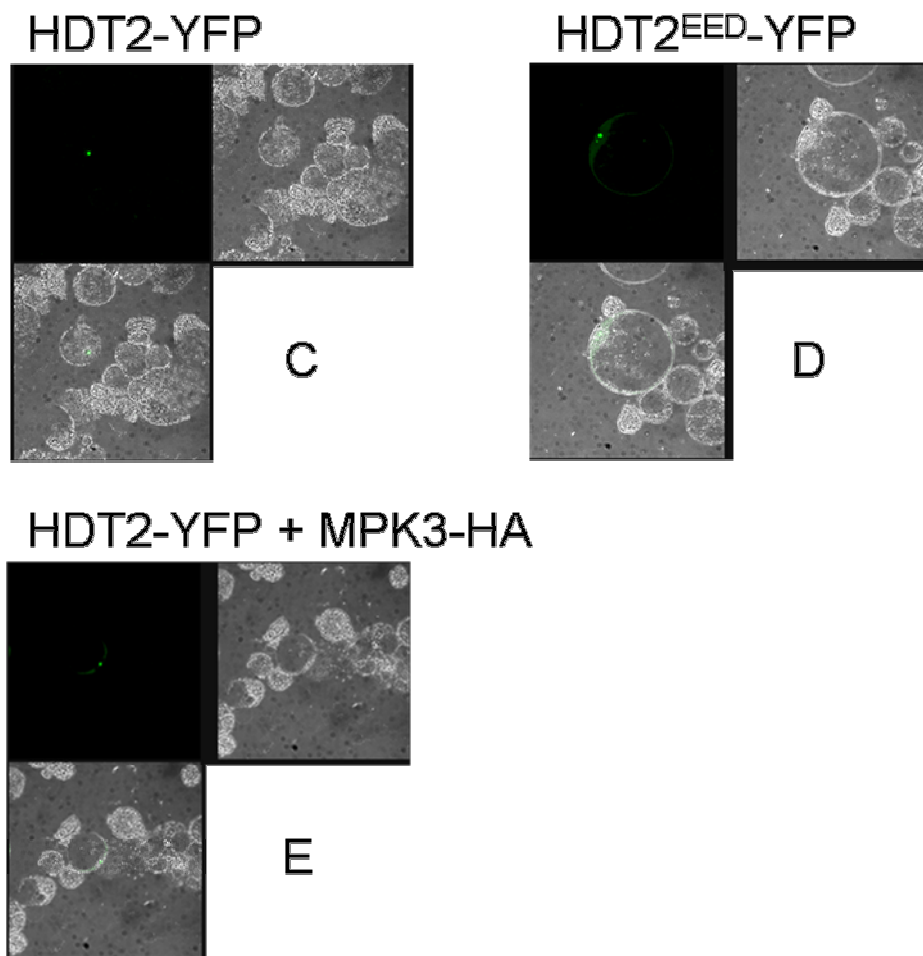
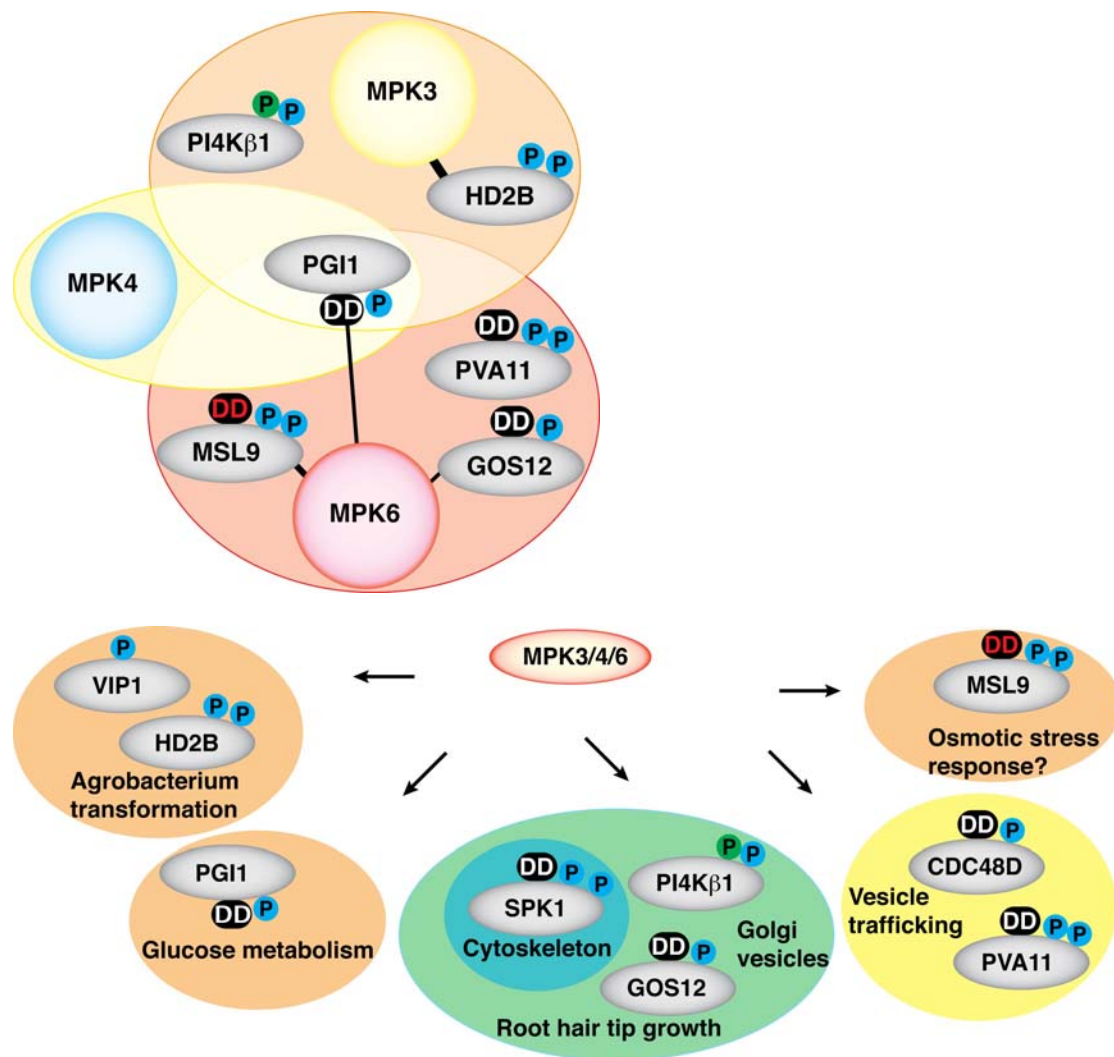


Figure 8

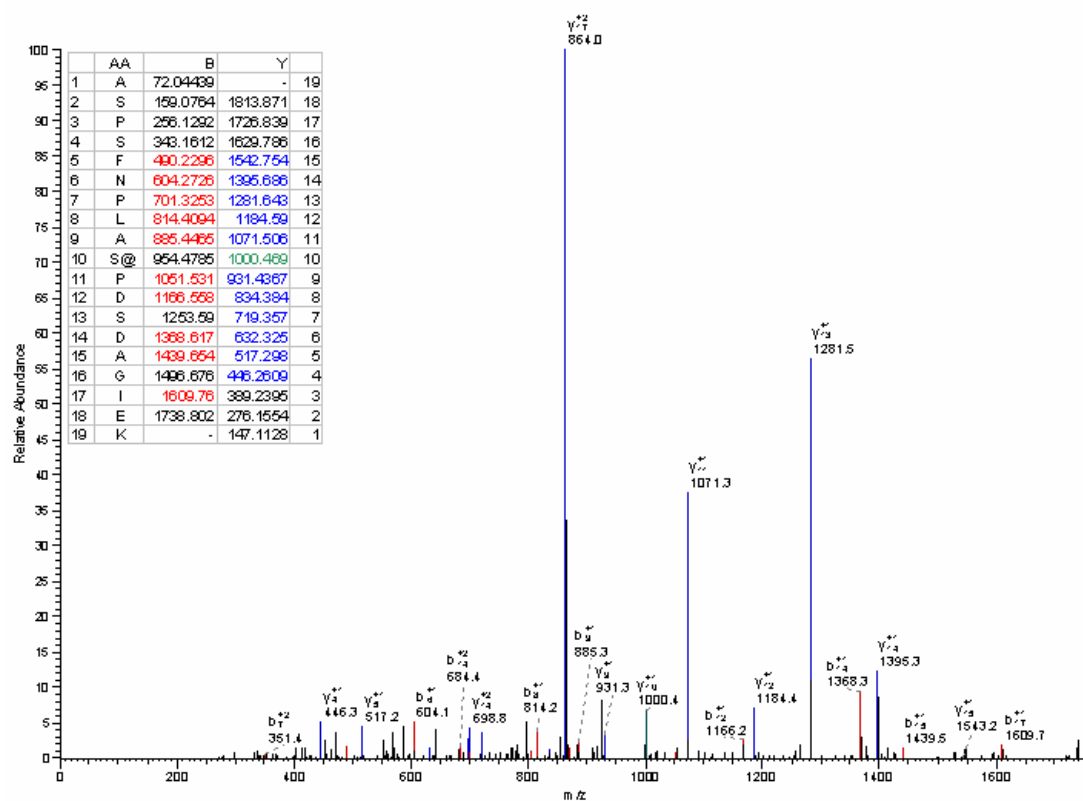


4.9 Supplemental Data

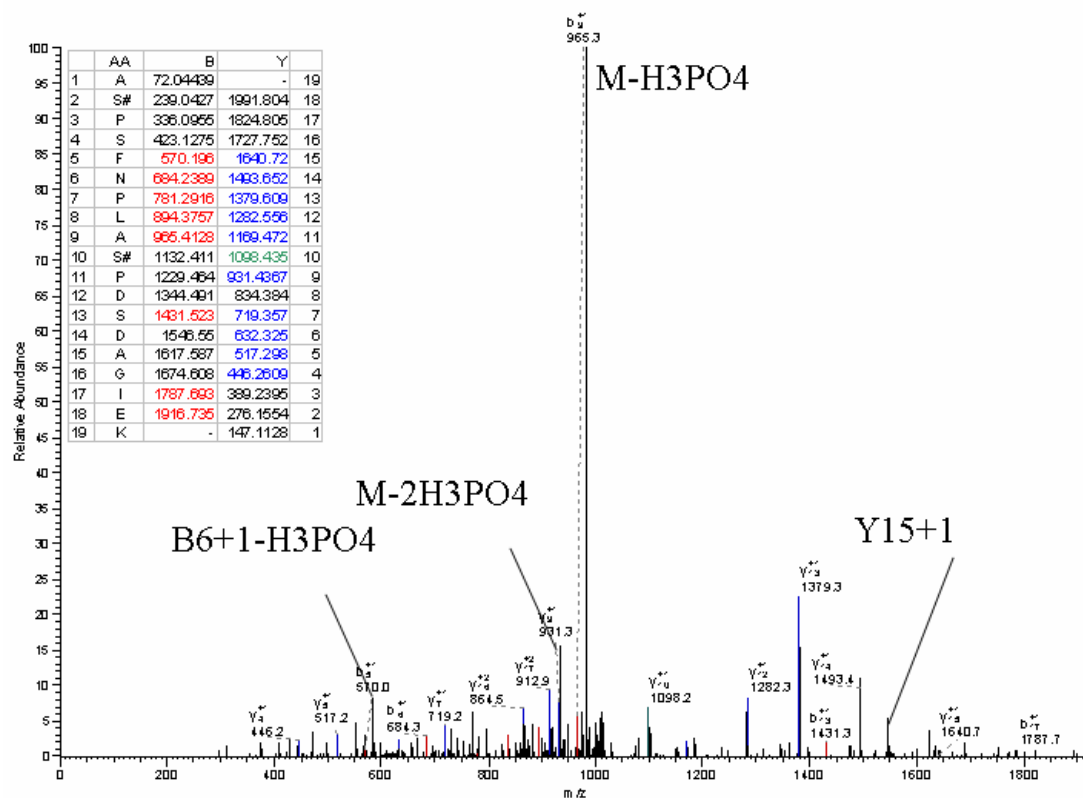
Supplemental Figure 1

MSL9 spectra

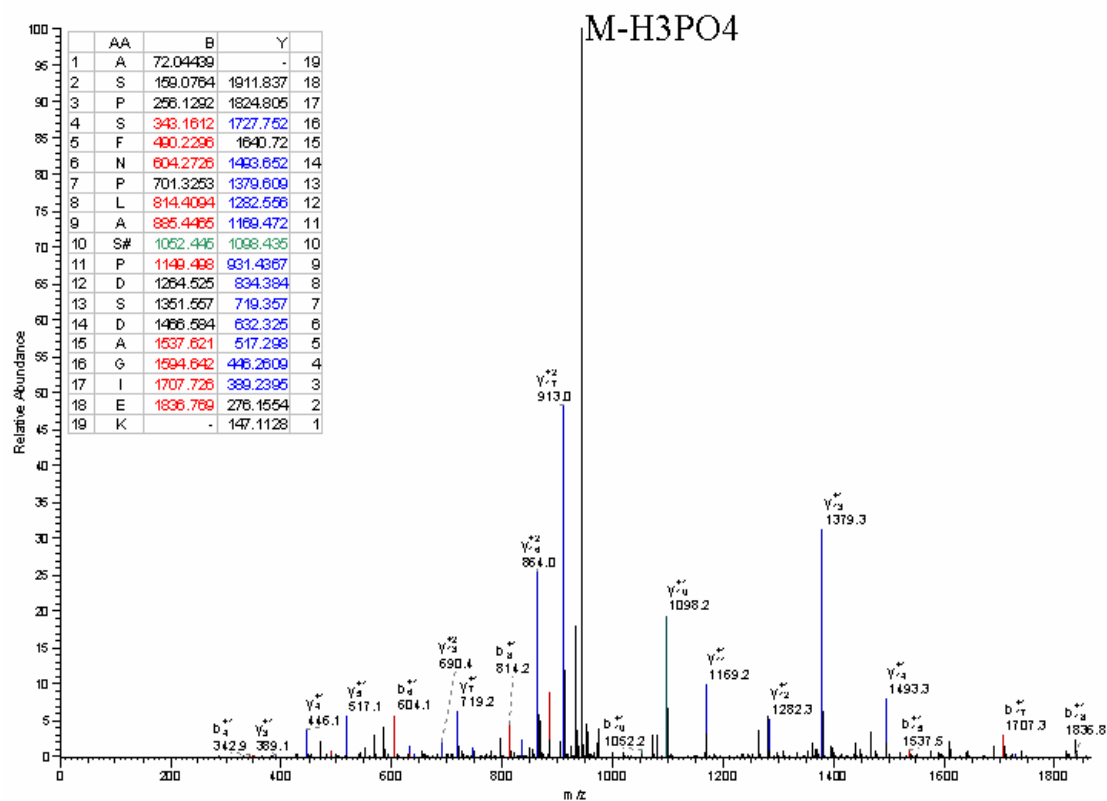
#13316-13316 NL:4.92E3



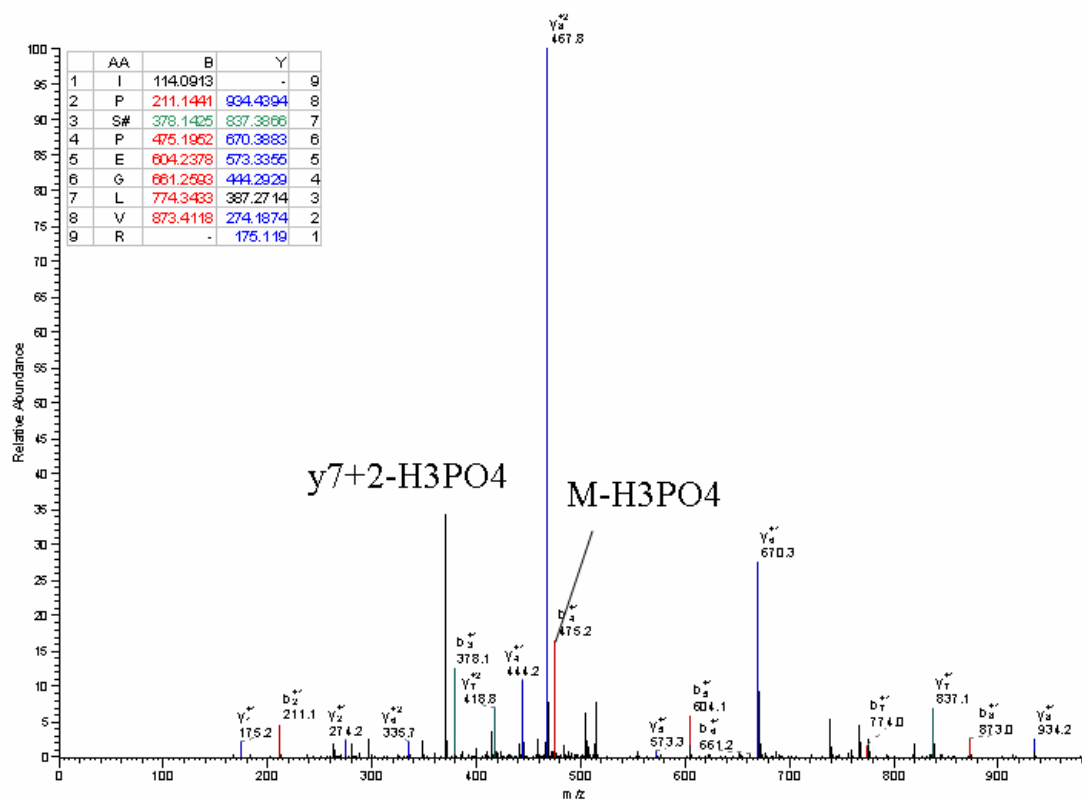
#14732-14732 NL:6.66E2



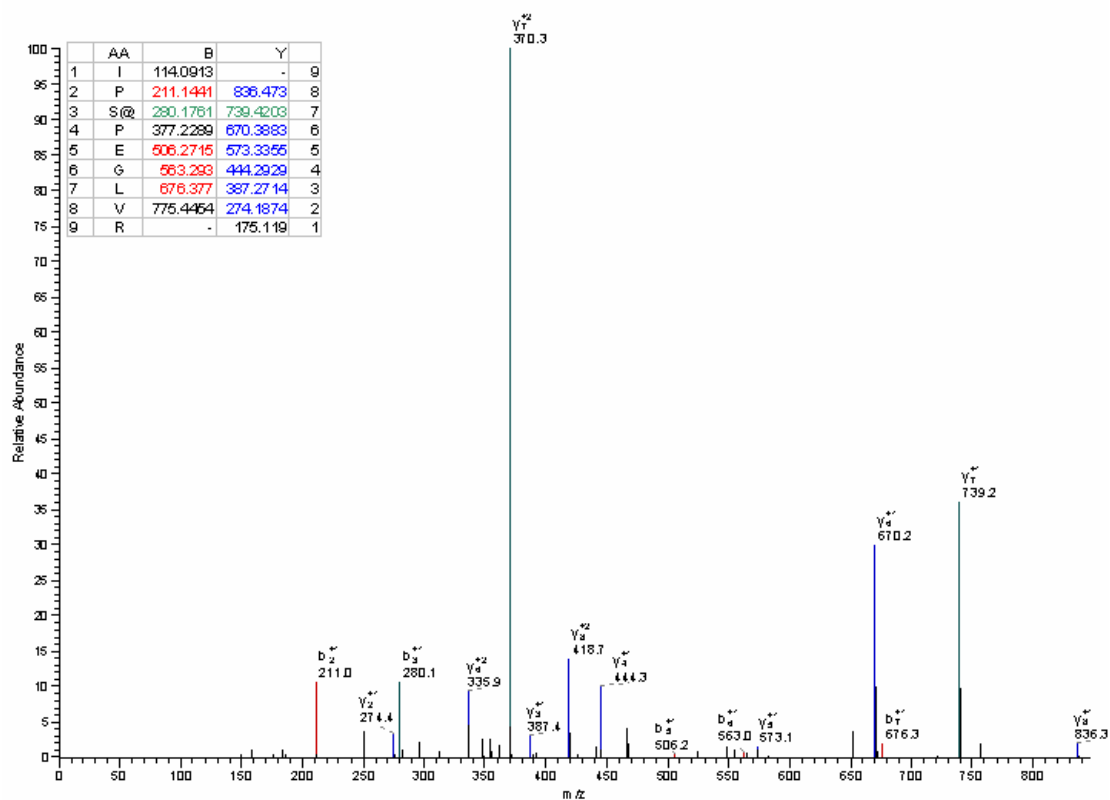
#13315-13315 NL:3.14E4



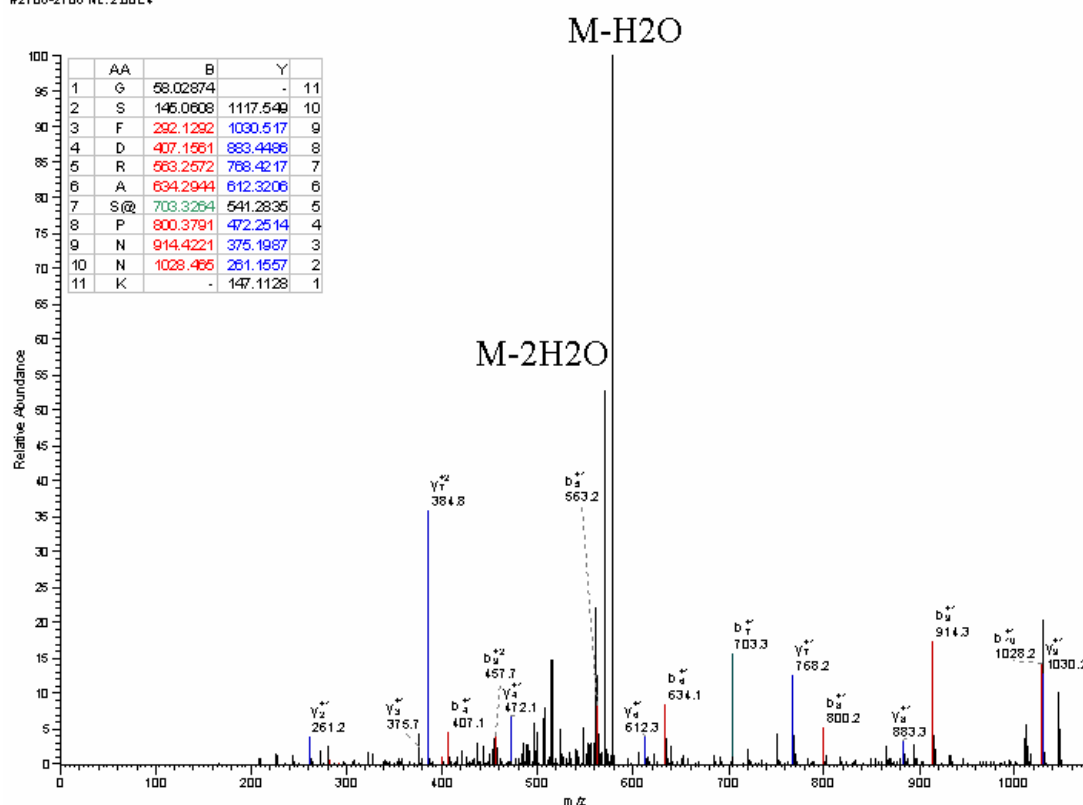
#11145-11146 NL:7.48E3



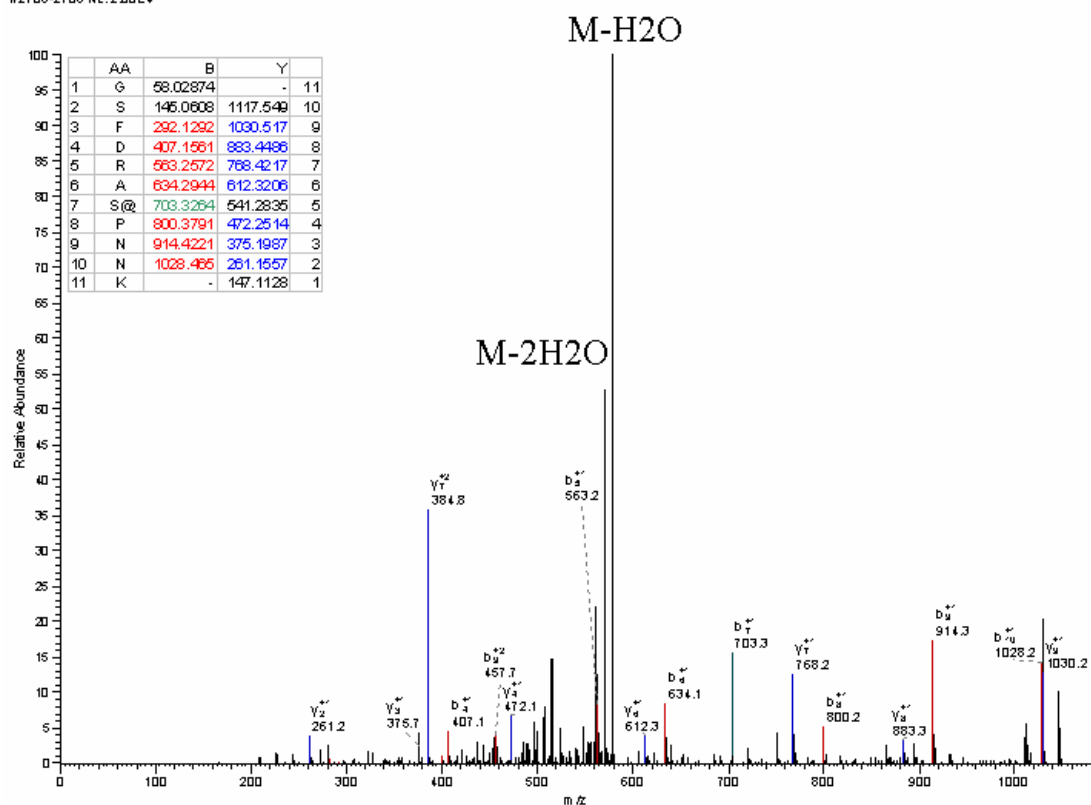
#11145-11146 NL:4.63E2



#27D6-27D6 NL:2.00E4

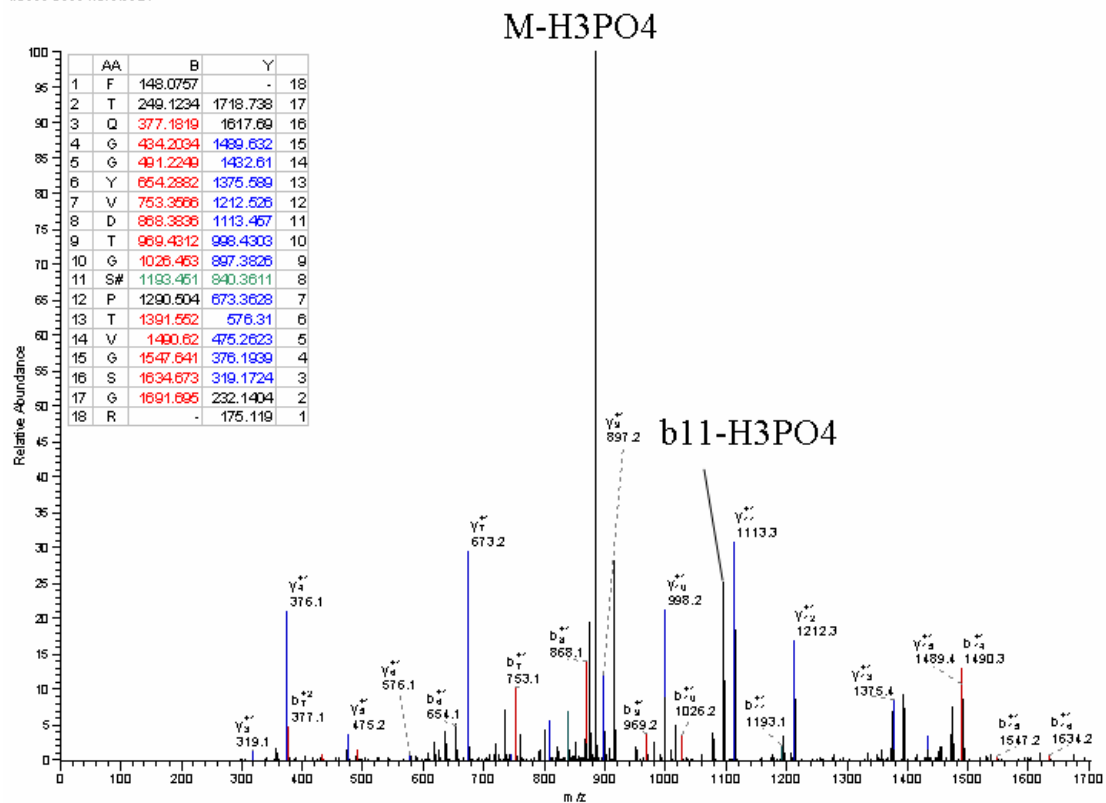


#27D6-27D6 NL:2.00E4

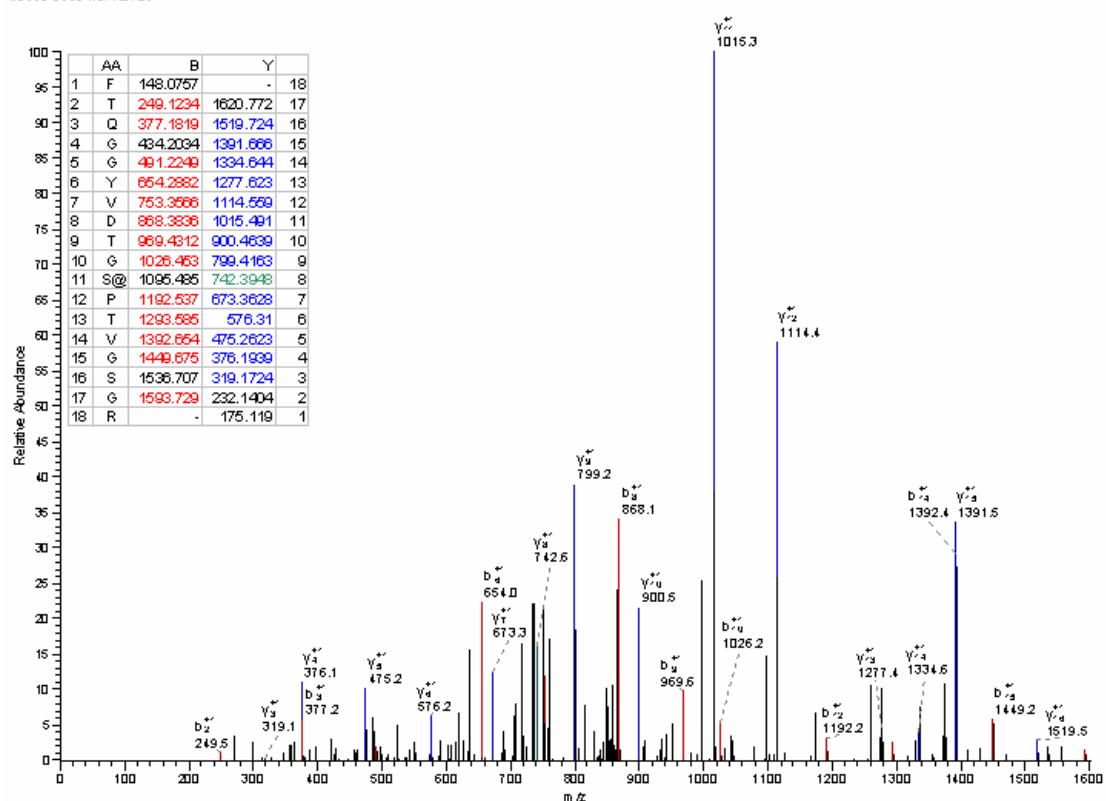


GOS12 spectra

#9688-9688 NL:6.65E4

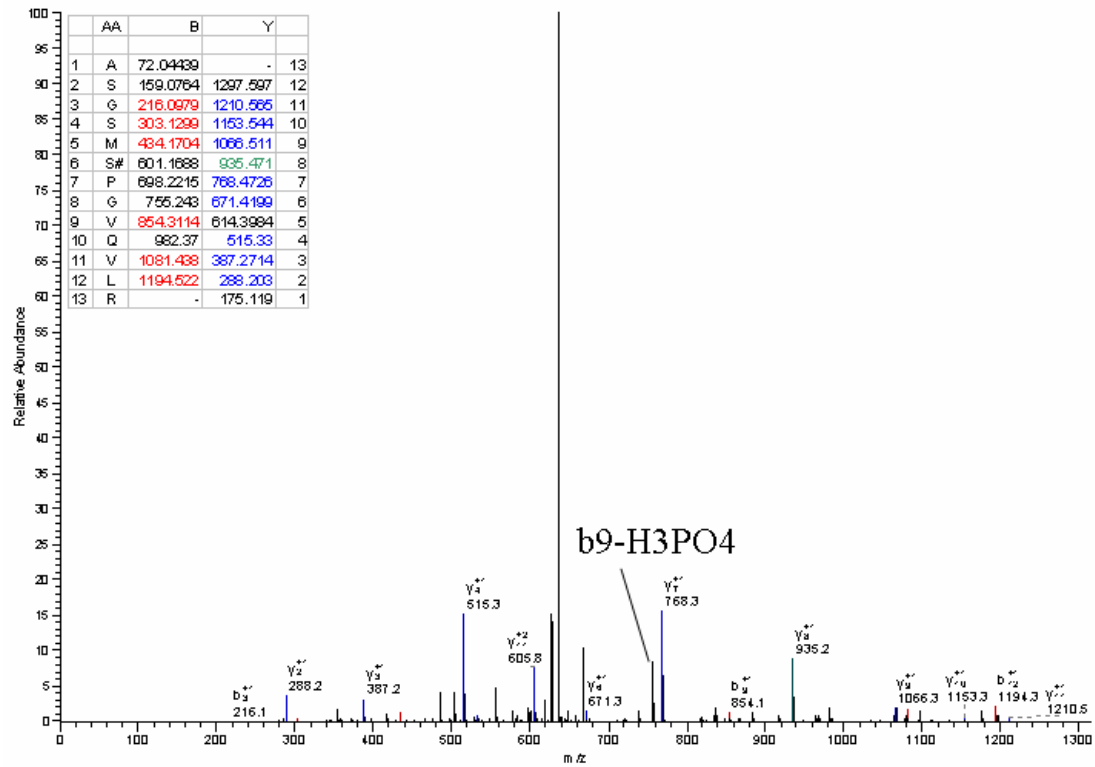


#9689-9689 NL:4.24E3

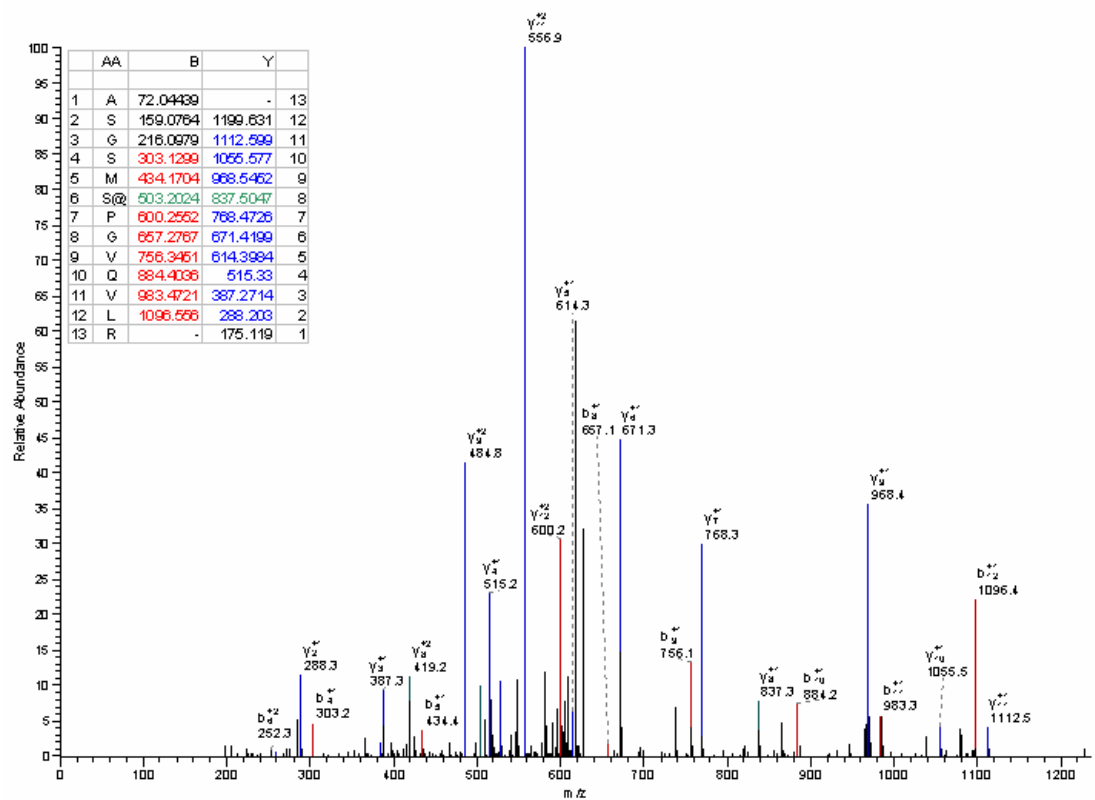


#10404-10404 NL:2.10E5

M-H3PO4

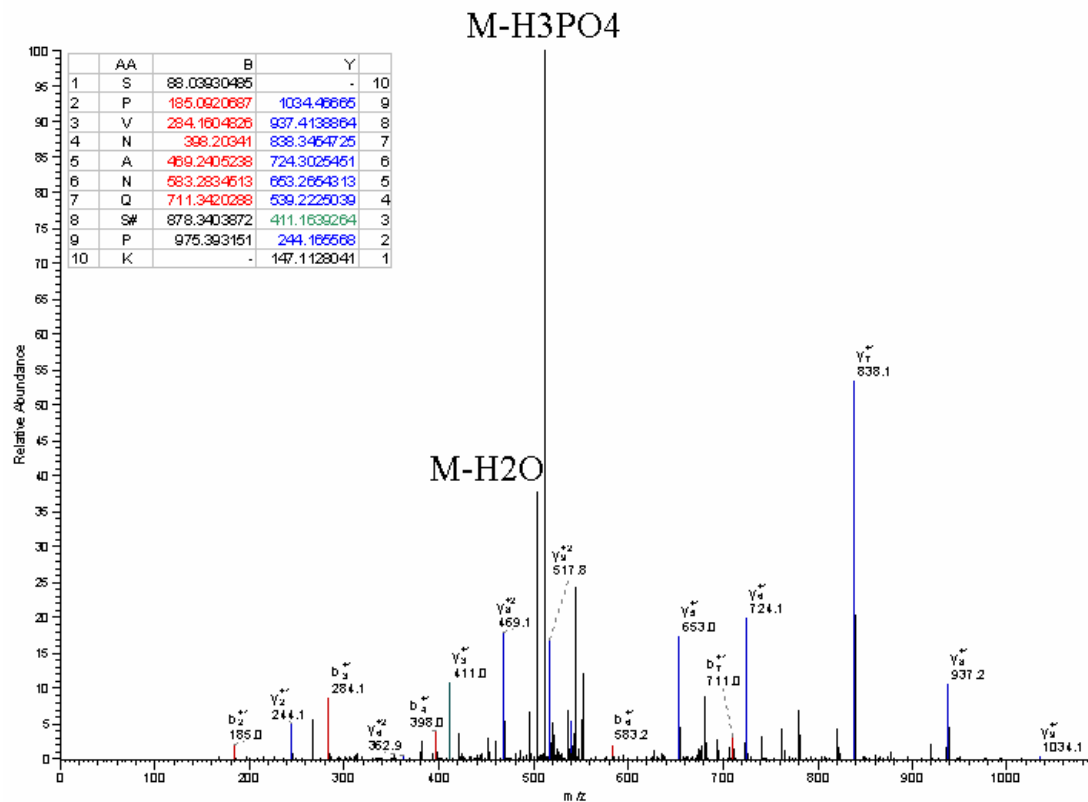


#10405-10405 NL:1.81E4

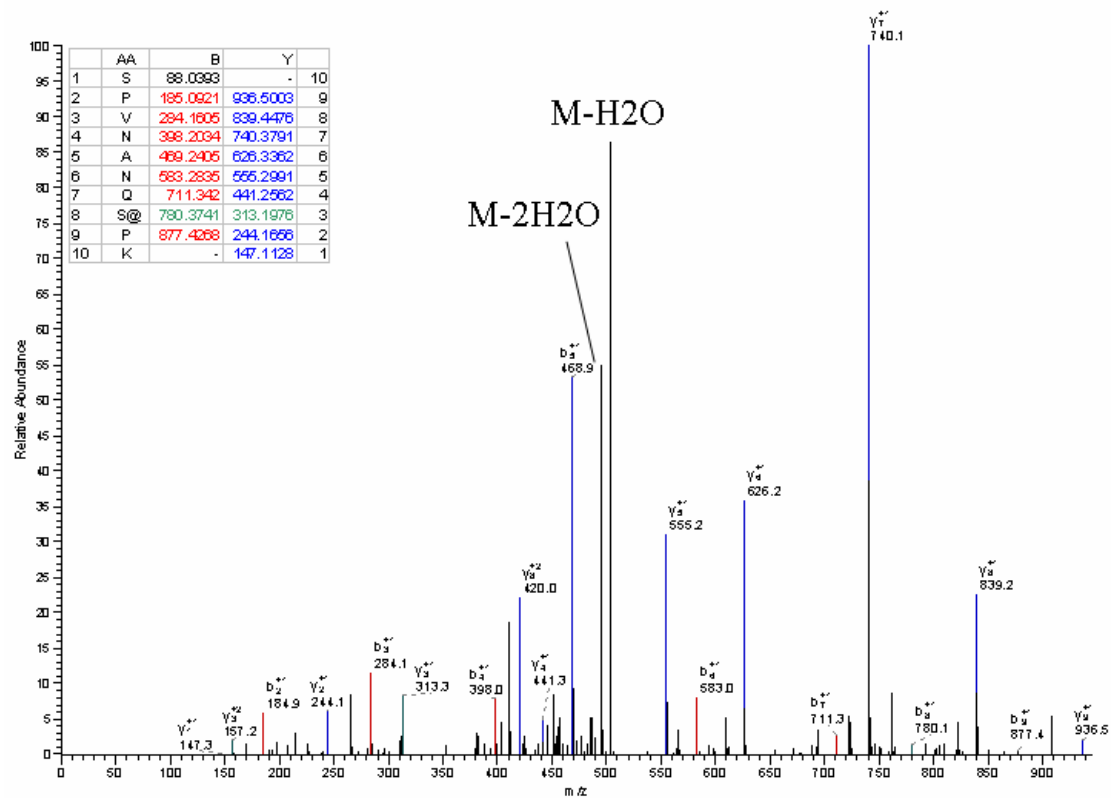


HD2B spectra

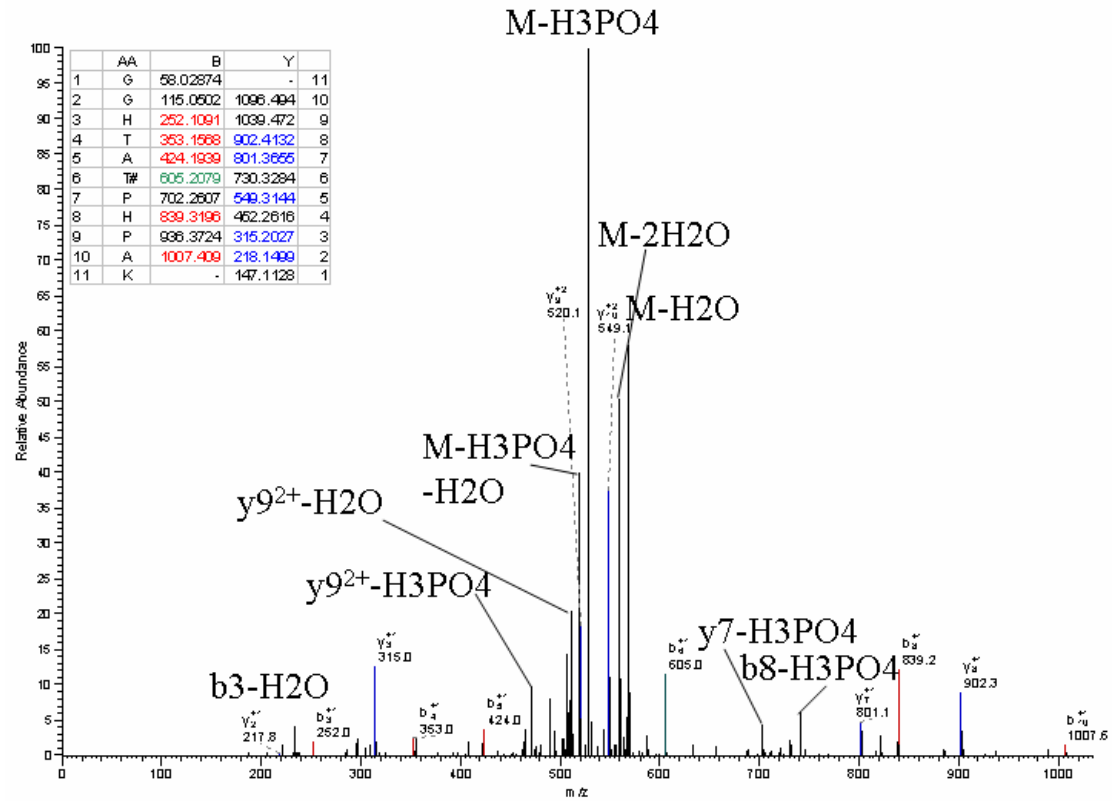
#2811-2811 NL:3.41E3



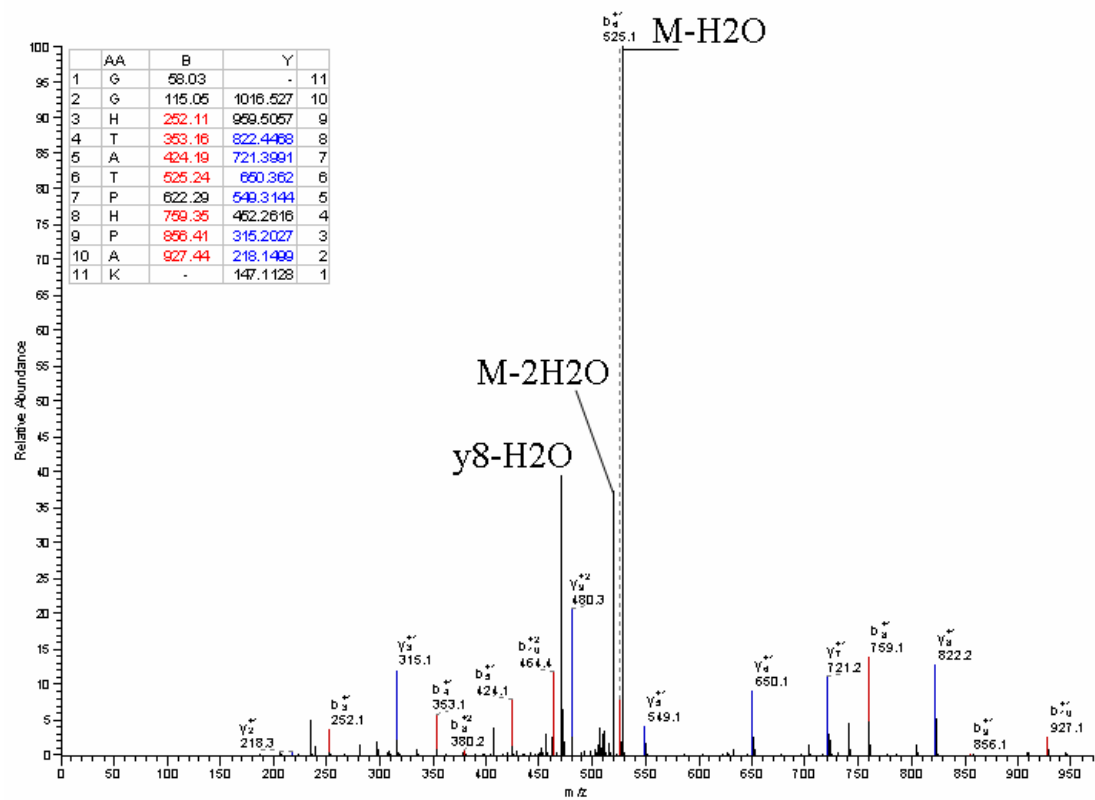
#2812-2812 NL:3.60E2



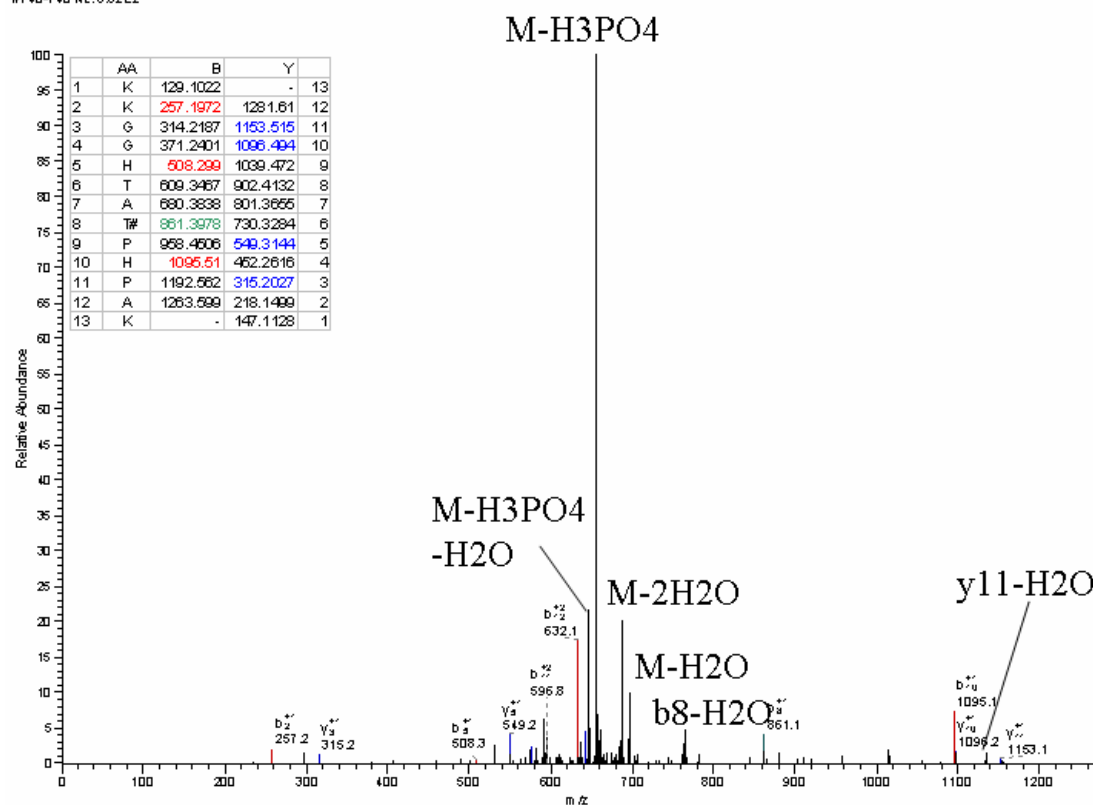
#1074-1074 NL:6.04E2



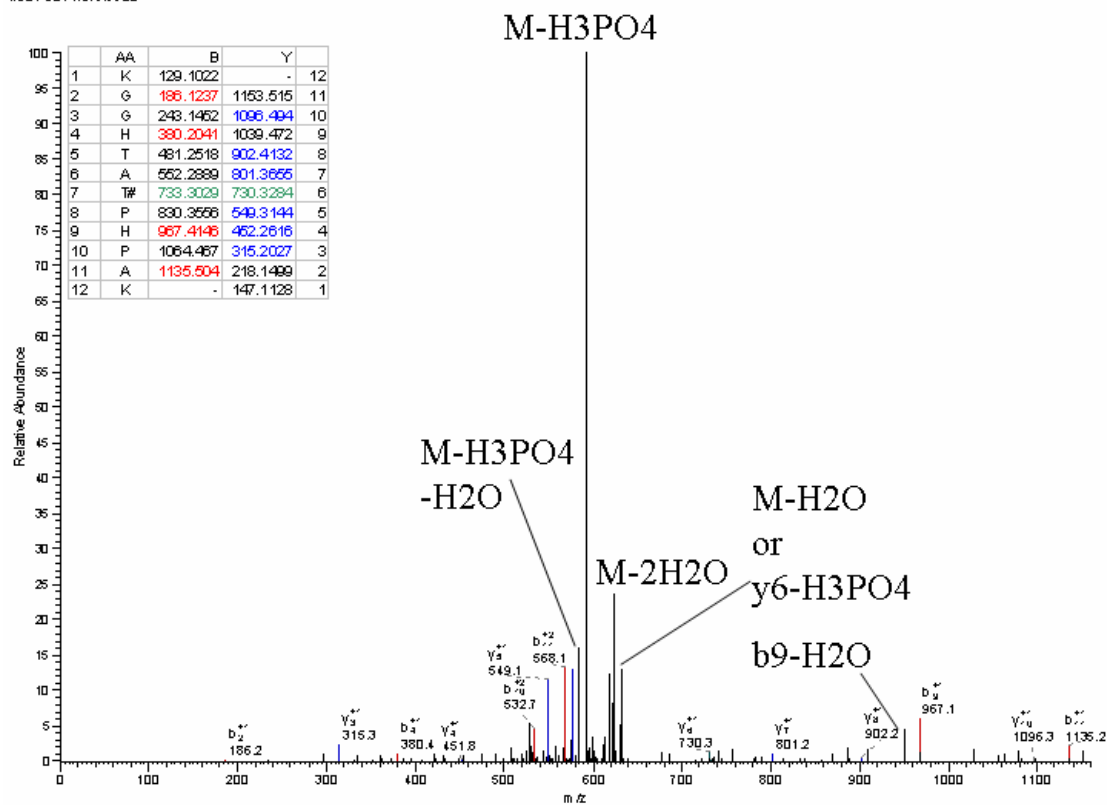
#1078-1078 NL:2.75E4



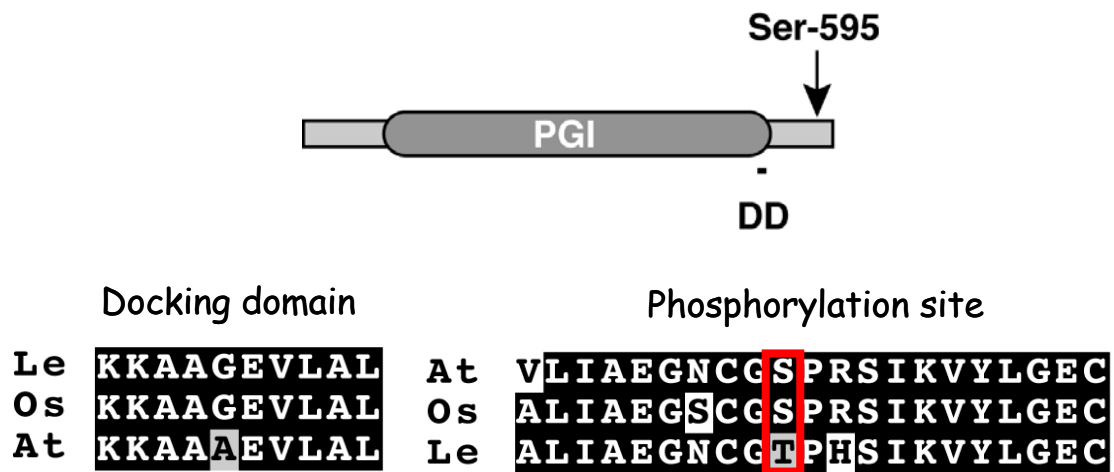
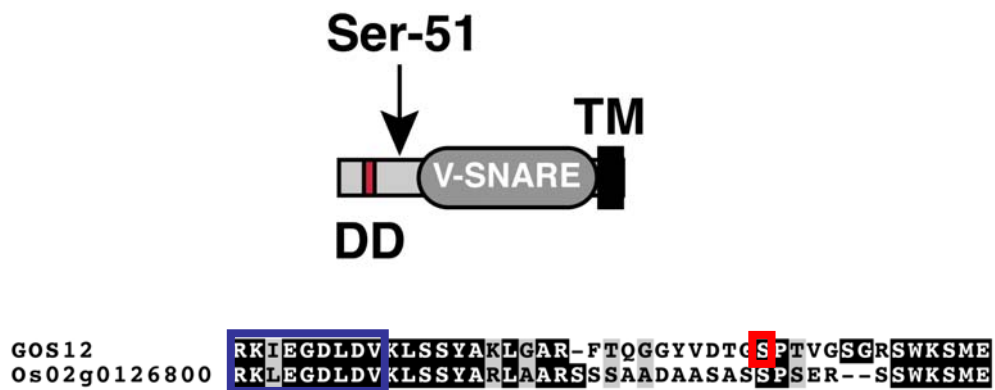
#740-740 NL:5.62E2



#904-904 NL:5.68E2



Supplemental Figure 2



Supplemental Table 1

	total SP/TP sites	proteins	with docking domain	
signalling	9	7	0	
trafficking	14	12	6	1 docking domain conserved in two homologues (PVA11 and PVA12)
ubiquitylation	3	3	0	
RNA metabolism	7	6	1	
chromatin remodelling and transcription	12	10	0	
protein folding and translation	2	2	1	
metabolic enzymes	14	12	1	
other	30	21	3	
total	91	73	12	

4.10 References

1. Bass RB, Strop P, Barclay M, Rees DC: **Crystal structure of Escherichia coli MscS, a voltage-modulated and mechanosensitive channel.** *Science* 2002, **298**: 1582-1587.
2. Benschop JJ, Mohammed S, O'Flaherty M, Heck AJ: **Quantitative phosphoproteomics of early elicitor signaling in Arabidopsis.** *Mol. Cell. Proteomics* 2007, **6**: 1198-1214.
3. Cardinale F, Jonak C, Ligterink W, Niehaus K, Boller T, Hirt H: **Differential activation of four specific MAPK pathways by distinct elicitors.** *J. Biol. Chem.* 2000, **24**: 36734-36740.
4. Chang CI, Xu BE, Akella R, Cobb MH, Goldsmith EJ: **Crystal structures of MAP kinase p38 complexed to the docking sites on its nuclear substrate MEF2A and activator MKK3b.** *Mol Cell.* 2002, **9**: 1241-1249.
5. Crane YM, Gelvin SB: **RNAi-mediated gene silencing reveals involvement of Arabidopsis chromatin-related genes in Agrobacterium-mediated root transformation.** *Proc Natl Acad Sci U S A.* 2007, **104**: 15156-15161.
6. De la Fuente van Bentem S, Anrather D, Roitinger E, Djamei A, Hufnagl T, Barta A, Csaszar E, Dohnal I, Lecourieux D, Hirt H: **Phosphoproteomics reveals extensive in vivo phosphorylation of Arabidopsis proteins involved in RNA metabolism.** *Nucleic Acid Res.* 2006, **34**: 3267-3278.
7. De la Fuente van Bentem S, Wieslawa IM, de la Fuente A, Hirt H: **Towards functional phosphoproteomics by mapping differential phosphorylation events in signaling networks.** *Proteomics* 2008, **8**: 4453-4465.
8. Djamei A, Pitzschke A, Nakagami H, Rajh I, Hirt H: **Trojan horse strategy in Agrobacterium transformation: abusing MAPK defense signaling.** *Science* 2007, **318**: 453-456.
9. Feilner T, Hultschig C, Lee J, Meyer S, Immink RGH, Koenig A, Possling A, Seitz H, Beveridge A, Scheel D, Cahill DJ, Lehrach H, Kreutzberger J, Kersten B: **High Throughput Identification of Potential Arabidopsis Mitogen-activated Protein Kinases Substrates.** *Mol. Cell. Proteomics* 2005, **4**: 1558-1568.
10. Haswell ES, Peyronnet R, Barbier-Brygoo H, Meyerowitz EM, Frachisse JM: **Two MscS homologs provide mechanosensitive channel activities in the Arabidopsis root.** *Curr Biol.* 2008, **18**: 730-734.
11. M Krishna, H. Narang: **The complexity of mitogen-activated protein kinases (MAPKs) made simple.** *Cell. Mol. Life Sci.* 2008, **65**: 3525 – 3544.
12. Linding R, Jensen LJ, Ostheimer GJ, van Vugt, MA *Et al.*: **Systematic discovery of in vivo phosphorylation networks.** *Cell* 2007, **129**: 1415-1426.
13. Nühse TS, Stensballe A, Jensen ON, Peck SC: **Phosphoproteomics of the Arabidopsis plasma membrane and a new phosphorylation site database.** *Plant Cell.* 2004, **16**: 2394-2405.

14. Nühse TS, Bottrill AR, Jones AM, Peck SC: **Quantitative phosphoproteomic analysis of plasma membrane proteins reveals regulatory mechanisms of plant innate immune responses.** *Plant J.* 2007, **51**: 931–940.
15. Mayor F Jr, Jurado-Pueyo M, Campos PM, Murga C: **Interfering with MAP kinase docking interactions: implications and perspective for the p38 route.** *Cell Cycle.* 2007, **6**: 528-533.
16. Matsuoka, S, Ballif BA, Smogorzewska A, McDonald ER: **ATM and ATR substrate analysis reveals extensive protein networks responsive to DNA damage.** *Science* 2007, **316**: 1160–1166.
17. Menges M, Hennig L, Gruissem W, Murray JA: **Genome-wide gene expression in an Arabidopsis cell suspension.** *Plant Mol Biol.* 2003, **53**: 423-442.
18. McNew JA, Coe JG, Søgaard M, Zemelman BV, Wimmer C, Hong W, Söllner TH: **Gos1p, a Saccharomyces cerevisiae SNARE protein involved in Golgi transport.** *FEBS Lett.* 1998, **435**: 89-95.
19. Merkouropoulos G, Andreasson A: **An Arabidopsis protein phosphorylated in response to microbial elicitation, atPHOS32, is a substrate of map kinase 3 and 6.** *J. Biol. Chem.* 2008, **283**: 10493-10499.
20. Joo S, Liu Y, Lueth A, Zhang S: **MAPK phosphorylation-induced stabilization of ACS6 protein is mediated by the non-catalytic C-terminal domain, which also contains the cis-determinant for rapid degradation by the 26S proteasome pathway.** *Plant J* 2008, **54**: 129-140.
21. Kramer A, Feilner T, Possling A, Radchuk V, Weschke W, Bürkle L, Kersten B: **Identification of barley CK2alpha targets by using the protein microarray technology.** *Phytochemistry.* 2004, **65**: 1777-1784.
22. Olsen JV, Blagoev B, Gnäd F, Macek B, Kumar C, Mortensen P, Mann M: **Global, in vivo, and site-specific phosphorylation dynamics in signaling networks.** *Cell.* 2006, **127**: 635-648.
23. Pandey R, Mueller A, Napoli CA, Selinger DA, Pikaard CS, Richards EJ, Bender J, Mount DW, Jorgensen RA: **Analysis of histone acetyltransferase and histone deacetylase families of Arabidopsis thaliana suggests functional diversification of chromatin modification among multicellular eukaryotes.** *Nucleic Acids Res.* 2002, **30**:5036-5055.
24. Pratelli R, Sutter JU, Blatt MR: **A new catch in the SNARE.** *Trends Plant Sci.* 2004, **9**: 187-95.
25. Preuss ML, Serna J, Falbel TG, Bednarek SY, Nielsen E: **The Arabidopsis Rab GTPase RabA4b localizes to the tips of growing root hair cells.** *Plant Cell.* 2004, **16**: 1589-1603.
26. Preuss ML, Schmitz AJ, Thole JM, Bonner HK, Otegui MS, Nielsen E: **A role for the RabA4b effector protein PI-4Kbeta1 in polarized expansion of root hair cells in Arabidopsis thaliana.** *J Cell Biol.* 2006, **172**: 991-998.

27. Pulvirenti T, Giannotta M, Capestrano M, Capitani M, Pisanu A, Polishchuk RS, San Pietro E, Bezoussenko GV, Mironov AA, Turacchio G, Hsu VW, Sallese M, Luini A: **A traffic-activated Golgi-based signalling circuit coordinates the secretory pathway.** *Nat Cell Biol.* 2008, **10**: 912-22.
28. Uemura T, Ueda T, Ohniwa RL, Nakano A, Takeyasu K, Sato MH: **Systematic analysis of SNARE molecules in Arabidopsis: dissection of the post-Golgi network in plant cells.** *Cell Struct Funct.* 2004, **29**: 49-65.
29. Ueno Y, Ishikawa T, Watanabe K, Terakura S, Iwakawa H, Okada K, Machida C, Machida Y: **Histone deacetylases and ASYMMETRIC LEAVES2 are involved in the establishment of polarity in leaves of Arabidopsis.** *Plant Cell.* 2007, **19**: 445-457.
30. Samaj J, Ovecka M, Hlavacka A, Lecourieux F, Meskiene I, Lichtscheidl I, Lenart P, Salaj J, Volkmann D, Bögre L, Baluska F, Hirt H: **Involvement of the mitogen-activated protein kinase SIMK in regulation of root hair tip growth.** *EMBO J.* 2002, **21**: 3296-3306.
31. Samaj J, Ovecka M, Hlavacka A, Lecourieux F, Meskiene I, Lichtscheidl I, Lenart P, Salaj J, Volkmann D, Bögre L, Baluska F, Hirt H: **Involvement of MAP kinase SIMK and actin cytoskeleton in the regulation of root hair tip growth.** *Cell Biol Int.*, 2003, **27**: 257-259.
32. Shevchenko A, Keller P, Scheffele P, Mann M, Simons K: **Identification of components of trans-Golgi network-derived transport vesicles and detergent-insoluble complexes by nanoelectrospray tandem mass spectrometry.** *Electrophoresis* 1997, **14**: 2591-2600.
33. Schweighofer A, Kazanaviciute V, Scheikl E, Teige M, Doczi R, Hirt H, Schwanninger M, Kant M, Schuurink R, Mauch F, Buchala A, Cardinale F, Meskiene I: **The PP2C-type phosphatase AP2C1, which negatively regulates MPK4 and MPK6, modulates innate immunity, jasmonic acid, and ethylene levels in Arabidopsis.** *Plant Cell.* 2007, **19**: 2213-2224.
34. Stokes MP, Rush J, Macneill J, Ren JM: **Profiling of UV-induced ATM/ATR signaling pathways.** *Proc. Natl. Acad. Sci. USA* 2007, **104**: 19855-19860.
35. Stulemeijer IJ, Stratmann JW, Joosten MH: **Tomato mitogen-activated protein kinases LeMPK1, LeMPK2, and LeMPK3 are activated during the Cf-4/Avr4-induced hypersensitive response and have distinct phosphorylation specificities.** *Plant Physiol.* 2007, **144**: 1481-1494.
36. Sugiyama N, Nakagami H, Mochida K, Daudi A, Tomita M, Shirasu K, Ishihama Y: **Large-scale phosphorylation mapping reveals the extent of tyrosine phosphorylation in Arabidopsis.** *Mol Syst Biol.* 2008, **4**: 193.
37. Zhou C, Labbe H, Sridha S, Wang L, Tian L, Latoszek-Green M, Yang Z, Brown D, Miki B, Wu K: **Expression and function of HD2-type histone deacetylases in Arabidopsis development.** *Plant J.* 2004, **38**: 715-724.

V. Previous projects

The Dark Side of the Salad: *Salmonella typhimurium* Overcomes the Innate Immune Response of *Arabidopsis thaliana* and Shows an Endopathogenic Lifestyle

Adam Schikora¹, Alessandro Carreri², Emmanuelle Charpentier³, Heribert Hirt^{1,2*}

1 Unité de Recherche en Génomique Végétale, Institut National de la Recherche Agronomique/Centre National de la Recherche Scientifique/University of Evry Val d'Essonne, Evry, France, **2** Department of Plant Molecular Biology, Max F. Perutz Laboratories, Vienna, Austria, **3** Department of Microbiology and Immunobiology, Max F. Perutz Laboratories, Vienna, Austria

Abstract

Salmonella enterica serovar *typhimurium* contaminated vegetables and fruits are considerable sources of human infections. Bacteria present in raw plant-derived nutrients cause salmonellosis, the world wide most spread food poisoning. This facultative endopathogen enters and replicates in host cells and actively suppresses host immune responses. Although *Salmonella* survives on plants, the underlying bacterial infection mechanisms are only poorly understood. In this report we investigated the possibility to use *Arabidopsis thaliana* as a genetically tractable host system to study *Salmonella*-plant interactions. Using green fluorescent protein (GFP) marked bacteria, we show here that *Salmonella* can infect various *Arabidopsis* tissues and proliferate in intracellular compartments. *Salmonella* infection of *Arabidopsis* cells can occur via intact shoot or root tissues resulting in wilting, chlorosis and eventually death of the infected organs. *Arabidopsis* reacts to *Salmonella* by inducing the activation of mitogen-activated protein kinase (MAPK) cascades and enhanced expression of pathogenesis related (*PR*) genes. The induction of defense responses fails in plants that are compromised in ethylene or jasmonic acid signaling or in the MKK3-MPK6 MAPK pathway. These findings demonstrate that *Arabidopsis* represents a true host system for *Salmonella*, offering unique possibilities to study the interaction of this human pathogen with plants at the molecular level for developing novel drug targets and addressing current safety issues in human nutrition.

Citation: Schikora A, Carreri A, Charpentier E, Hirt H (2008) The Dark Side of the Salad: *Salmonella typhimurium* Overcomes the Innate Immune Response of *Arabidopsis thaliana* and Shows an Endopathogenic Lifestyle. PLoS ONE 3(5): e2279. doi:10.1371/journal.pone.0002279

Editor: David M. Ojcius, University of California Merced, United States of America

Received: February 26, 2008; **Accepted:** March 23, 2008; **Published:** May 28, 2008

Copyright: © 2008 Schikora et al. This is an open-access article distributed under the terms of the Creative Commons Attribution License, which permits unrestricted use, distribution, and reproduction in any medium, provided the original author and source are credited.

Funding: Austrian Science Fund, Centre National de Recherche France

Competing Interests: The authors have declared that no competing interests exist.

* E-mail: Heribert.Hirt@evry.inra.fr

Introduction

Salmonella enterica serovar *typhimurium* (*S. typhimurium*) is a facultative endopathogen and the causative agent of various human diseases ranging from enteritis to typhoid fever. It is responsible for salmonellosis, which is the most frequent food-borne disease with around 1.5 billion yearly infections world wide (WHO). Disease in mammals occurs after consumption of contaminated food or water. Systemic infection can follow, which depends on the ability of the bacteria to survive the harsh conditions of the gastric tract before crossing the intestinal epithelium. Owing to its importance, the mechanism of *Salmonella* invasion of human cells is under intense study. Two *Salmonella* pathogenicity islands (SPI-1 and SPI-2) encoding structural elements of type III secretion systems (T3SS) and effectors injected into the host cells, are necessary for entry and proliferation within mammalian cells [1]. Infection occurs in several well-organized and adjusted steps. The first one includes docking of *Salmonella* to the epithelial cell and injection of SPI-1 encoded effectors, which suppress the host immune system and modify the actin and tubulin cytoskeleton [2]. Endocytosis is the second step and requires formation of *Salmonella* Containing Vacuoles (SCVs). Retainment of SCVs in the host cytoplasm is assured by SPI-2 encoded

effectors [3] and strains not capable to sustain intact SCVs are avirulent [4].

Salmonella-contaminated vegetables and fruits were recently identified as a widespread source of human infection [5]. Although diverse plant species support growth of *Salmonella* [6], the underlying molecular mechanisms of the *Salmonella*-plant interaction are largely unknown.

The plant immune system functions at different levels during pathogen attack. Pathogen-associated molecular patterns (PAMPs) and effectors injected into plant cells, trigger activation of defence mechanisms [7,8,9,10]. PAMPs are recognized by plant receptors and trigger a defence mechanism referred to as “basal” defence [11]. On the other hand, pathogens have developed mechanisms to overcome detection by injecting effectors into plant cells, which interfere with signalling cascades and thereby abolish basal defence response. In some cases, pathogen effectors can be recognized by plant resistance proteins (R proteins), triggering a hypersensitive response (HR) and thereby limit pathogen infection [12]. Systemic acquired resistance (SAR) represents another level of defence resulting in resistance to a broad spectrum of pathogens throughout the plant [13]. SAR requires signal molecules activating the expression of pathogenesis-related (*PR*) genes and salicylic acid (SA), jasmonic acid (JA) and ethylene (ET) are

involved in regulating their expression. These molecules play important roles in the induction of plant defence responses upon pathogen attack and are implicated in different forms of resistance [14,15]. While SA-dependent pathways are generally important in defence against biotrophic pathogens and lead to hypersensitive response (HR) and/or local resistance [13], JA and ET pathways seem to be involved in defence mechanisms against herbivore attack and necrotrophic pathogens [16].

Mitogen-activated protein kinase (MAPK) cascades play a crucial role in mediating defence responses to plant pathogen attack [17]. In *Arabidopsis*, MPK3 and MPK6 are activated by different bacterial elicitors [18,19] and trigger enhanced expression of *PR* genes [7,20]. Silencing of *MPK6* results in compromised resistance to plant pathogens [21]. MEKK1, MKK4/5, MPK3/6/4 were identified downstream of the FLS2 receptor recognizing bacterial flagellin [7] and are also involved in regulating reactive oxygen species (ROS) production [22,23,24]. Recently, MKK3 was shown to have a dual function; activating either MPK6 in response to JA signalling [25], or MPK7 in response to ROS and plant pathogens [26].

Comparing the defence response to classical plant pathogens, the response to human pathogens is much less understood. The human pathogen *S. aureus* triggers SA-dependent defence responses in *Arabidopsis* plants [27] and its spreading can be diminished by SA treatment. In addition, the SA-depleted isochlorismate synthase defective *ics1* mutants and transgenic *Arabidopsis* lines, overexpressing the bacterial SA hydroxylase (*NahG*), are hypersensitive to *S. aureus* infection [27]. Recently, it was reported that treating plants with the ethylene precursor ACC, significantly diminishes colonization of *Medicago sativa* and *Arabidopsis* by *Klebsiella pneumoniae* or *Salmonella* [28].

The present study shows that the human pathogen *S. typhimurium* triggers the activation of plant immune responses including enhanced transcription of *PR* genes. We show that *Salmonella* can overcome plant defence mechanisms and enter and proliferate inside various *Arabidopsis* tissues, causing wilting and chlorosis as disease symptoms. Among different possible immune responses of *Arabidopsis*, the ET- and JA-dependent signalling pathways were found of major importance for inducing defence responses during *S. typhimurium* infection. Moreover, the JA-mediating MKK3-MPK6 MAPK pathway was identified to be essential for restricting *Salmonella* proliferation and disease in *Arabidopsis* plants. Our results indicate that *Arabidopsis* can serve as a valuable model system to study *Salmonella*-host interaction, suggesting the necessity to modify agricultural practices to improve food safety.

Results

Salmonella is pathogenic to Arabidopsis

Three different types of experiments were performed to assess the question whether *Salmonella* can actively invade, proliferate and spread through plants. To test whether *Salmonella* is capable to proliferate inside plants, whole rosettes of *Arabidopsis thaliana* Col-0 wild-type plants were vacuum-infiltrated with *S. typhimurium* wild-type strain 14028s and the internal bacterial population was then counted over the following four days. The number of colony forming units (cfu) in discs excised from infiltrated leaves drastically increased over the first 2 days before reaching plateau levels (Fig. 1a). Two weeks after dipping the plants in bacterial solutions, invasion of *Salmonella* into *Arabidopsis* caused a defined disease phenotype as revealed by severe chlorosis and wilting of leaves (Fig. 1c–d). To evaluate whether *Salmonella* is also able to actively recognize and invade *Arabidopsis*, liquid media in which

Arabidopsis seedlings were immersed, were inoculated with bacteria. Over the following days, the bacterial population inside seedlings was monitored after surface-sterilization and homogenisation of the seedlings (Fig. 1b). A 40-fold increase in cfu of internal bacteria was observed over a period of 2 days (Fig. 1b). Altogether these results indicate that *Salmonella* can actively invade and proliferate in *Arabidopsis* plants and cause disease.

Most pathogenic bacteria can spread through susceptible host plants very rapidly. We investigated whether *Salmonella* can also systemically infect plants. For this purpose we selectively infected roots with *Salmonella* and analyzed its presence in leaves two weeks later. While bacteria were growing on and in *Arabidopsis* roots two weeks after infection, we were not able to detect *Salmonella* in leaf homogenates from these plants (data not shown). Alternatively, to determine whether *Salmonella* can spread from leaf-to-leaf, we syringe-infiltrated single leaves and monitored the presence of bacteria in non-infiltrated neighbouring leaves two weeks later. Although *Salmonella* effectively infected single leaves, no bacteria were detected in non-infiltrated neighbouring leaves (Fig. S1). These data indicate that *S. typhimurium* is not able to spread to other non-exposed parts of the *Arabidopsis* plant, suggesting that *Salmonella* cannot migrate via the xylem (root-to-shoot) nor via the phloem (leaf-to-leaf) systems.

From the epidemiological standpoint, it is important to know the duration of *Salmonella* persistence in infected plants. We therefore determined how long *Salmonella* could stay alive in *Arabidopsis* plants. For this purpose, whole rosettes of three weeks old *Arabidopsis* plants were vacuum-infiltrated and the presence of internal bacteria was monitored over the period of one month. Although the infiltrated leaves died within 5 days, apical meristems survived the infection and produced new leaves. One month after infiltration, newly formed leaves contained significant albeit much lower *Salmonella* cfu, possibly indicating that meristems are poor *Salmonella* targets or that meristematic tissues are particularly resistant to bacterial infection (Fig. S2).

Endopathogenic lifestyle of Salmonella in Arabidopsis

In animals and humans, *Salmonella* actively enters epithelial and other cells in order to replicate and spread through the organism. We focused our attention on the question whether, similar to the situation in mammals, *Salmonella* can also invade plant cells. For this purpose, *S. typhimurium* was transformed with a plasmid constitutively expressing green fluorescent protein (GFP) [29]. Three hours post-inoculation of liquid medium with immersed seedlings, GFP-marked *Salmonella* were localized inside root hairs (Fig. 1e) and at 20 hours post-inoculation, inside rhizodermal cells (Fig. 1f–g). At this time point, large numbers of motile bacteria were observed inside single host cells, confirming that *Salmonella* can proliferate in plant cells. To our knowledge, this is the first report of an infection of the plant cytoplasm by a human enteropathogen. *Salmonella* was also found to form biofilm-like structures on the surface of roots and leaves, preferentially colonizing regions around emerging lateral roots and wounded tissues (data not shown). To extend our *in planta* observations to the single cell level, inoculation experiments were also performed using *Arabidopsis* protoplasts. Probably due to the high sucrose concentration in the medium, infection rates in this system were low. However, protoplasts were clearly invaded by GFP-marked *Salmonella* within 3 hours (Fig. 1h). Optical Z-stacking allowed the exact positioning of the GFP-marked *Salmonella* to the cytoplasmic compartment of infected protoplasts (Fig. S3). These data demonstrate that *Salmonella* has the ability to enter and proliferate inside plant cells.

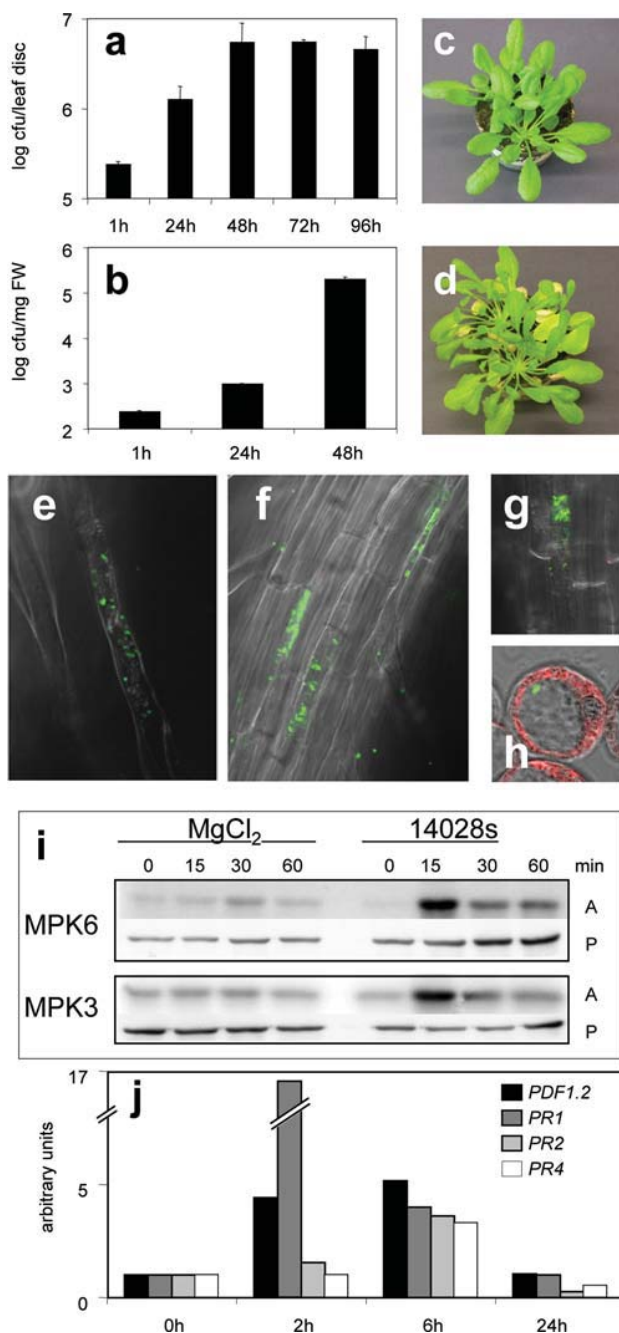


Figure 1. *Salmonella* can invade and grow in *Arabidopsis* cells and induce plant innate defence mechanisms. **a–b**, Three weeks old *A. thaliana* plants were vacuum-infiltrated (a) and 14 days old *A. thaliana* seedlings were incubated in medium inoculated (b) with *S. typhimurium* wild type 14028s. Proliferation of *Salmonella* was analyzed over a period of 4 (a) and 2 (b) days by determination the cfu of internal bacteria in homogenates of leaf discs (a) or seedlings (b). **c–d**, Disease symptoms after dipping in *Salmonella*. Three weeks old *A. thaliana* plants were dipped for 5 min in *S. typhimurium* 14028s solution and macroscopic changes were observed over a 2 weeks period, c: before dipping, d: 14 days after dipping in bacterial solution. **e–h**, *Salmonella* enters plant cells. GFP marked *S. typhimurium* 14028s were localized in *A. thaliana* root cells after 3 (e) or 20 h (f, g). **h**; 3 h after infection, cell culture protoplasts contain bacterial cells. Images were taken using a confocal microscope with 488 nm excitation and 505–530 nm emission filters. **i**, Treatment with *Salmonella* induces MPK3 and MPK6 kinase activities. Two weeks old *A. thaliana* seedlings were treated with either

10 mM MgCl₂ or *S. typhimurium* 14028s. Endogenous MPK6 was immunoprecipitated from total protein extraction. Myelin basic protein (MBP) was used as substrate. A, activity; P, protein amounts were detected by Western blotting with antibodies specific for MPK3/6. **j**, Treatment with *Salmonella* induces defence responses. 14 days old *A. thaliana* seedlings were treated with *S. typhimurium* 14028s. Quantitative RT-PCR analysis was performed on 5 µg reverse transcribed total mRNA; *clathrin*, *ubiquitin4* and *actin2* were used for normalization. doi:10.1371/journal.pone.0002279.g001

Arabidopsis induces defence responses upon infection with *S. typhimurium*

Under normal conditions, plants react to pathogens by activating various defence responses, thereby diminishing the proliferation of bacteria, fungi or viruses. We tested whether plants recognize *Salmonella* as a pathogen and actively induce defence responses in order to limit infection, as observed with other bacterial plant pathogens [30]. In *Arabidopsis*, a variety of PAMPs were shown to activate the MAPKs: MPK3 and MPK6 [18,19], followed by the transcription of a number of *PR* genes [7,20]. To determine whether these defence responses also occur upon *S. typhimurium* infection, we used MPK3 and MPK6 specific antibodies to analyze the activation of these kinases in seedlings exposed to *Salmonella*. The activities of both MPK3 and MPK6 strongly increased at 15 min after contact with the bacteria (Fig. 1i). To examine whether recognition of *Salmonella* results in activation of other MAPKs, the activities of 9 MAPKs, representing all 4 phylogenetic groups of the MAPK family in *Arabidopsis* [31], were analyzed after infection of protoplasts with *S. typhimurium*. From the nine investigated kinases, only MPK3 and MPK6 showed activation, confirming our previous *in planta* results. Activities of two other MAPKs; MPK2 and MPK17 were reduced (Fig. 2). Interestingly, *Arabidopsis* appeared to sense multiple *Salmonella* PAMPs, because *S. typhimurium* 14028s infection of an *A. thaliana* *fls2–17* mutant, which is defective in flagellin perception [20], still resulted in MPK6 activation (Fig. 3).

To study the role of the plant innate immune system during *Salmonella* infection in more detail, we turned our attention to the SA-, JA-, and ET-dependent signalling pathways. To clarify their role during infection of *Arabidopsis* with *Salmonella*, quantitative RT-PCR analysis of marker genes for SA-, JA- and ET-dependent defence gene expression was performed. *PDF1.2*, encoding an antifungal defensin, is commonly used as a marker for JA- and ET-induced resistance [32]. In *A. thaliana* Col-0 infected with *Salmonella*, expression of the *PDF1.2* gene increased rapidly during the first 6 h (Fig. 1j). Expression of other JA-regulated genes, such as *PR2* and *PR4* [33] as well as the SA marker *PR1* gene were also induced during *Salmonella* infection (Fig. 1j, Fig. 4). These results show that *Arabidopsis* reacts to *Salmonella* infection by activating multiple defence pathways of the innate immune system.

JA- and ET-dependent signalling pathways are involved in resistance against *S. typhimurium*

It was previously shown that lack of SA promotes and that treatment with the ethylene precursor ACC lowers *Salmonella* colonization of plants [28]. Therefore, we investigated whether defects in any of the three signalling pathways affect *Salmonella*'s ability to infect *Arabidopsis* plants. We performed infection experiments with SA depleted *NahG* plants [34], *ein2* (ethylene insensitive 2) [35] and *coi1* (coronatine insensitive 1) [36,37] mutant plants compromised in either the ET or JA signalling pathways, respectively. Liquid media with immersed seedlings were inoculated with *S. typhimurium* for 48 hours before determination of cfu of the internal bacteria. When compared with wild type *A.*

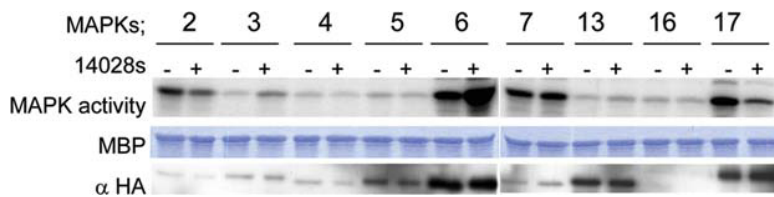


Figure 2. Activation of MAP kinases transiently expressed in protoplasts. MPK3 and MPK6 are activated and MPK2 and MPK17 are inhibited upon infection with *Salmonella*. Nine of 20 MAPKs were expressed in cell culture derived protoplasts for 24 h and protoplasts were exposed to bacteria for 20 min. All MAPKs were expressed as HA-tagged versions and immunoprecipitated for 2 h with 2 μ l HA specific antibody and 25 μ l protein A-Sepharose beads. Kinase activity assays were performed as described above.
doi:10.1371/journal.pone.0002279.g002

thaliana Col-0 plants, *coi1-16* and *ein2-1* plants contained 35 and 50 times more *Salmonella*, respectively (Fig. 5e). In contrast, only a small difference in *Salmonella* infection levels was detected between wild type and *NahG* plants (Fig. 5e), indicating that the JA and ET pathways are important for resistance against *S. typhimurium*. Comparing the disease symptoms in *coi1-16*, *ein2-1* and *NahG* plants challenged with *Salmonella* by dipping plants for 5 min into a bacterial solution, the JA-signalling pathway appeared to be of primary importance for *Arabidopsis* resistance to *Salmonella* infection. *coi1-16* plants revealed severe senescence symptoms and wilting two weeks after dipping (Fig. 5c–d). Although *ein2-1* plants showed even higher proliferation levels of *Salmonella* than *coi1-16* plants (Fig. 5e), these plants did not show enhanced disease symptoms (Fig. 5a–b). In contrast, *NahG* plants showed similar *Salmonella* proliferation rates and symptoms as Col-0 wild type plants (data not shown).

To better understand the different signalling events, we monitored native MPK6 kinase activities in *coi1-16*, *ein2-1* and *NahG* plants upon *Salmonella* exposure. The activation pattern of MPK6 in *ein2-1* plants was very similar to that observed in wild type *A. thaliana* Col-0 plants and strong transient MPK6 activation was observed at 15 min after bacterial contact (Fig. 5f). *NahG* plants also showed a similar activation pattern of MPK6, although total activities were generally lower (Fig. 5f). In contrast, the level of MPK6 activation was poorly above background and the activation peak was shifted towards 30 min in *coi1-16* plants (Fig. 5f).

To monitor another level of the *Arabidopsis* innate immune system, the *coi1-16*, *ein2-1* and *NahG* plants were also analysed for

the expression of different defence response marker genes upon *Salmonella* treatment. In comparison to wild type *Arabidopsis* plants, *coi1-16* mutants showed no enhanced accumulation of *PDF1.2* and *PR1* transcripts (Fig. 5g–h). In *ein2-1* mutants, *PDF1.2* and *PR1* transcript accumulation was delayed upon *Salmonella* infection (Fig. 5g–h). *Salmonella* treatment of *NahG* plants resulted in accumulation of *PDF1* transcripts, but no induction of *PR1* expression was detected (Fig. 5g–h). These results reveal that the *Arabidopsis* SA, ET and JA pathways differentially contribute to disease development and the induction of defence responses upon *Salmonella* infection.

The MKK3-MPK6 cascade plays a crucial role in resistance to *Salmonella*

Of the *Arabidopsis* mutants, *coi1-16* was compromised in MPK6 activation, all defence responses and moreover showed enhanced disease symptoms (Fig. 5). These results identify the JA signalling pathway to be of outstanding importance in *Salmonella*-*Arabidopsis* interaction. COI1 is an F-box protein acting in an E3 ubiquitin ligase containing complex, which degrades the repressors of JA-responsive genes [38,39]. The JA-dependent activation of MPK6 is consistent with recent data, suggesting that full activation of MPK6 by JA requires mitogen-activated protein kinase kinase 3 (MKK3) [25]. To test this model during *Arabidopsis*-*Salmonella* interaction, we analyzed the *Salmonella*-induced activation of native MPK6 in *mkk3* mutants (Fig. 6a). Like in *mpk6* knock-out plants, no activation of MPK6 was detected in *mkk3* mutants, revealing that *Salmonella* induces MPK6 by MKK3 activation. A corollary of

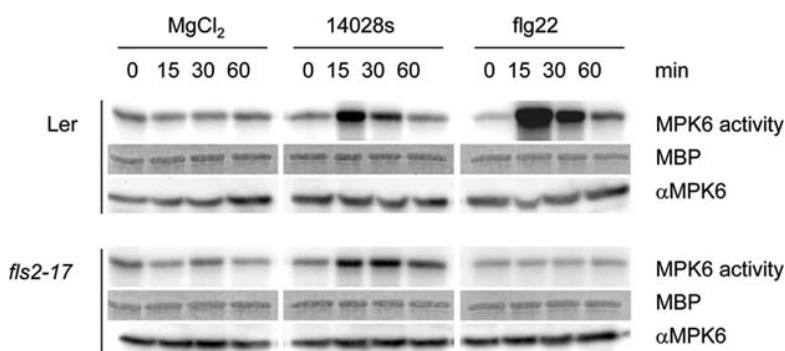


Figure 3. *Arabidopsis* responds to multiple *Salmonella*-derived PAMPs. Plants can recognize several *Salmonella*-derived molecules, and this recognition leads to defence mechanisms. We tested whether *Arabidopsis*, in order to activate its response to *Salmonella*, relies on the most prominent flagellum and/or other bacterial effectors. The native MPK6 can be activated by *S. typhimurium* wild type 14028s in *A. thaliana* *fls2-17* mutant, which is not able to recognize the flagellar protein flagellin. This result shows that the interaction between plants and *Salmonella* involves other signalling molecules, probably lipopolysaccharide (LPS), lipoproteins or other effectors. Kinase activity assays were performed on equal amounts of total protein extracted from 14 days old plants immunoprecipitated with MPK6 specific antibody. The *A. thaliana* wild type Ler was used as control in the experiment with the *A. thaliana* *fls2-17* mutant. Flg22 is a 22 amino-acid peptide derived from flagellin.
doi:10.1371/journal.pone.0002279.g003

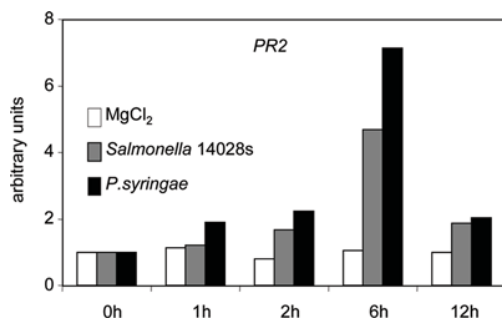


Figure 4. Quantitative RT-PCR analysis of JA-inducible *PR2* expression upon infection with *Salmonella* and *Pseudomonas syringae*. Transcript amounts of *PR2* (pathogenesis related2), similarly to *PDF1.2*, are induced by MeJA treatment. Transcript levels accumulate also after contact with *Salmonella*, pointing to a central role of the JA pathway in response to this bacterium. Moreover, the induction follows the kinetics of induction caused by the plant specialized pathogen *P. syringae*. Q-RT-PCR was performed as described above. doi:10.1371/journal.pone.0002279.g004

these results suggests that MPK6 might play an important role in defence against *Salmonella* infection. In agreement with this hypothesis, *mpk6* plants were significantly more susceptible to *Salmonella* infection, showing a 17-fold higher cfu after 24 hours of culture in liquid medium inoculated with *Salmonella* (Fig. 6b). Moreover, *mpk6* plants showed enhanced *Salmonella* proliferation levels when the bacteria were vacuum-infiltrated into leaves (Fig. 6c). These data indicate that the MKK3/MPK6 module of the JA signalling pathway plays an important role in restricting *Salmonella* infection in *Arabidopsis*.

Discussion

The results presented in this report demonstrate that the human pathogen *Salmonella enterica* serovar *typhimurium* (*S. typhimurium*) may also be a true plant endopathogen. This bacterium can actively invade various tissues, enter into and proliferate in cells of *Arabidopsis*. Although infection of *Arabidopsis* triggers immune responses similar to those known from other plant pathogens, *S. typhimurium* is able to overcome the host defence mechanisms and multiply in *Arabidopsis* plants. Using a panel of plant defence

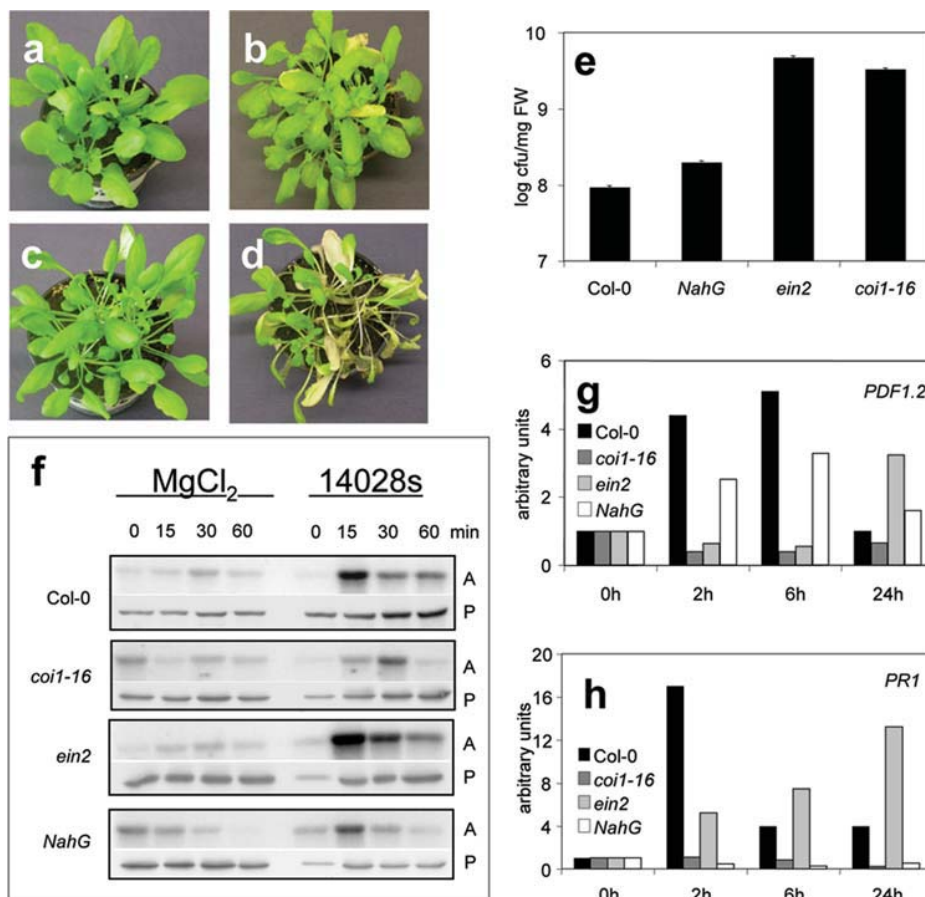


Figure 5. Jasmonate and ethylene signalling pathways are necessary for defence response to *Salmonella*. a–d, Disease symptoms in JA and ET insensitive mutants *ein2* (a,b) and *coi1-16* (c,d) plants dipped for 5 min in *S. typhimurium* 14028s solution; (a, c) before dipping, (b, d) 14 days after dipping. e, *coi1-16* and *ein2* are susceptible to *Salmonella* invasion. 14 days old *A. thaliana* wild type Col-0, *coi1-16* and *ein2* mutants or *NahG* transgenic seedlings were inoculated with *S. typhimurium* 14028s for 48 h, and cfu of internal bacteria in the seedling homogenates were determined. f, Activities of native MPK6. MPK6 activity was poorly induced in *coi1-16* plants after *Salmonella* treatment. Kinase activity assays were performed as described above. g–h, Quantitative analysis of JA-regulated *PDF1.2* (g) and SA-dependent *PR1* (h) expression upon *Salmonella* infection. Induction of *PDF1.2* expression was abolished in *coi1-16* and delayed in *ein2*. Expression of *PR1* was not induced in *coi1-16* or *NahG* plants. Quantitative RT-PCR analysis was performed on 5 µg reverse transcribed total mRNA. *clathrin*, *ubiquitin4* and *actin2* were used for normalization. doi:10.1371/journal.pone.0002279.g005

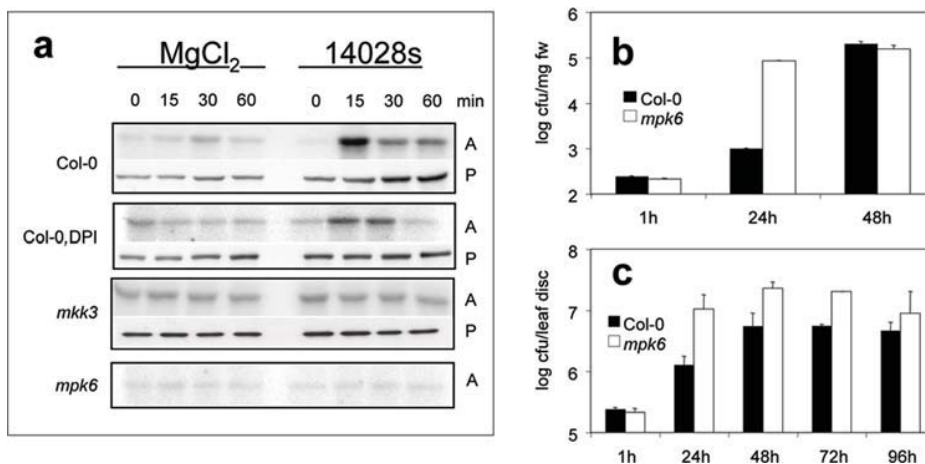


Figure 6. *Salmonella* induction of MPK6 depends on MKK3. **a**, Kinase activity assays on native MPK6 immunoprecipitated from *mkk3* and *mpk6* mutants treated with 10 mM $MgCl_2$ or *S. typhimurium* 14028s. Myelin basic protein (MBP) was used as substrate. A, activity; P, protein amounts were detected by Western blotting with antibodies specific for MPK6. **b**, Infection assays. 14 days old seedlings incubated in MS/2 medium inoculated with *S. typhimurium* 14028s during 2 days, cfu of internal bacteria were determined from plant homogenates. **c**, Proliferation of bacteria in infiltrated plants is faster in *mpk6* mutants. A *S. typhimurium* 14028s solution was used to vacuum-infiltrate 3 weeks old leaves of *mpk6* or Col-0, cfu of internal bacteria were determined in homogenates of leaf discs. doi:10.1371/journal.pone.0002279.g006

mutants, the JA signalling pathway was identified to be of major importance for resistance of *Arabidopsis* plants to *Salmonella* infection. Overall, these results demonstrate that *Arabidopsis* can be used as a valuable genetic host model system to study *Salmonella* pathogenesis in plants.

Salmonella is a plant endopathogen

Infection of animals or humans with *S. typhimurium* is dependent on various factors. The ability of *S. typhimurium* to enter mammalian host epithelial cells is tightly controlled by SPI-1 encoded factors and results in the formation of *Salmonella* containing vacuoles (SCVs), which are necessary for survival and subsequent systemic bacterial infection [4] [1]. The survival of *S. typhimurium* outside of the host organism is less well understood, but *Salmonella* can clearly adapt to different external conditions including low pH or high temperature [40]. *Salmonella* was not only shown to persist in soil for as long as 900 days after inoculation [41], but these bacteria can also survive in a variety of fruits, explaining why mangos and tomatoes are often causally linked to human salmonellosis. Although in these cases, food contamination is rather thought to occur during post-harvest processing, a number of recent reports indicated soil-grown vegetables as the source of human *Salmonella* infection [5]. The presence of *Salmonella* in soil might mostly originate from animal-derived contamination such as organic fertilizers or slaughter waste. The question arising now is whether infection of plants by *Salmonella* in the soil occasionally occurs via passive and nonselective mechanisms or whether infection underlies active bacterial infection processes employed by *Salmonella*. Our results, as well as other recently published data [42], demonstrate that *Arabidopsis* and a number of other plants have to be considered as true hosts for *Salmonella*. Inoculation experiments suggest that in the cases of *Medicago truncatula* and *Arabidopsis*, *Salmonella* is able to recognize plants as a suitable host and actively enters root tissues (Fig. 1b and [42]). Furthermore, when infiltrated into leaves, *Salmonella* are also able to proliferate in this environment (Fig. 1a and [28]). Most reports so far suggested the presence of *Salmonella* in the apoplast (the interspace between cells) [5], or in the form of

biofilms, as shown for parsley [43]. Using GFP-marked bacteria, we show here that, *Salmonella* also inhabits the cytoplasmic compartment (Fig. 1e–h). Only after three hours post inoculation *Salmonella* were present inside root hairs, and 17 hours later also non-root hair rhizodermal cells were infected. By confocal microscopy, bacteria were observed to be moving in the cytoplasm. It is presently unclear whether *Salmonella* are present in endocytotic vesicles comparable to the SCVs in animal host cells. Further studies are also necessary to clarify the exact mechanism how *Salmonella* can penetrate through cell walls and enter into plant cells. Our present findings may however provide an explanation for the common *S. typhimurium* infection after consuming raw, contaminated fruits or vegetables, even after washing or surface sterilization. As shown by our investigation, bacteria present inside plant tissues and/or inside plant cells are resistant to these kinds of treatments and other precautions are required to fulfil current food safety standards.

Importance of the JA-dependent signaling pathway for defence gene induction

The first event in plant-pathogen interaction is recognition of the pathogen by the plant. Although a number of PAMPs were already identified, only a few receptors have so far been identified. FLS2 [20] and EFR [44] (receptors for flg22 and EF-Tu, respectively) are closely related LRR receptor kinases from the LRR-XII subfamily of receptor-like kinases. In the presence of the respective elicitors, both receptors trigger the activation of downstream kinases and defence responses. A nonproteinaceous binding site for harpinPspH PAMP was identified in tobacco plasma membranes that is required for triggering MAP kinase activation [9]. Activation of MAPK cascades is an essential step to induce defence reactions in response to pathogen attack. Several MAPKs are activated by different plant pathogenic bacteria as well as by treatment with several PAMPs [7,18,19,44]. *Salmonella* attack of *Arabidopsis* plants also results in the activation of MPK3 and MPK6 with a similar kinetics (Fig. 1i), showing a transient activation maximum at 15 min. Since MPK3 and MPK6 are implicated in various pathways, the respective signalling complex-

es rather than the MAP kinases themselves, are thought to provide the necessary signalling specificity. Since a recent report reveals the MAPK kinase MKK3 to be involved in activating MPK6 in response to JA [25], we investigated a possible involvement of this MAPKK in triggering MPK6 activation in response to *Salmonella* infection. MPK6 activation was totally compromised when *mkk3* mutants were treated with *Salmonella*, revealing that *Salmonella*-induced activation is mediated by MKK3 (Fig. 6a). In agreement with a role of MKK3 and MPK6 in the defence response against *Salmonella*, we recently found that MKK3 is also involved in defence against bacterial and fungal pathogens and becomes activated by reactive oxygen species [26]. Although MPK6 can also be activated by other MAPKKs besides MKK3 [7], [45], our observation that MPK6 could not be activated to any extent in *mkk3* mutant plants speaks against the involvement of other MAPKKs in *Salmonella*-induced activation of the MPK6 pathway. The role of MPK6 is also underscored by the fact that *mpk6* mutant plants were significantly less resistant to *Salmonella* attack, allowing infection to occur significantly faster and the development of higher *Salmonella* levels inside *Arabidopsis* plant tissues (Fig. 6b–c).

Arabidopsis infected by *Salmonella* initiates transcription of a number of defence genes, including the antifungal defensin gene *PDF1.2* [32] and the *PR2* and *PR4* pathogenesis related genes (Fig. 1j, Fig. 4). The transcription of these genes is generally upregulated in response to pathogens as well as by JA and ET [33]. The well-studied SA-regulated *PR1* gene was also upregulated when plants came into contact with *Salmonella* (Fig. 1j). Together, these data indicate that *Salmonella* attack induces in *Arabidopsis* a complex defence response similar to that observed upon attack by other typical plant pathogens [12].

In a simplified view, defence reactions of plants can be divided into SA- and JA/ET-dependent immune responses. SA-dependent responses (further subdivided into NPR1-dependent and NPR1-independent reactions) are important in defence against biotrophic pathogens [13] whereas JA and ET are mainly involved in responses against herbivores and necrotrophic pathogens [16]. We used *Arabidopsis* plants blocked in these three signalling pathways (*NahG*, *coi1-16* and *ein2-1*) in order to determine which if any of these pathways is relevant for resistance against infection by *Salmonella*. The *coi1-16* mutant is defective in an F-box protein required for degradation of repressors of JA-responsive genes [38], [39], and is highly susceptible to *Salmonella* attack (Fig. 5d). The *Arabidopsis coi1-16* mutants were not able to induce activation of MPK6 kinase, nor transcription of any of the tested pathogenesis-related marker genes (Fig. 5f–h), indicating that the JA signaling pathway is absolutely required to induce downstream defence reactions against *Salmonella*. In contrast to Iniguez [28] who reported that *NahG* plants are more susceptible to *Salmonella*, we found slightly enhanced proliferation rates (Fig. 5e), but this may be due to different experimental procedures. Finally, ET was also identified to play a role in *Arabidopsis* defence against *Salmonella*. Although the ET signalling *ein2-1* mutant plants showed delayed expression of defence genes that was correlated with enhanced proliferation rates similar to those observed in *coi1-16* mutants, *Salmonella* infected *ein2-1* plants did not produce enhanced disease phenotypes (Fig. 5b). However, this phenomenon does not seem to be a particularity of the interaction between *Salmonella* with *Arabidopsis* plants. Upon infection with pathogenic *Pseudomonas syringae*, *ein2-1* mutant plants showed similar bacterial growth rates as wild type Col-0, plants but only minimal chlorophyll loss [46], indicating that marker gene expression and disease phenotype are not necessarily causally related.

Overall our findings give rise to the following human health considerations. The present work provides an explanation why

commonly used practices like washing or surface sterilization of *Salmonella*-infected plants fail to prevent human infection, suggesting that current safety regulations should undergo a serious reconsideration. Alternative strategies to ensure food safety might be achieved by controlling the quality of organic fertilizers and water for irrigation. Moreover, breeding crops and fruits for improved defence signalling could also help to prevent *Salmonella* infection already at the plant level. If plants can be infected with *Salmonella* and thus have be considered as intermediate hosts to spread human diseases, then other human endopathogens could possibly use similar strategies. We therefore also suggest to investigate the potential of other human and animal endopathogenic bacteria to use plants as alternative hosts.

Materials and Methods

Plants and bacterial strains

Arabidopsis thaliana plants were grown on half MS medium, pH 5.4, 0.7% w/v agar at 22°C under 16 h light conditions (60 $\mu\text{M m}^{-2}\text{s}^{-1}$ light) or in soil at 22°C under 16 h light conditions. *Escherichia coli* XL1blue (host for cloning experiments) and *S. typhimurium* LB5010 (for generation of recombinant strains), 14028s (wild type), were cultured in LB medium aerobically at 37°C with antibiotic selection, when required.

GFP marked bacteria

The *gfpmut2* [29] gene encoding green fluorescent protein (forward: ttgaattcgtaactaactaattaattgaaggagatag, reverse: aaaaaaagcttcctcgtagacattattgtatag) was cloned downstream of the constitutive *rpsM* promoter (forward: tctagaaaggctacggccgttaattgg, reverse: gttacgccaggatgcttagaacggg) and upstream of *rrbB*-based transcriptional terminators in a high-copy number replicating vector pEC75 (composed of a pUC19-based origin of replication and the pUC19-ampicillin resistance gene). The GFP plasmid was introduced in *S. typhimurium* 14028s. Constitutive expression of GFP in the recombinant strain throughout the growth *in vitro* was verified using Zeiss LSM 510 META confocal microscope.

Infection of plants with *S. typhimurium*

Bacteria used in infection experiments were grown to late-logarithmic phase. All infections were performed using a bacterial solution with a density of 3×10^8 cfu/ml. Plants were either cultivated in half MS medium without sucrose and inoculated with bacteria (inoculation experiments) or vacuum-infiltrated with a bacterial solution in 10 mM MgCl_2 (infiltration experiments). At specific times after infection, plants were surface sterilized in 50 mM PBS pH 7.4 supplemented with 1% v/v bleach, 0.1% w/v SDS and 0.2% v/v Tween20 for 2 min and washed 4 times (2 min each) in H_2O . Seedlings (inoculation experiments) or 0.7 cm^3 excised leaf discs (infiltration experiments) were homogenized in 20% glycerol in 10 mM MgCl_2 , and appropriate dilutions of homogenates were plated on selective LB agar media in triplicates. The cfu number was calculated per mg fresh weight per seedling or per leaf disc

Kinase assays

Kinase activity assays were performed on extracts from 14 days old seedlings treated with *Salmonella* for 0, 15, 30 or 60 min. Cleared cell extracts with equal amounts of proteins were subjected for 2 h immunoprecipitation with 2 μl MPK specific antibodies and 25 μl protein A-Sepharose beads. The kinase reactions of immunoprecipitated proteins were performed at 24°C for 30 min in 15 μl kinase buffer containing 10 μg myelin basic

protein (MBP), 0.1 mM ATP and 2 μ Ci γ - 32 P-ATP. Phosphorylation levels of MBP were analyzed with a Phosphorimager.

Quantitative RT-PCR

Transcript levels were analyzed using the Eppendorf system (*realplex* and *RealMaster Mix*). 5 μ g of total RNA extract were used for reverse transcription. PCRs were run at 95°C, 15 sec: denaturation; 60°C, 15 sec: annealing and 68°C, 15 sec: elongation, for 40 cycles. RNA concentrations were normalized using transcript levels of *clathrin*, *ubiquitin4* and *actin2* genes, and values were plotted as a function of non-infected control samples.

Supporting Information

Figure S1 *Salmonella* cannot spread between different *Arabidopsis* organs. Single leaves from soil grown 3 weeks old *A. thaliana* wild type Col-0 were infiltrated with a bacterial solution. The plants were cultivated for two additional weeks and cfu of internal bacteria in both infiltrated and non-infiltrated leaves were determined. *S. typhimurium* 14028s was not detected in the non-infiltrated organs. In contrast, bacteria were still present in infiltrated leaves.

Found at: doi:10.1371/journal.pone.0002279.s001 (0.05 MB PDF)

Figure S2 *Salmonella* are present in newly formed *Arabidopsis* leaves even one month after infiltration. a–b, *A. thaliana* wild type Col-0 plants were infiltrated with *S. typhimurium* 14028s strain and

incubated for an additional month in control growing conditions. Infiltrated leaves died within 5 days (arrowheads in b), however, newly formed leaves were present (arrows in b). cfu number was calculated in discs excised from those leaves two days after infiltration or from newly developed leaves one month after infiltration (a). As control non-infiltrated plants were used.

Found at: doi:10.1371/journal.pone.0002279.s002 (0.34 MB PDF)

Figure S3 Z-stacking through an *Arabidopsis* protoplast infected with GFP-marked *Salmonella* cells. One μ m optical sections of two infected protoplasts (a–b) were taken using a LSM 510 META confocal microscope and reassembled with the Zeiss LSM Software. 488 nm excitation and 505–530 nm emission filters were used.

Found at: doi:10.1371/journal.pone.0002279.s003 (0.45 MB PDF)

Acknowledgments

Authors would like to thank Sergio de la Fuente van Bentem, Bénédicte Sturbois and Thorsten Nünberger for comments on this manuscript.

Author Contributions

Conceived and designed the experiments: HH EC AS. Performed the experiments: AS AC. Analyzed the data: AS. Contributed reagents/materials/analysis tools: EC. Wrote the paper: HH EC AS.

References

- Holden DW (2002) Trafficking of the Salmonella Vacuole in Macrophages doi:10.1034/j.1600-0854.2002.030301.x. *Traffic* 3: 161–169.
- Guignot J, Caron E, Beuzon C, Bucci C, Kagan J, et al. (2004) Microtubule motors control membrane dynamics of *Salmonella*-containing vacuoles. *Journal of Cell Science* 117: 1033–1047.
- Waterman SR, Holden DW (2003) Functions and effectors of the Salmonella pathogenicity island 2 type III secretion system doi:10.1046/j.1462-5822.2003.00294.x. *Cellular Microbiology* 5: 501–511.
- Fields PI, Swanson RV, Haidaris CG, Heffron F (1986) Mutants of *Salmonella typhimurium* That Cannot Survive within the Macrophage are Avirulent doi:10.1073/pnas.83.14.5189. *PNAS* 83: 5189–5193.
- Brandl MT (2006) Fitness of Human Enteric Pathogens on Plants and Implications for Food Safety doi:10.1146/annurev.phyto.44.070505.143359. *Annual Review of Phytopathology* 44: 367–392.
- Jablone J, Warriner K, Griffiths M (2005) Interactions of *Escherichia coli* O157:H7, *Salmonella typhimurium* and *Listeria monocytogenes* plants cultivated in a gnotobiotic system. *International Journal of Food Microbiology* 99: 7–18.
- Asai T, Tena G, Plotnikova J, Willmann MR, Chiu W-L, et al. (2002) MAP kinase signalling cascade in *Arabidopsis* innate immunity. 415: 977–983.
- Fellbrich G, Romanski A, Varet A, Blume B, Brunner F, et al. (2002) NPP1, a Phytophthora-associated trigger of plant defense in parsley and *Arabidopsis* doi:10.1046/j.1365-313X.2002.01454.x. *The Plant Journal* 32: 375–390.
- Lee J, Klessig DF, Nurnberger T (2001) A Harpin Binding Site in Tobacco Plasma Membranes Mediates Activation of the Pathogenesis-Related Gene HIN1 Independent of Extracellular Calcium but Dependent on Mitogen-Activated Protein Kinase Activity 10.1105/tpc.13.5.1079. *Plant Cell* 13: 1079–1093.
- Navarro L, Zipfel C, Rowland O, Keller I, Robatzek S, et al. (2004) The Transcriptional Innate Immune Response to flg22. Interplay and Overlap with Avr Gene-Dependent Defense Responses and Bacterial Pathogenesis 10.1104/pp.103.036749. *Plant Physiol* 135: 1113–1128.
- Gomez-Gomez L, Felix G, Boller T (1999) A single locus determines sensitivity to bacterial flagellin in *Arabidopsis thaliana* doi:10.1046/j.1365-313X.1999.00451.x. *The Plant Journal* 18: 277–284.
- Jones JDG, Dangl JL (2006) The plant immune system. 444: 323–329.
- Durrant WE, Dong X (2004) SYSTEMIC ACQUIRED RESISTANCE doi:10.1146/annurev.phyto.42.040803.140421. *Annual Review of Phytopathology* 42: 185–209.
- Beckers GJM, Spoel SH (2006) Fine-Tuning Plant Defence Signalling: Salicylate versus Jasmonate. *Plant Biology*. pp 1–10.
- Halim VA, Vess A, Scheel D, Rosahl S (2006) The Role of Salicylic Acid and Jasmonic Acid in Pathogen Defence. *Plant Biology*. pp 307–313.
- Zimmerli L, Stein M, Lipka V, Schulze-Lefert P, Somerville S (2004) Host and non-host pathogens elicit different jasmonate/ethylene responses in *Arabidopsis* doi:10.1111/j.1365-313X.2004.02236.x. *The Plant Journal* 40: 633–646.
- Nakagami H, Pitzschke A, Hirt H (2005) Emerging MAP kinase pathways in plant stress signalling. *Trends in Plant Science* 10: 339–346.
- Desikan R, Hancock JT, Ichimura K, Shinozaki K, Neill SJ (2001) Harpin Induces Activation of the Arabidopsis Mitogen-Activated Protein Kinases AtMPK4 and AtMPK6 10.1104/pp.126.4.1579. *Plant Physiol* 126: 1579–1587.
- Nuhse TS, Peck SC, Hirt H, Boller T (2000) Microbial Elicitors Induce Activation and Dual Phosphorylation of the Arabidopsis thaliana MAPK 6 10.1074/jbc.275.11.7521. *J Biol Chem* 275: 7521–7526.
- Gomez-Gomez L, Boller T (2000) FLS2: An LRR Receptor-like Kinase Involved in the Perception of the Bacterial Elicitor Flagellin in *Arabidopsis*. *Molecular Cell* 5: 1003–1011.
- Menke FLH, van Pelt JA, Pieterse CMJ, Klessig DF (2004) Silencing of the Mitogen-Activated Protein Kinase MPK6 Compromises Disease Resistance in *Arabidopsis* 10.1105/tpc.015552. *Plant Cell* 16: 897–907.
- Ichimura K, Casais C, Peck SC, Shinozaki K, Shirasu K (2006) MEKK1 Is Required for MPK4 Activation and Regulates Tissue-specific and Temperature-dependent Cell Death in *Arabidopsis* 10.1074/jbc.M605319200. *J Biol Chem* 281: 36969–36976.
- Nakagami H, Soukupova H, Schikora A, Zarsky V, Hirt H (2006) A Mitogen-activated Protein Kinase Kinase Kinase Mediates Reactive Oxygen Species Homeostasis in *Arabidopsis* 10.1074/jbc.M605293200. *J Biol Chem* 281: 38697–38704.
- Suarez-Rodriguez MC, Adams-Phillips L, Liu Y, Wang H, Su S-H, et al. (2007) MEKK1 Is Required for flg22-Induced MPK4 Activation in *Arabidopsis* Plants 10.1104/pp.106.091389. *Plant Physiol* 143: 661–669.
- Takahashi F, Yoshida R, Ichimura K, Mizoguchi T, Seo S, et al. (2007) The Mitogen-Activated Protein Kinase Cascade MKK3-MPK6 Is an Important Part of the Jasmonate Signal Transduction Pathway in *Arabidopsis* 10.1105/tpc.106.046581. *Plant Cell* 19: 805–818.
- Doczi R, Brader G, Pettko-Szandner A, Rajh I, Djamei A, et al. (2007) The Arabidopsis Mitogen-Activated Protein Kinase Kinase MKK3 Is Upstream of Group C Mitogen-Activated Protein Kinases and Participates in Pathogen Signaling 10.1105/tpc.106.050039. *Plant Cell*: tpc.106.050039.
- Prithiviraj B, Bais HP, Jha AK, Vivanco JM (2005) *Staphylococcus aureus* pathogenicity on *Arabidopsis thaliana* is mediated either by a direct effect of salicylic acid on the pathogen or by SA-dependent, NPR1-independent host responses doi:10.1111/j.1365-313X.2005.02385.x. *The Plant Journal* 42: 417–432.
- Iniguez LA, Dong Y, Carter HD, Ahmer BMM, Stone JM, et al. (2005) Regulation of Enteric Endophytic Bacterial Colonization by Plant Defenses. *Molecular Plant Microbe Interaction* 18: 169–178.

29. Cormack BP, Valdivia RH, Falkow S (1996) FACS-optimized mutants of the green fluorescent protein (GFP). *Gene Fluorescent Proteins and Applications* 173: 33–38.
30. Chisholm ST, Coaker G, Day B, Staskawicz BJ (2006) Host-Microbe Interactions: Shaping the Evolution of the Plant Immune Response. *Cell* 124: 803–814.
31. MAPK Group, Ichimura K, Shinozaki K, Tena G, Sheen J, et al. (2002) Mitogen-activated protein kinase cascades in plants: a new nomenclature. *Trends in Plant Science* 7: 301–308.
32. Penninckx I, Eggermont K, Terras F, Thomma B, Samblanx G, et al. (1996) Pathogen-Induced Systemic Activation of a Plant Defensin Gene in Arabidopsis Follows a Salicylic Acid-Independent Pathway 10.1105/tpc.8.12.2309. *Plant Cell* 8: 2309–2323.
33. Jung C, Lyou S, Yeu S, Kim M, Rhee S, et al. (2007) Microarray-based screening of jasmonate-responsive genes in Arabidopsis thaliana. *Plant Cell Rep* 26: 1053–1063.
34. Heck S, Grau T, Buchala A, Metraux J-P, Nawrath C (2003) Genetic evidence that expression of NahG modifies defence pathways independent of salicylic acid biosynthesis in the Arabidopsis-Pseudomonas syringae pv. tomato interaction doi:10.1046/j.1365-313X.2003.01881.x. *The Plant Journal* 36: 342–352.
35. McGrath R, Ecker JR (1998) Ethylene signalling in Arabidopsis: events from the membrane to the nucleus. *Plant Physiol Biochem* 14: 119–126.
36. Xie D-X, Feys BF, James S, Nieto-Rostro M, Turner JG (1998) COI1: An Arabidopsis Gene Required for Jasmonate-Regulated Defense and Fertility 10.1126/science.280.5366.1091. *Science* 280: 1091–1094.
37. Xu L, Liu F, Lechner E, Genschik P, Crosby WL, et al. (2002) The SCFCOII Ubiquitin-Ligase Complexes Are Required for Jasmonate Response in Arabidopsis 10.1105/tpc.003368. *Plant Cell* 14: 1919–1935.
38. Chini A, Fonseca S, Fernandez G, Adie B, Chico JM, et al. (2007) The JAZ family of repressors is the missing link in jasmonate signalling. 448: 666–671.
39. Thines B, Katsir L, Melotto M, Niu Y, Mandaokar A, et al. (2007) JAZ repressor proteins are targets of the SCFCOII complex during jasmonate signalling. 448: 661–665.
40. Samelis J, Ikeda JS, Sofos JN (2003) Evaluation of the pH-dependent, stationary-phase acid tolerance in *Listeria monocytogenes* and *Salmonella Typhimurium* DT104 induced by culturing in media with 1% glucose: a comparative study with *Escherichia coli* O157:H7 doi:10.1046/j.1365-2672.2003.02013.x. *Journal of Applied Microbiology* 95: 563–575.
41. Nicholson F, Groves S, Chambers B (2005) Pathogen survival during livestock manure storage and following land application *Bioresource Technology* 96: 135–143.
42. Dong Y, Iniguez AL, Ahmer BMM, Triplett EW (2003) Kinetics and Strain Specificity of Rhizosphere and Endophytic Colonization by Enteric Bacteria on Seedlings of *Medicago sativa* and *Medicago truncatula* 10.1128/AEM.69.3.1783-1790.2003. *Appl Environ Microbiol* 69: 1783–1790.
43. Lapidot A, Romling U, Yaron S (2006) Biofilm formation and the survival of *Salmonella Typhimurium* on parsley. *International Journal of Food Microbiology* 109: 229–233.
44. Zipfel C, Kunze G, Chinchilla D, Canierd A, Jones JDG, et al. (2006) Perception of the Bacterial PAMP EF-Tu by the Receptor EFR Restricts Agrobacterium-Mediated Transformation. *Cell* 125: 746–760.
45. Meszaros T, Helfer A, Hatzimasoura E, Magyar Z, Serazetdinova L, et al. (2006) The Arabidopsis MAP kinase kinase MKK1 participates in defence responses to the bacterial elicitor flagellin doi:10.1111/j.1365-313X.2006.02888.x. *The Plant Journal* 48: 485–498.
46. Bent AF, Innes RW, Ecker JR, Staskawicz BJ (1992) Disease Development in Ethylene-Insensitive *Arabidopsis thaliana* Infected with Virulent and Avirulent Pseudomonas and Xanthomonas Pathogens. *Mol Plant Microbe Interact* 5: 372–378.

Site-Specific Phosphorylation Profiling of *Arabidopsis* Proteins by Mass Spectrometry and Peptide Chip Analysis

Sergio de la Fuente van Bentem,^{*,†} Dorothea Anrather,[‡] Ilse Dohnal,[‡] Elisabeth Roitinger,^{§,#}
Edina Csaszar,[‡] Jos Joore,^{||} Joshua Buijnink,^{||} Alessandro Carreri,[†] Celine Forzani,[†]
Zdravko J. Lorkovic,[⊥] Andrea Barta,[⊥] David Lecourieux,^{†,+} Andreas Verhounig,[▽]
Claudia Jonak,[▽] and Heribert Hirt^{†,○}

Department of Plant Molecular Biology, and Department of Biochemistry, Max F. Perutz Laboratories,
University of Vienna, Dr. Bohr-Gasse 9, 1030 Vienna, Austria, Research Institute of Molecular Pathology,
Dr. Bohr-Gasse 7, 1030 Vienna, Austria, Pepscan Presto, Zuidersluisweg 2, 8243 RC Lelystad, The Netherlands,
Department of Medical Biochemistry, Max F. Perutz Laboratories, Medical University of Vienna,
Dr. Bohr-Gasse 9, 1030 Vienna, Austria, Gregor Mendel Institute of Molecular Plant Biology, Austrian Academy
of Sciences, Vienna Biocenter, Dr. Bohrgasse 3, 1030 Vienna, Austria, URGV Plant Genomics,
2 rue Gaston Cremieux, 91057 Evry, France

Received January 10, 2008

An estimated one-third of all proteins in higher eukaryotes are regulated by phosphorylation by protein kinases (PKs). Although plant genomes encode more than 1000 PKs, the substrates of only a small fraction of these kinases are known. By mass spectrometry of peptides from cytoplasmic- and nuclear-enriched fractions, we determined 303 *in vivo* phosphorylation sites in *Arabidopsis* proteins. Among 21 different PKs, 12 were phosphorylated in their activation loops, suggesting that they were in their active state. Immunoblotting and mutational analysis confirmed a tyrosine phosphorylation site in the activation loop of a GSK3/shaggy-like kinase. Analysis of phosphorylation motifs in the substrates suggested links between several of these PKs and many target sites. To perform quantitative phosphorylation analysis, peptide arrays were generated with peptides corresponding to *in vivo* phosphorylation sites. These peptide chips were used for kinome profiling of subcellular fractions as well as H₂O₂-treated *Arabidopsis* cells. Different peptide phosphorylation profiles indicated the presence of overlapping but distinct PK activities in cytosolic and nuclear compartments. Among different H₂O₂-induced PK targets, a peptide of the serine/arginine-rich (SR) splicing factor SCL30 was most strongly affected. SRPK4 (SR protein-specific kinase 4) and MAPKs (mitogen-activated PKs) were found to phosphorylate this peptide, as well as full-length SCL30. However, whereas SRPK4 was constitutively active, MAPKs were activated by H₂O₂. These results suggest that SCL30 is targeted by different PKs. Together, our data demonstrate that a combination of mass spectrometry with peptide chip phosphorylation profiling has a great potential to unravel phosphoproteome dynamics and to identify PK substrates.

Introduction

The genomes of plant species encode more than 1000 protein kinases (PKs),^{1–3} substantiating the notion that protein phosphorylation is one of the most frequently occurring post-

translational modification targeting perhaps as much as 30% of all proteins in eukaryotes. Animal and yeast research have shown that different kinases can selectively phosphorylate multiple sites in their substrates^{4,5} and thereby fine-tune the activity of a particular substrate.⁶ In the recent past, several methods have been developed to identify *in vivo* phosphorylation sites on proteins on a large scale. These methods are based on selective phosphopeptide isolation from protease-digested protein mixtures and the subsequent sequencing of these peptides by mass spectrometry. Among various phosphopeptide purification methods, immobilized metal affinity purification (IMAC) and titanium dioxide (TiO₂) have been most successfully used for phosphorylation site mapping.^{7–10} Optimization of protocols and the introduction of mass spectrometers with high mass accuracy have recently achieved the identification of more than 5000 phosphorylation sites.^{11,12} Importantly, it seems that different phosphopeptide isolation

* To whom correspondence should be addressed. Phone: +43-1-4277-54612. Fax: +43-1-4277-9546. E-mail: delafus3@univie.ac.at.

† Department of Plant Molecular Biology, University of Vienna.

‡ Department of Biochemistry, University of Vienna.

§ Research Institute of Molecular Pathology.

Current address: Christian-Doppler-Laboratory for Proteome Analysis, Department of Biochemistry, Max F. Perutz Laboratories, University of Vienna, Dr. Bohr-Gasse 9, 1030 Vienna, Austria.

|| Pepscan Presto.

⊥ Department of Medical Biochemistry, Medical University of Vienna.

+ Current address: UMR CNRS 6161, Bâtiment de Botanique, 40 av. du recteur Pineau, F-86022, Poitiers cedex, France.

▽ Gregor Mendel Institute of Molecular Plant Biology.

○ URGV Plant Genomics.

methods purify different sets of phosphopeptides, suggesting that at present no single protocol achieves full phosphoproteome coverage.¹³

In addition to the general description of phosphorylation sites, the dynamics of stimulus-induced changes in the phosphoproteome has been studied by quantitative mass spectrometry.^{11,14–17} Among novel insights into protein phosphorylation, these studies have revealed that a remarkable specificity of signaling occurs at the level of individual phosphosites. Different sites on the same protein often respond in different ways to a changing environment. Indeed, it seems that many proteins integrate signals from various kinases, indicating that for the analysis of signaling networks, monitoring of individual sites is crucial.^{5,11}

Peptide or protein chips have been used to identify PK substrates.^{18–20} Such studies have revealed the substrate specificities of yeast PKs at a global scale^{21,22} and of two MAPKs in plants.²³ Large-scale site-specific phosphorylation profiling can be achieved by using arrays of short peptides that contain one or a few phosphorylation sites. This technique can suggest substrate phosphorylation sites for different PKs when tested individually on a peptide array.²⁴ Others have used peptide arrays to determine the optimal phosphorylation motif for a specific PK as well as stimulus-induced changes in kinase activities within animal cell extracts²⁵ and recently in plants.²⁶

In contrast to yeast and animal systems, phosphoproteomics in plants is still a largely unexplored field.²⁷ Phosphoproteomic analysis has mostly focused on identifying phosphoproteins rather than phosphosites. Although several approaches were successful in determining the identity of phosphoproteins, they identified no or just a small number of phosphosites.^{28–32} In contrast, several studies have used IMAC or TiO₂ to reveal numerous phosphorylation sites in *Arabidopsis* plasma membrane proteins,^{14,33} now made available through a database.³⁴ In contrast, knowledge of phosphorylation sites in intracellular proteins is scarce. Moreover, approaches such as those described for studies on animals⁵ are currently not feasible in plants, because contextual data to link kinases to substrates are largely lacking. Consequently, the knowledge of plant PKs, their substrates and the phosphorylation networks in which they participate is limited. Here, we focus on the intracellular phosphoproteome of *Arabidopsis* to allow us to propose potential phosphorylation networks. Purification of phosphopeptides from cytosolic and nuclear extracts by IMAC followed by mass spectrometric analysis allowed us to determine more than 300 *in vivo* phosphorylation sites. Microarrays of peptides corresponding to a subset of the identified phosphopeptides were developed. These peptide chips enabled us to identify differential phosphorylation of substrates by PKs from cytoplasmic and nuclear fractions. Furthermore, with the use of the peptide chips, we could determine an oxidative stress-induced PK activity that phosphorylates a peptide of the splicing factor SCL30. Further analysis suggested that SRPK4 and MAPKs act together to mediate constitutive and oxidative stress-induced phosphorylation of SCL30.

Materials and Methods

Mass Spectrometric Analysis of Phosphopeptides. Nuclear and cytosolic phosphoproteomes from *Arabidopsis* root cell culture were screened. Protein extractions, peptide esterification and mass spectrometry were performed as described previously.³⁵ Phosphopeptides from cytosolic and nuclear samples were, respectively, isolated with 5 μ L of IMAC material

(Phos-Select, Sigma) or POROS MC material (ABI), which was charged with FeCl₃. The LTQ linear ion trap mass spectrometer (ThermoElectron; San Jose, CA) was operated in the data-dependent mode: 1 full scan (m/z 450–1600) was followed by MS/MS (MS²) scans of the four most abundant ions. These ions were excluded from further selection for 30 s. For each MS² spectrum, the neutral loss algorithm in the Xcalibur 1.4 software was enabled. In this mode, MS/MS/MS (MS³) experiments are automatically triggered, if a neutral loss of phosphoric acid (98, 49, 32.7 Da for singly-, doubly-, or triply charged precursor ions, respectively) is detected among the most intense 8 fragment ions in the preceding MS² scan. Searches against the nonredundant *Arabidopsis thaliana* protein database from NCBI (for the latest search the version of the eighth of September 2007) were done with tryptic specificity allowing 2 missed cleavages. Peptide tolerance was set to 1.5 Da and fragment tolerance to 1.0 Da. The obtained result was filtered using XCorr cutoff scores of 1.5, 2.0, and 2.5 for singly-, doubly-, and triply charged peptides, respectively. In total, phosphopeptide spectra of two nuclear extracts and four cytosolic extracts were subjected to careful manual inspection using Bioworks Browser 3.1 SR1 (Thermo Electron) and later versions 3.2 and 3.3. For each peptide, the MS/MS (MS²) and, when available, MS/MS/MS (MS³) spectra were thoroughly inspected. An IMAC-purified phosphopeptide fraction of cytosolic proteins was analyzed by LTQ-MS coupled with Fourier Transform Ion Cyclotron Resonance-MS (FTICR-MS). SEQUEST-Bioworks data generation parameters for the LTQ-FT combination were the following: MW range, 600–4500 Da; precursor ion tolerance, 50 ppm; group scan, 1; minimum group count, 1; minimum ion count, 5. Subsequently, results were filtered with mass deviations of precursor ions of up to 5.0 ppm; XCorr scores of 1.5, 2.0, and 2.5 for singly-, doubly-, and triply charged peptides, respectively; and peptide probability ≤ 0.5 . Static modifications for the database search: carbamidomethylation of Cys (+57.02146 Da). Variable modifications: oxidation of Met (+15.99492 Da); phosphorylation of Ser/Thr/Tyr (+79.96633 Da); loss of water from Ser/Thr (−18.00000 Da; to interpret the MS³ spectra); and methylation on C-termini of peptides and on Asp and Glu (+14.01570 Da). We estimated the false-positive rates, with the use of a decoy database, to be 2.2% for the LTQ-FT-ICR experiment.

Bioinformatic analysis on the protein sequences was performed as described previously³⁵ and peptide sequences were aligned using BCM Search Launcher.

Stress Treatment of *Arabidopsis* Root Cell Cultures. Five-day-old *Arabidopsis* root cell cultures were treated for 5 min with water (control) or 4 mM H₂O₂. Harvested material was filtered, frozen in liquid nitrogen and ground with mortar and pestle. From the resulting cell material, proteins were isolated as described below.

Peptide Chip Experiments. Nuclear extracts from cell material were prepared as described.³⁵ Soluble (cytosolic) extracts were prepared by adding HEPES kinase buffer (50 mM HEPES pH 7.5, 10 mM MgCl₂, 10 mM MnCl₂, 5 mM EDTA, 1 mM EGTA, 1 mM NaF, 1 mM Na₃VO₄, 15 mM β -glycerophosphate, 15 mM 4-nitrophenylphosphate, 0.5 mM PMSF, 5 μ g/mL leupeptin, and 10 μ g/mL aprotinin) to cell material and centrifuging for 30 min at 20 000g. Extracts were filtered through 0.22 μ m GV Durapore spin filters (Millipore) to remove particle contaminants. A 6 \times reaction mixture (50% glycerol, 300 μ M ATP, 60 mM MgCl₂, 0.05% Brij-35, 0.25 mg/mL bovine serum albumin and 25 μ Ci [γ -³³]ATP) was freshly prepared

before each chip assay and filtered through 0.22 μm syringe filters (VBC-Genomics Bioscience Research, Vienna, Austria). Before the assay, cytosolic extracts were diluted four times in HEPES kinase buffer to reduce background noise on the chip.²⁶ After adding 10 μL of the reaction mixture to 50 μL of nuclear (100 μg of protein) or (diluted) cytosolic extract (25 μg of protein), the final mix was applied onto the slides (manufactured by Pepscan Presto, Lelystad, The Netherlands) as described in the PepChip kinase manual (Pepscan Presto, Lelystad, The Netherlands). Protein array slides were incubated for 2–3 h at 30 °C. Afterward, the slides were shortly washed in PBS containing 1% Triton X-100, then twice for 15 min in 2 M NaCl containing 1% Triton X-100 and twice for 15 min in water. The slides were then shortly washed twice with water and dried. Subsequently, the slides were exposed to a phosphorimager screen for 5 days and scanned with a Storm scanner. Spots were quantified using Imagequant and spots with an average of more than 3500 arbitrary units were considered positive as only these were found to be consistently phosphorylated in three independent biological replicate experiments. Each chip contained three replicate sets of the peptides, and spot intensities were normalized by taking the average of the spot intensities from one slide. To test whether the SCL30 peptide is phosphorylated by SRPK4 and MPK3, 5 μg of purified glutathione *S*-transferase (GST)-SRPK4 or GST-MPK3 (see below for purification) was incubated for 2 h at 30 °C on the chip. Subsequent steps were performed as described for cell extracts. This experiment was repeated once.

Mutagenesis of ASK α . Full-length ASK α (At5g26751) was cloned into pGEX5x3. For mutagenesis, PCR was performed on this plasmid with Pfu Ultra. ASK α Y229A was produced with primers ASK α Y229A-F (accaaacatttcgcccattgctcgaggta) and Y229A-R (tacctcgagcagatggcggaatgtttggt). ASK α S228A was generated with primers ASK α S228A-F (agaaccaaacattgctacatctgctcgag) and S228-R (ctcgagcagatgtaggcaatgtttggtct). PCR mixtures were digested for 2 h with *DpnI* and transformed into *Escherichia coli*. Different clones were sequenced and one for each mutation was used for protein purification (see below).

Protein Purification and *in Vitro* Kinase Assays. GST, GST-SCL30, GST-MPK3 and GST-SRPK4 were expressed from pGEX4-T1, while GST-ASK α , ASK α Y229A and ASK α S228A were expressed from pGEX5x3 and purified from *E. coli* BL21. GST and GST-SCL30 were tested as substrates for GST-SRPK4, and MBP was tested as substrate for GST-ASK α , GST-ASK α Y229A and GST-ASK α S228A. For this purpose, proteins were assayed in a total volume of 20 μL kinase buffer (20 mM HEPES, pH 7.5, 15 mM MgCl₂, 5 mM EGTA, and 1 mM DTT). The reaction was started with 2 μCi [γ -³²P]ATP and incubated at room temperature for 30 min. The reaction was stopped by the addition of 8 μL of 4 \times SDS loading buffer. Proteins were resolved by 15% SDS-polyacrylamide gel electrophoresis. The gel was dried and exposed overnight to a phosphorimager screen.

To determine whether SRPK4 is activated by H₂O₂, 10 μg of pDEDH plasmid containing SRPK4-HA was transformed into protoplasts of *Arabidopsis* root cell culture.³⁶ Approximately 20 h after transformation, protoplasts were treated for 5 min with 4 mM H₂O₂, harvested by a short centrifugation step, and frozen in liquid nitrogen. Protein extraction buffer (25 mM Tris, pH 7.8, 75 mM NaCl, 10 mM MgCl₂, 15 mM EGTA, 1 mM DTT, 1 mM NaF, 0.5 mM Na₂VO₃, 15 mM β -glycerophosphate, 15 mM *p*-nitrophenylphosphate, 0.1% Tween 20, 0.5 mM phenylmethylsulfonyl fluoride, 5 $\mu\text{g}/\text{mL}$ leupeptin, and 5 $\mu\text{g}/\text{mL}$

aprotinin) was added and extracts were centrifuged at 14 000g for 30 min. SRPK4-HA was immunoprecipitated overnight with anti-HA antibodies and immunocomplex kinase assays were performed as described before.³⁷ Samples were handled further as described above.

For testing whether MAPKs phosphorylate SCL30, cytosolic extracts were prepared from untreated cell material with protein extraction buffer. Extracts were centrifuged at 14 000g for 30 min. From the soluble fraction (500 μg of protein), MPK3, -4 and -6 were immunoprecipitated with 2 μL of specific antibody and immunocomplex kinase assays with GST, GST-SCL30 or myelin basic protein were performed. Subsequent steps were carried out as described above.

Immunoblotting with Anti-Phosphotyrosine Antibodies. Purified GST-ASK α , GST-ASK α Y229A and GST-ASK α S228A were subjected to SDS-PAGE and blotted onto PVDF membrane. The membrane was incubated with P-TYR-100 anti-phosphotyrosine antibodies (Cell Signaling Technology) in a 1:4000 dilution. The blot was washed, incubated with a Fab-specific, alkaline phosphatase-conjugated goat anti-mouse secondary antibody and washed. The blot was incubated with 1.5 mL of CDP-star reagent and chemiluminescence was detected by using a light-sensitive film.

Results

A Phosphoproteomic Approach Identifies 303 *in Vivo* Phosphorylation Sites of *Arabidopsis* Proteins. On the basis of the technique of IMAC purification of phosphopeptides, a mass spectrometry approach was taken to identify *in vivo* phosphorylation sites of *Arabidopsis* proteins.³⁸ Phosphopeptide spectra were subjected to stringent manual verification of phosphopeptides to obtain a reliable data set. This is reflected in (1) the high percentage of corresponding MS³ spectra of each peptide that confirm the sequence, (2) the high percentage of unambiguously identified sites (86%), (3) the large number of redundant phosphopeptides with miscleavages or different phosphorylation states, (4) the large number of conserved sites identified in different homologous proteins, and (5) the confirmation of many phosphopeptides (57% of the phosphopeptides identified in cytosolic extracts and 49% of all phosphopeptides) by one FTICR-MS experiment with phosphopeptides of cytosolic proteins. This analysis led to the disclosure of 303 phosphorylation sites on 205 proteins (Supplemental Table S1). The ratio between phosphorylated residues was 91.8%/7.5%/0.7% for serine/threonine/tyrosine (Figure 1A), indicating that, as in animals and yeast,^{10,11} the phosphorylation on tyrosine in *Arabidopsis* is far less abundant than on serine and threonine. We compared our data set with published *Arabidopsis* phosphorylation site studies and found 10 sites previously described by Nühse et al.,³³ 2 by Laugesen et al.,³² 2 by Wolschin and Weckwerth³⁹ and 49 by Benschop et al.¹⁴ (although in many cases the actual position of the phosphorylation site was not defined in the latter study). We also confirmed sites in HY5 (40) and fructose-6-phosphate 2-kinase/fructose-2,6-bisphosphatase.^{14,41} More than 80% of our data set includes novel phosphorylation sites, including two phosphotyrosine sites. Phosphoproteins were assigned to eight different classes, based on their domain composition or functional description in the literature (Figure 1B). Similar to Moser and White,⁴² we observed a high percentage of singly phosphorylated peptides (Figure 1C). Evolutionarily conserved phosphorylation was identified in putatively highly abundant proteins, such as metabolic enzymes (Supplemental Figure S1)

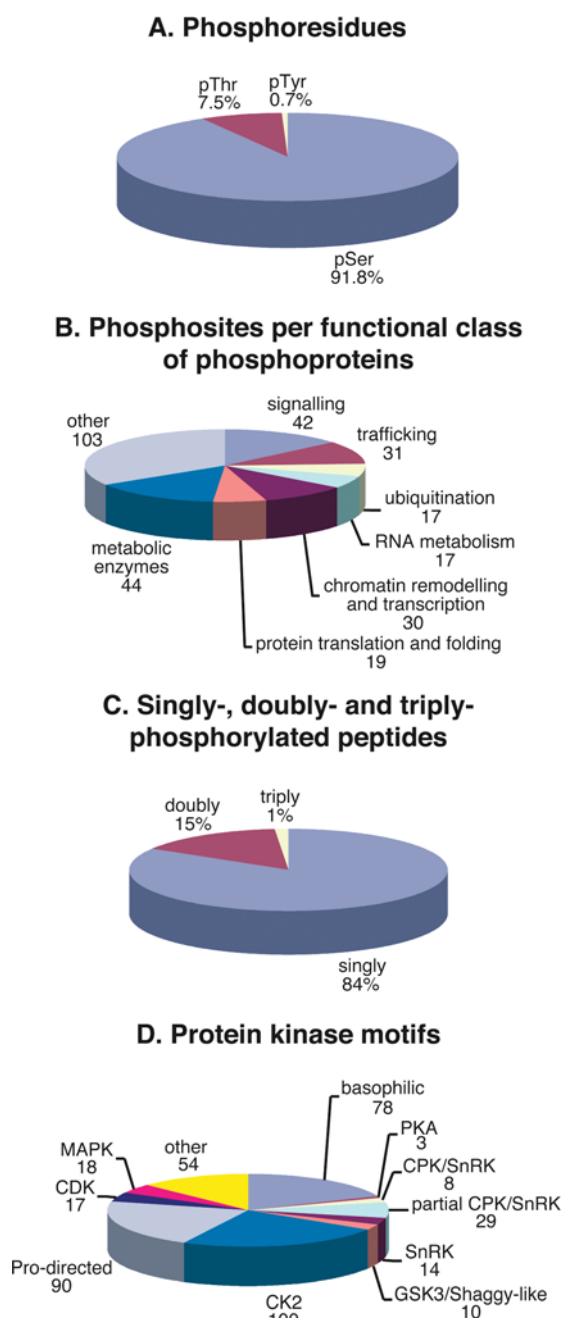


Figure 1. Overview phosphoproteomic data. (A) Percentage of phosphorylated amino acids (among a total of 292 unambiguously identified residues). pSer, phosphoserine; pThr, phosphothreonine, pTyr, phosphotyrosine. (B) Identified phosphoproteins were assigned to eight classes depending on their domain composition or known function. Shown here is the number of phosphorylation sites per class of phosphoproteins. (C) Percentage of singly-, doubly- and triply phosphorylated peptides among a total of 294. (D) Identified protein kinase motifs. Basophilic motif, R/K-X₂-pS/pT; CK2 motif, pS/pT-X₂-D/E; proline-directed motif, pS/pT-P.

and ribosomal proteins (Supplemental Table S1). However, also phosphorylation sites of proteins of expected low abundance were found, such as a nucleotide binding domain-leucine-rich-repeat-type disease resistance protein and various signaling proteins (Supplemental Table S1).

Linking Protein Kinases to Their Downstream Targets. One way to screen the obtained data set is to select for phos-

phorylation sites within PKs and protein phosphatases actively involved in reversible phosphorylation modification of proteins. Phosphorylation sites of 21 PKs and two protein phosphatases were identified (Table 1), including several RAF-like kinases, AGC kinases, cyclin-dependent kinases (CDKs), SNF1-related kinase 2 (SnRK2) isoforms and calcium-dependent PKs (CDPKs). More than half (14 out of 26) of the phosphorylation sites of PKs are located within activation loops. In general, phosphorylation of the PK activation loop correlates with an active state,⁴ suggesting that the PKs that we found to be phosphorylated in their activation loops were active. Consequently, these PKs potentially phosphorylated a number of the PK substrate sites described here. In line with this hypothesis, we identified a CDK site in the C-terminal region of retinoblastoma-related protein 1 (RBR1), which is a known target of a PSTAIRE CDKA/cyclin D complex *in vitro*,^{43,44} however, the actual site(s) had not been identified. In agreement with our hypothesis, we found T161 as a phosphorylation site in the activation loop of the *Arabidopsis* PSTAIRE CDKA, CDC2A/CDKA;1 (Figure 2A), which has recently been identified as important for activation.⁴⁵ Strikingly, we also found the upstream CDK-activating PK CDKF;1 that phosphorylates CDKA;1 in *Arabidopsis*.⁴⁶ Although mutational analysis has indicated that T290 is essential for CDKF;1 activity, we determined two other sites: a serine in the activation loop and a second site that is located C-terminally of the kinase domain. Indeed, a T290A mutant CDKF;1 has still some activity toward kinase-dead CDKA;1,⁴⁷ suggesting that another residue in the activation loop might be functional. Interestingly, the second site matches with a CDK motif, suggesting feedback regulation of CDKF;1 by a CDK, perhaps CDKA;1 itself or CDKC;1/2 (Figure 2A). Since we found CDKF;1 to be active (according to its phosphoprofile), we speculate that in addition to CDKA;1, CDKC;1/2 might also be a target of CDKF;1.

Phosphotyrosine sites were identified in a glycogen synthase kinase 3 (GSK3)/shaggy-like kinase (GSK) and in an unknown PK (Table 1). Both sites are located in the activation loop at a position analogous to the tyrosine in MAPK activation loops (Figure 3). The same tyrosine residue is phosphorylated in animal GSK3.^{48,49} Alignment of the activation loops of PKs belonging to the subgroup 4.5 (PlantP database) shows that more members of this group contain a tyrosine residue at the analogous position and therefore might become phosphorylated on this site as well (Figure 3). All 10 of the *Arabidopsis* GSK3/shaggy-like PKs⁵⁰ contain a tyrosine at the corresponding position (data not shown). This suggests that phosphorylation on tyrosine residues in PK activation loops could be a more general phenomenon than previously thought. It has been suggested that the peanut (non-MAPK) serine/threonine/tyrosine (STY) kinase is phosphorylated on a tyrosine residue in its activation loop.⁵¹ This residue was claimed to be analogous to a tyrosine phosphorylation site in human dual-specificity tyrosine-(Y)-phosphorylation regulated kinase 2 (DYRK2). However, this DYRK2 residue has not been described as a phosphorylation site. Instead, mutational analysis and *in vivo* phosphosite mapping have shown that the previous tyrosine is the correct phosphorylation site.^{52,53} This residue is located at the same position as the two tyrosine phosphorylation sites identified in our study and the tyrosine in the activation loop of MAPKs (Figure 3). This suggests that the

Table 1. Phosphorylation Sites in Protein Kinases and Phosphatases

gene identifier	protein kinase	phosphopeptide sequence	in activation loop
Protein Kinases			
Class 1-transmembrane receptor kinase and related nontransmembrane kinases			
At3g14350	LRR-TM-PK SRF7	R.HKpSFDDDDSTMR.K ^{a,b}	No
At1g27190	LRR-TM-PK	K.NMADKHGVpSEHYDEFPLVFNK.Q	No
At5g10020	LRR-TM-PK	R.FSDQPVMMLDVYpSPDR.L ^{a,b}	No
Class 2-ATN1/CTR1/EDR1/GmPK6 like kinase			
At1g16270	RAF18	R.TVpSGGGIETEAR.N	No
At1g16270/ At3g24720/ At1g04700/ At1g79570	RAF18/RAF16/RAF20/RAF40	K.RNpTLVpSGGVR.G	Yes
At2g17700	RAF21	R.VQIESGVMpTAETGTYR.W	Yes
At4g38470	RAF30	K.AQTGVMpTAETGTYR.W	Yes
At5g58950	RAF36	R.SVpSPSPQMAVPDVFKE ^b	No
Class 4-nontransmembrane protein kinases			
Family 4.2.1-calcium dependent protein kinase			
At4g04700	calcium-dependent protein kinase CPK27	R.TEpSSLQPEGELLPIIN ^c	No
At2g17290/ At4g35310	calcium-dependent protein kinase CPK5/6	K.NpSLNISM.RD ^b	No
Family 4.2.4-Snf1-related protein kinase (SnRK)			
At5g08590 or	SNF1-related kinase SnRK2.1 (ASK2) or SnRK2.4/.5	K.ppSSLHSRPKSTVGTPAYIAPEVLSR.R ^d or K.ppSSLHSRPKSTVGTPAYIAPEVLSR.R ^d	Yes
At5g63650/ At1g10940 At3g50500/ At5g66880/ At4g33950/ At4g40010	SNF1-related kinase SnRK2.2/.3/.6/.7	K.SSVLHpSQPK.S	Yes
Family 4.2.6-IRE/NPH/PI dependent/S6 kinase			
At5g09890	AGC kinase NDR-8	R.ALAYpSTVGTLDDYMAPEVLLK.K	Yes
At4g14350/ At1g03920/ At3g23310	AGC kinase NDR-1/-2/-3	R.MLAYpSTVGTPDYIAPEVLLK.K ^b	Yes
At3g17850	IRE homologue 1 (IRE-H1)	R.HKDSLAAEpSPDGMK.V	No
Family 4.5.2-CDC2-like kinase family			
At3g48750	CDC2A/CDKA;1	R.TEpTHEVVTWYR.A ^b	Yes
At1g67580	cdc2-like protein kinase	K.pSPDPLEEQR.R	No
At5g10270/ At5g64960	cdc2-like protein kinase (cdc2MsC/CDKC;1/CDKC;2)	R.MVKpSPDPLEEQR.R R.SYSHDHTGNLpTNR.V	Yes
Family 4.5.4-GSK3/Shaggy-like protein kinase family			
At5g26751/ At1g06390/ At3g05840/ At5g14640/ At1g57870	GSK3/shaggy-like kinase $\alpha/\gamma/\delta/\epsilon/\iota$	K.GEPNISpYICSR.Y	Yes
Family 4.5.8-unknown function kinase			
At5g35980	protein kinase-like	K.TVYSpYIQSR.Y	Yes
At3g17750	At3g17750/MIG5_4	K.HPWLTYPYEIPSA ^{b,c}	No
At1g73450/ At1g73460	protein kinase, putative	K.HPWLSYPYEIPSA ^{2,3}	No
Unclassified Protein Kinase			
At4g28980	CDK-activating kinase CAK1AT/CDKF;1	R.ILMEHDIVApSDENQQAYK.L K.YLSEELPVPVSELYVPPTMSGPDpSPR.K	Yes No
Protein Phosphatases			
Group 6.1-Serine/Threonine (ST) phosphatases			
At2g27210	kelch repeat-containing protein Ser/Thr phosphatase BSL3	K.LIHPLPPAIP TSPEpTSPER.H ^b	
Group 6.3-PP2C (Protein Phosphatase 2C) phosphatases			
At1g22280	protein phosphatase 2C	K.TDQAILSNpSSDLGR.G ^{a,b}	

^a Site described by Nühse et al.³³ ^b site described by Benschop et al.¹⁴ ^c C-terminus. ^d Peptides are identical in mass and cannot be distinguished between them. Unambiguous sites are preceded by a lower case p and in bold, while ambiguous sites are indicated in italics.

peanut STY kinase might rather be phosphorylated on a threonine residue (Figure 3).

Tyrosine-229 Phosphorylation of GSK3/Shaggy-like Kinase ASK α Is Required for Its Transphosphorylation Activity. To verify the tyrosine phosphorylation of one of the targets that we identified, the GSK3/Shaggy-like kinase ASK α was selected.

The tyrosine residue that was determined in this protein, Y229, is located in the activation loop and is analogous to the phosphotyrosine in human GSK3s (Tyr279 in GSK α and Y216 in GSK3 β) that is an autophosphorylation site required for activity.^{54,55} Full-length ASK α was produced in *E. coli* and purified as a glutathione S-transferase (GST) fusion protein. In

addition, two mutants were generated and also purified as GST fusion proteins, GST-ASK α Y229A and GST-ASK α S228A. First, it was tested whether the GST fusion proteins were phosphorylated on tyrosine by immunoblotting with a specific anti-phosphotyrosine antibody. Indeed, ASK α was found to be phosphorylated on tyrosine (Figure 4A, left lane). Mutation of tyrosine 229 to alanine resulted in an almost complete loss of the tyrosine phosphorylation signal. In contrast, the ASK α S228A mutant displayed normal tyrosine phosphorylation (Figure 4A). This indicates that Y229 in *Arabidopsis* ASK α is autophosphorylated and corresponds to the *in vivo* tyrosine phosphorylation site identified by mass spectrometry.

Because Y229 lies within the activation loop of the GSKs, we then asked whether phosphorylation of tyrosine 229 is required for protein kinase activity toward substrates. For this purpose, we tested the different ASK α variants for their ability to phosphorylate the artificial substrate myelin basic protein (MBP). Although both the wild-type protein and the S228A mutant phosphorylated MBP, ASK α Y229A showed a clearly diminished activity (Figure 4B). Concluding, these data suggest that tyrosine 229 in ASK α is phosphorylated and that this event is required for its transphosphorylation activity.

Grouping of Phosphosites According to Kinase Consensus Motifs. The substrate specificity of many PKs is partly based on the stereochemistry of the amino acids adjoining the phosphorylation site.⁴ Therefore, phosphorylation sites can be grouped into distinct kinase consensus motifs.^{11,12,33} We identified 100 sites that match a casein kinase 2 (CK2) motif, 90 for proline-directed kinases (including MAPKs and CDKs) and 78 basophilic PK motifs (with an affinity for basic amino acids, including PKAs, CDPKs and SnRKs) (Figure 1D). Within the basophilic data set, a novel “dipolar” motif¹² R/K-X₂-pS/pT-X₂-D/E/pS/pT was observed 33 times (Supplemental Figure S2). An example of this well-conserved motif is shown in Figure 5 for AGD6 and -7. In addition, we observed 21 times the motif R/K-X₂-pS/pT-P, which combines basophilic with proline-directed kinase motifs. In contrast, the double motif pS/pT-P-X-D/E (combining proline-directed with CK2 motifs) was observed only three times among 100 CK2 sites. Although the data set does not allow comprehensive analysis of phosphosites, there seems to be a bias to some of the functional classes for certain motifs. For instance, 50% and 72% of the sites of proteins involved in RNA metabolism and protein folding and translation are part of proline-directed and CK2 motifs, respectively.

It has been proposed that CK2 sites account for 10–20% of eukaryotic phosphoproteomes.⁵⁶ Alignment of all 100 predicted CK2 sites shows a bias toward acidic residues at the +1 and +2 positions (Supplemental Figure S2). Since CK2 favors the phosphorylation of such motifs,⁵⁷ these sites are good candidates for true CK2 targets. Several of the potential CK2 targets were known CK2 substrates in animal and yeast systems, like HSP90 isoforms, ribosomal proteins and high mobility group B (HMGB) proteins. Plant HMGB proteins are also CK2 targets,⁵⁸ but to our knowledge, no sites have been described. In addition to known CK2 targets, we found novel putative CK2 sites in for instance the chromatin remodelling factor BRM and SUMO activating enzyme 2 (Supplemental Figure S2).

Phosphorylation often occurs in an ordered fashion, by one or multiple kinases. Twenty-three out of 48 doubly- and triply phosphorylated peptides were found in a less phosphorylated form (48%), suggesting ordered phosphorylation (or dephosphorylation) of the respective proteins. Doubly- and triply

phosphorylated peptides were found with a spacing of 0–7 amino acids between the phosphosites. The common double phosphorylation motifs pS-X-pS-P and pS/pT-P-X₂-pS-P motifs were both found six times (Supplemental Figure S2), implying proline-directed kinases in ordered phosphorylation. GSK3-like kinases often require prephosphorylation (or priming) of a site at the +4 position. Among 10 potential GSK3 sites (Supplemental Figure S2), we observed for five sites a phosphopeptide with only the priming site phosphorylated, but with the GSK3 site unphosphorylated (Supplemental Table S1). As described above, a tyrosine phosphorylation site in the activation loop of GSK3-like kinase isoforms was determined, suggesting that they were in their active states. With this information, a putative network model centering *Arabidopsis* GSK3-like kinases was constructed (Figure 2B).

Concluding, in our phosphoproteomic screen, we found several phosphosites in activation loops of PKs that might be linked to downstream targets directly, either by analysis of phosphomotifs in substrates or by comparing the data with protein chip experiments such as those performed for MAPKs and CK2.^{23,59}

Phosphorylation of Vesicular Trafficking Machineries.

Plants contain RAB, RHO, ARF, and RAN GTPases, but no RAS GTPases.⁶⁰ We identified 19 sites in 12 proteins that are predicted to regulate RAB, ARF and RAN GTPases, including five in ARF-GTPase activating proteins (ARF-GAPs) (Figure 5). ARF-GAP DOMAIN (AGD) 5, 6, 7 and a previously undescribed AGD (At4g13350) are phosphorylated on serine residues in a similar region C-terminally of the ARF-GAP domain. The site in AGD6 and 7 has a well-conserved dipolar kinase motif in related AGDs of other plant species (Figure 5). SCARFACE (SCF or AGD3/VAN3) is involved in trafficking of the auxin efflux facilitator PIN-FORMED1 (PIN1) and leaf vein pattern formation.^{61,62} Not only ARF-GAPs, but also a member of the ARF guanine nucleotide exchange (GEF) protein family was found to be phosphorylated (Supplemental Table S1).

Important Effectors of RNA Interference Are Protein Kinase Targets. We found two proteins, ARGONAUTE1 (AGO1) and SERRATE (SE), which function in miRNA-mediated silencing.^{63,64} The AGO1 site located right after the PIWI domain, which is an RNase H-like domain that likely mediates the RNA cleavage activity of AGO1 (Figure 6A). The site is conserved in the closely related AGO5 (At2g27880) and orthologues in other plants but not in mammalian Argonaute proteins (data not shown). The MS² and MS³ fragmentation patterns of the AGO1 peptide are shown in Supplemental Figure S3.

SE is involved in shoot meristem function and leaf axial patterning by regulating miRNA-mediated downregulation of genes involved in meristem activity and adaxial leaf fate.⁶⁴ SE is phosphorylated at four sites in the N-terminal region of the protein. Phosphorylation of AGO1 and SE suggests that phosphorylation regulates RNA-based silencing in plants.

Key Regulators of Plant Development Are Phosphorylated. Several of the identified phosphoproteins are involved in plant development. BRAHMA (BRM) and SPLAYED (SYD) are SWI/SNF-like chromatin-remodelling factors that control developmental programs in *Arabidopsis*.^{65,66} Both proteins have partially redundant functions⁶⁷ and were found to be phosphorylated on single sites. The region surrounding the phosphosites suggests that the identified sites might be targeted by different kinases. BRM is an *in vitro* target of MAP kinase 6 (MPK6).²³ However, our identified phosphosite does not match with a

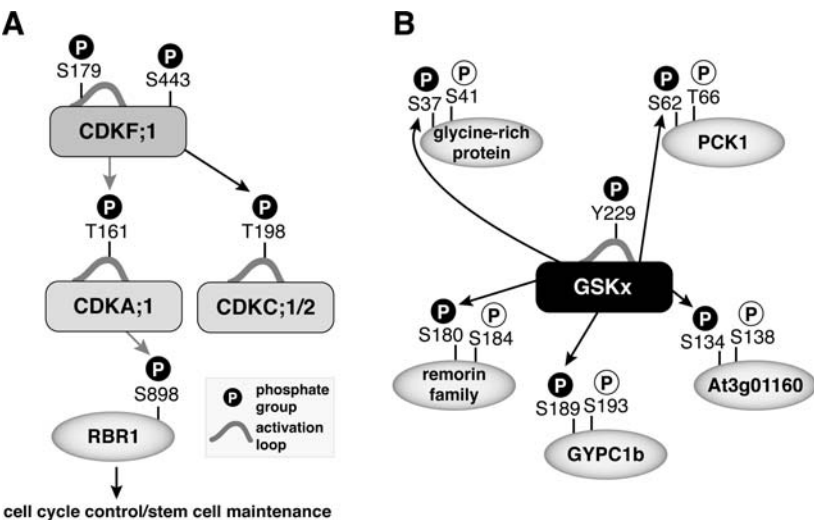


Figure 2. Identified phosphorylation sites within potential cascades of cyclin-dependent kinase and GSK3-like kinase signaling. (A) Two phosphorylation sites were determined in the upstream kinase CDKF;1: one in the activation loop (S179) and a C-terminal one (S443) that matches with a CDK consensus motif, suggesting potential feedback regulation by a CDK. Although only CDKA;1 has been described as a CDKF;1 target, the phosphorylation of CDKC;1 might be caused by CDKF;1 as well. The C-terminal S898 site in RBR1 also matches a CDK consensus. Since RBR1 is an *in vitro* target of CDKA;1, it is plausible to assume that this kinase is responsible for this event. Arrows between proteins for which experiments have suggested that they are kinase-substrate pairs are indicated in gray. (B) Putative network of GSK3/shaggy-like kinases and their substrates. A tyrosine phosphorylation site in the activation loop of a GSK3/shaggy-like kinase (GSKx, *Arabidopsis* GSK3/shaggy-like kinase isoform alpha, gamma, delta, eta or iota) was determined, indicating that this PK was in its active state. Potential GSK3 consensus motifs were found in 10 phosphoproteins (Supplemental Figure S2), but for the five substrates shown here, phosphopeptides were found with only the priming site phosphorylated (white circles), in addition to the potential GSK3 site (black circles).

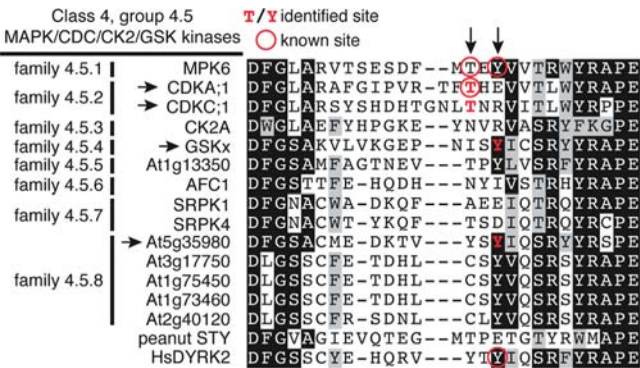


Figure 3. Tyrosine phosphorylation of protein kinases. In this phosphoproteomic study, four phosphopeptides were identified that were derived from the activation loops of a group of PKs belonging to class 4 out of the 5 classes of plant kinases (PlantsP database, <http://plantsp.genomics.purdue.edu>). The identified pY residues of the GSK3/shaggy-like and the unknown At5g35980 kinases are located at the same position as the well-known tyrosine of MPK6. Multiple members of group 4.5 kinases have a tyrosine at the corresponding position, suggesting that they might be phosphorylated on tyrosine as well. CK2A, casein kinase 2 alpha; SRPK, SR protein-specific kinase; GSK, *Arabidopsis* GSK3/Shaggy-like kinase. The x in GSKx denotes isoform α , γ , η or ι since the activation loop sequences of these isoforms are identical. The arrows indicate the positions of one or more phosphorylation sites within the activation loops.

typical MAPK consensus site, but with a CK2 site (Supplemental Figure S2). Although the potential MAPK site has not been determined, this could suggest that BRM is targeted by different PKs on distinct sites.

VERNALISATION INDEPENDENCE 4 (VIP4) is involved in the regulation of flowering time⁶⁸ and was found to be phosphorylated on seven sites (Figure 6B). Five sites match with

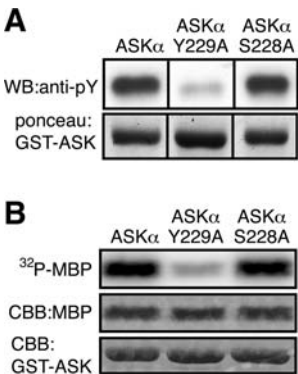


Figure 4. Phosphorylation of *Arabidopsis* GSK3/shaggy-like kinase ASK α on Y229 is required for transphosphorylation activity. (A) ASK α and two mutant versions, ASK α S228A and ASK α Y229A, were purified from *E. coli* as GST fusion proteins, separated by SDS-PAGE and blotted. The blot was probed with an anti-phosphotyrosine antibody (WB:anti-pY). Loading of the GST fusion proteins was determined by ponceau staining (lower panel). (B) Activity of ASK α and ASK α mutants towards myelin basic protein (MBP). Phosphorylation of MBP was tested in a kinase assay. Incorporation of ³²P into MBP was determined by autoradiography (upper panel). Equal loading of the GST fusion proteins and MBP was verified by coomassie brilliant blue (CBB) staining (lower panels).

a CK2 motif, one with a proline-directed kinase motif and one that shares both these motifs. VIP4 likely acts in a transcriptional regulator complex related to budding yeast Paf1c.⁶⁹

WUSCHEL-INTERACTING PROTEIN 1 (WSIP1)/TOPLESS (TPL) and four TOPLESS-RELATED (TPR) proteins are functionally redundant putative transcriptional corepressors that regulate apical embryonic fate.^{70,71} A conserved phosphorylation site was determined in WSIP1/TPL and TPR1 (Figure 6C

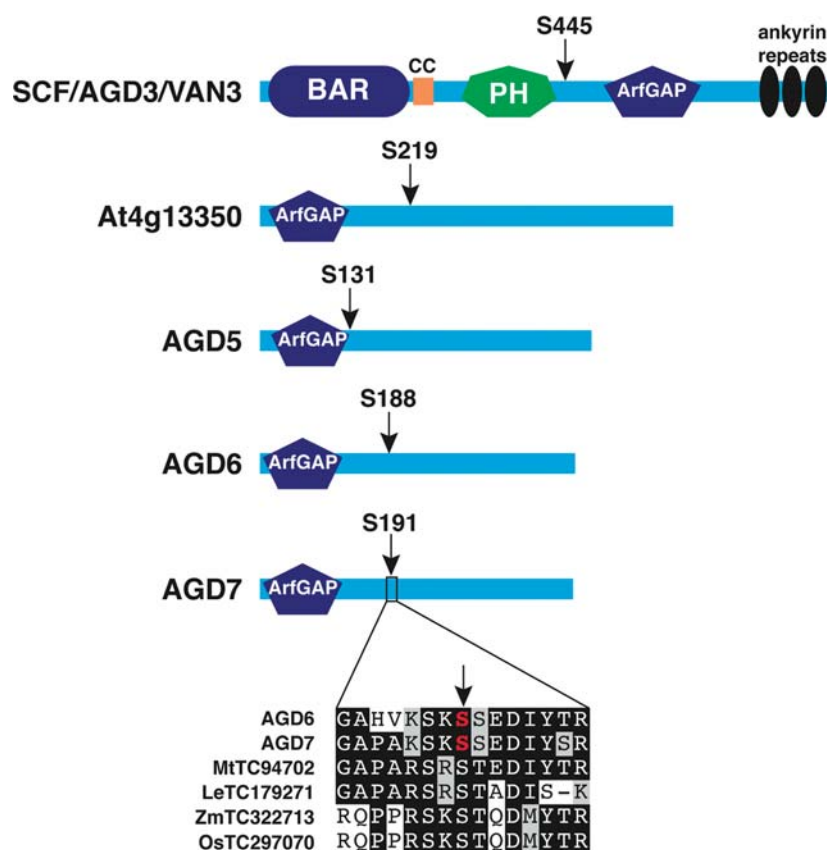


Figure 5. Phosphoserine residues identified in different ARF GTPase-activating proteins (ARF-GAPs). At4g13350 has not been assigned to the ARF-GAP DOMAIN (AGD) family, but contains a well-conserved ARF-GAP domain. The alignment of the region surrounding the phosphosite in AGD6 and -7 with *Medicago truncatula* (Mt), *Zea mays* (maize, Zm) and *Oryza sativa* (rice, Os) proteins shows the conservation of the site in orthologues throughout the plant kingdom. The localization of the phosphorylation sites with AGD5–7 and At4g13350 suggests a common mode of regulation of these ARF-GAPs by phosphorylation. BAR, Bin-Amphiphysin-Rvs; CC, coiled coil; PH, pleckstrin homology.

and D). The site is conserved in TPR2–4, as well as in proteins from other species that are similar to TPL (Figure 6D). The sites identified in TPL and TPR1 both match a proline-directed/basophilic kinase double phosphorylation motif. Although this motif is present in TPL, TPR1 and -2, it is not found in TPR3 and -4 (Figure 6D).

Phosphorylation Site Profiling by a Peptide Array Approach. Alternative approaches to phosphoproteomics include peptide chips to identify kinase substrates as well as to quantitatively determine changes in the activities of a mixture of PKs under different experimental conditions.²⁵ So far, however, no chips were available with peptides corresponding to *in vivo* phosphorylation sites of plant substrates. Therefore, we developed a trial chip with a set of 47 peptide sequences which were selected out of different functional groups of phosphoproteins from our data sets of this and a previous study.³⁵ Peptides of 11 amino acid length were synthesized and spotted in triplicate sets on glass slides. We applied PK mixtures consisting of cytoplasmic and nuclear fractions onto the peptide slides and determined which peptides are phosphorylated. Seventeen peptides were phosphorylated by the cytosolic extract, and 20 by the nuclear extract (Figure 7). In total, 22 different peptides were phosphorylated on the chip. In general, spot intensities of chips phosphorylated by PKs of the nuclear extracts were higher than in PK mixtures of the cytosolic extracts, which have to be diluted to reduce background noise on the chips.²⁶ Visual inspection and quantitative

analysis (Figure 7 and Supplemental Table S2) of the phosphoprofiles revealed a large overlap of peptides that can be phosphorylated by PKs of both cellular fractions. However, although it is difficult to quantitatively compare the peptide phosphorylation values between the cytosolic and nuclear extracts, several clear differences between kinome activities in these extracts could be seen. Overall, we observed selective phosphorylation of five peptides by PKs in the nuclear extract, and two peptides by cytosolic PKs (Figure 7). Three of the peptides phosphorylated by only the nuclear extract are derived from the activation loops of the RAF-like kinase RAF36 and SnRK2 isoforms. This observation points to a possible role of RAF36 and SnRK2s in the nucleus. In agreement with this hypothesis, it was recently reported that two (other) SnRK2 isoforms directly phosphorylate transcription factors.⁷² In addition, a number of peptides corresponding to five proteins involved in mRNA splicing (SCL30, SCL30a, SRp34a, SR45 and CypRS64) all show a relative higher phosphorylation by PKs in the nuclear fraction. In contrast, peptides corresponding to an unknown protein (At5g09850) and to the activation loop of the AGC kinase NDR-8 were phosphorylated by a PK present or active only in the cytosolic extract. Overall, these results suggest that the PKs that target the activation loops of the respective PKs may be either localized or active in particular subcellular compartments. In summary, these data indicate that the

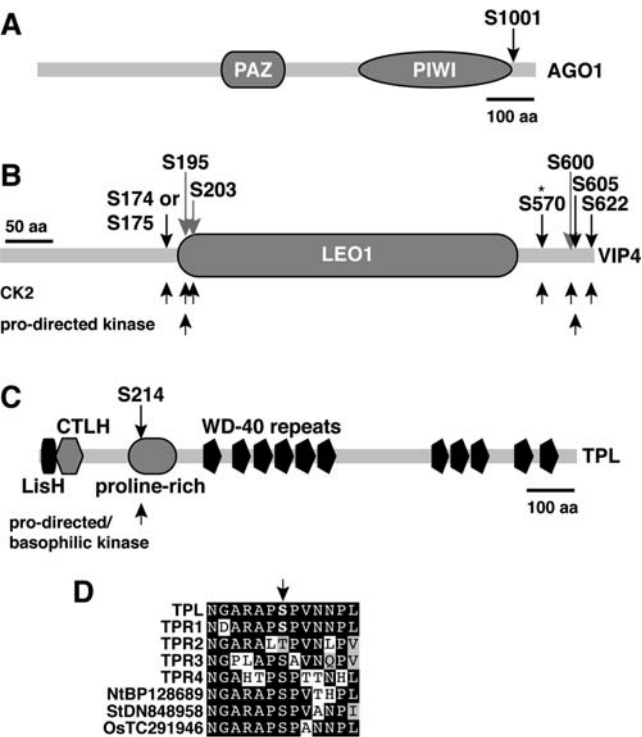


Figure 6. Phosphorylation of proteins involved in RNA interference and development. (A) Phosphorylation sites in ARGONAUTE1 (AGO1). PAZ, domain shared by the proteins Piwi, Argonaute and Zwillie. PIWI, RNase H-like domain. (B) Phosphorylation sites in VERNALIZATION INDEPENDENCE 4 (VIP4). Gray arrows indicate sites that have been observed in nonphosphorylated form. The asterisk indicates a splicing variant-specific phosphosite. (C) Phosphorylation site in TOPLESS (TPL). (D) Conservation of the sites identified in TPL and TPR1 in other *Arabidopsis* TPRs and proteins homologous to TPL from other plant species.

peptide chip approach provides a quantitative source for the analysis of PK activities in different subcellular fractions of plant extracts.

Differential Screening for Oxidative Stress-Regulated Phosphorylation Events Using Peptide Chips and Identification of Responsible Protein Kinases. Another application of phosphopeptide profiling on chips is the analysis of complex PK mixtures in response to changing conditions.²⁵ To test this idea for plants, *Arabidopsis* cells were treated by oxidative stress for 5 min with 4 mM H₂O₂ that induces activities of the MAPKs MPK3, -4 and -6 (Figure 8A and Supplemental Figure S4).⁷³ Separate peptide chips were incubated with cytosolic extracts of control and oxidative stress treated cells. In two independent experiments, we observed an increased phosphorylation of a peptide derived from a putative chromatin remodelling protein (At5g07350) and a peptide from the activation loop of the PK At5g35980 (Figure 8B). Interestingly, the PK is phosphorylated *in vivo* on the tyrosine residue, suggesting that a tyrosine-directed kinase is activated by oxidative stress. Phosphorylation of a peptide derived from the mRNA splicing factor SCL30 increased most strongly in all experiments (Figure 8B), and was therefore selected for further analysis.

Our data suggested that a PK targeting SCL30 is rapidly activated by H₂O₂. Inspection of the peptide sequence revealed putative phosphorylation motifs for SR-specific PKs and MAPKs. SRPK4 is one of four SRPKs in *Arabidopsis* and might be a

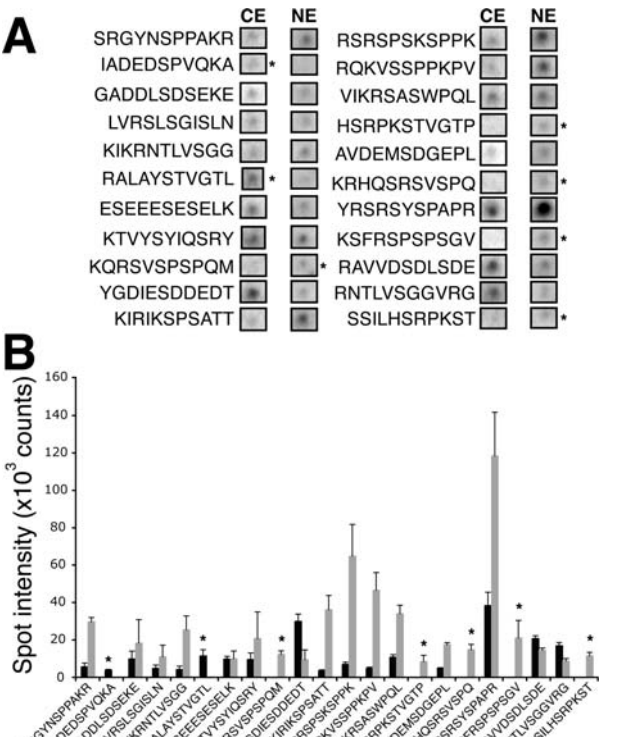


Figure 7. Peptide chip phosphorylation. For phosphosite-specific profiling of phosphorylation, 47 peptides containing *in vivo* phosphorylation sites identified in this study were spotted onto glass slides. (A) Slides were incubated with either cytosolic (CE) or nuclear extracts (NE). (B) Quantification of spot intensities. Asterisks indicate spots that were phosphorylated by only the CE (black bars) or the NE (gray bars). Spot intensity values, identified phosphosites in these peptides and the corresponding protein identities are given in Supplemental Table S2.

plausible candidate because it can phosphorylate another SR protein.³⁵ However, it was not clear whether SRPK4 is activated by H₂O₂. On the other hand, MAPKs are activated by H₂O₂ (Figure 8A), but it was unclear whether they can target SCL30. To test whether any of these PKs could be responsible for the oxidative stress-induced phosphorylation of SCL30, SRPK4 was purified as a glutathione S-transferase (GST) fusion from *E. coli* and tested for phosphorylation activity toward purified GST (control) and GST-SCL30. As shown in Figure 8C, GST-SRPK4 phosphorylated SCL30, but not GST. In addition to full-length GST-SCL30, several truncated products were phosphorylated by SRPK4, suggesting that N-terminal sites are also targeted by SRPK4. These kinase assays suggested that SRPK4 might be the kinase mediating oxidative stress-induced phosphorylation of SCL30. However, by expression of SRPK4 in *Arabidopsis* protoplasts, we observed no activation of SRPK4 by H₂O₂ (Figure 8D). This might be explained by the fact that SRPK4 contains an aspartic acid at the position analogous to the phosphotyrosine in the activation loop of MAPKs and the two PKs that we found to be phosphorylated (Figure 3). Since mutation of phosphosites to acidic residues often mimics the phosphorylated state, this might render SRPK4 constitutively active. So we wondered whether H₂O₂-inducible MAPKs can act on SCL30. For this purpose, MPK3, MPK4 and MPK6 were immunoprecipitated from *Arabidopsis* cells with specific antibodies. By a radioactive kinase assay, it was shown that all three MAPKs can phosphorylate GST-SCL30, but not GST

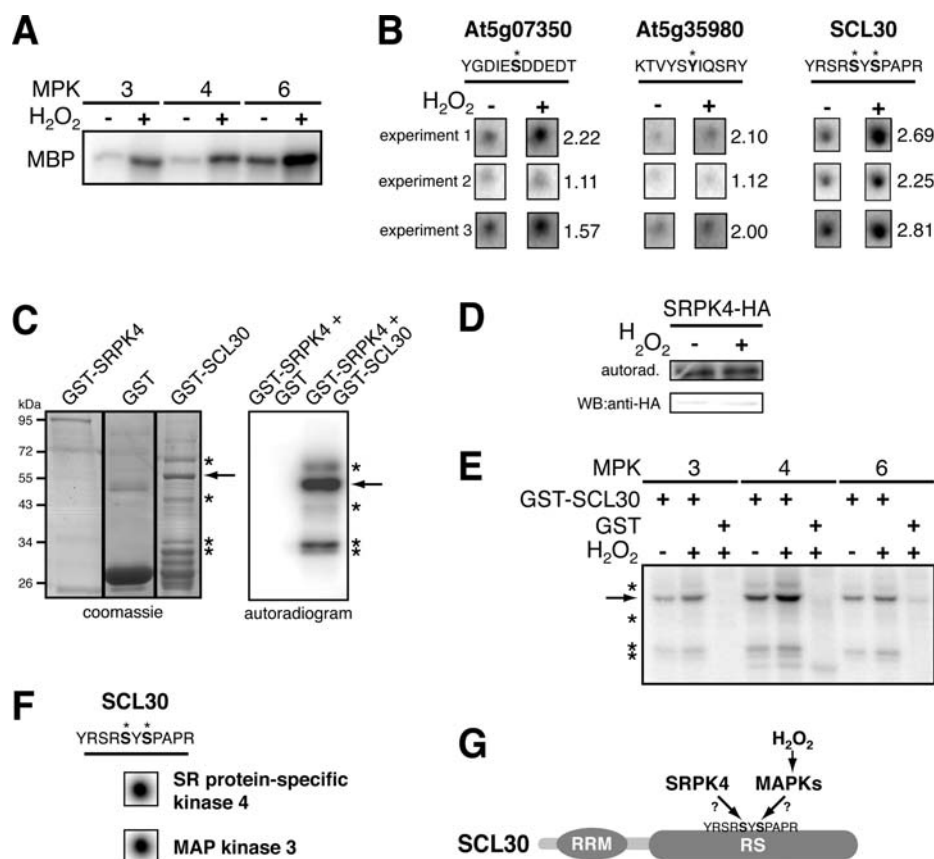


Figure 8. H₂O₂-induced phosphorylation of an SCL30-derived peptide and *in vitro* phosphorylation of SCL30 by different kinases. (A) Activity of MPK3, -4 and -6 in cell cultures after a 5 min treatment with water (-) or H₂O₂ (+). MPK3, -4 and -6 were immunoprecipitated from cell culture extracts and tested in a radioactive kinase assay towards MBP. (B) Cytosolic extracts of 5 min water-treated (-) and H₂O₂-treated (+) *Arabidopsis* cells were incubated on peptide chips. The three indicated spots were induced in at least two independent experiments. Identified *in vivo* sites within the peptide sequences are indicated by bold letters and asterisks. Values indicate induction of phosphorylation by H₂O₂-treated extracts compared to control extracts. (C) GST-SRPK4 was tested for kinase activity towards GST (control) and GST-SCL30 purified from *E. coli* (see coomassie-stained gel). After the kinase assay, proteins were separated by SDS-PAGE and the gel was dried and exposed to a phosphorimager screen (see autoradiogram). The arrow indicates full-length GST-SCL30 (expected mass 56 kDa), asterisks indicate C-terminally truncated forms or a slower migrating band on top of full-length GST-SCL30. (D) SRPK4-HA was expressed in *Arabidopsis* protoplasts and its activity tested towards GST-SCL30 (only the full-length band is shown here). (E) Phosphorylation of GST-SCL30 by MAPKs that were immunopurified from suspension cultured cells treated for 5 min with water (-) or H₂O₂ (+). As a negative control, GST was tested with the kinases immunoprecipitated from the H₂O₂-treated cells. (F) Phosphorylation of the SCL30-derived peptide on the chip by GST-SRPK4 (SRPK4) and GST-MPK3 (MPK3). The peptide originates from the Ser/Arg-rich (RS) domain and contains two of the nine previously identified phosphorylation sites (35). (G) Model for the phosphorylation of SCL30 by SRPK4 and MAPKs. Although SRPK4 constitutively phosphorylates SCL30, MAPKs do this primarily during oxidative stress (and potentially other stresses). We hypothesize that SRPK4 targets the first *in vivo* site, whereas MAPKs likely phosphorylate the second, proline-directed site.

(Figure 8E). A slight autophosphorylation activity of MPK4 and -6 can also be seen (Figure 8E).

Since both SRPK4 and stress-responsive MAPKs phosphorylate full-length SCL30, we addressed the question whether the SCL30 peptide was phosphorylated on the peptide array by these kinases. To use kinases immunoprecipitated from plant extracts is not possible, since they are immobilized on beads that cannot be applied on peptide chips. Therefore, recombinant GST fusion proteins of SRPK4 and MPK3 were separately incubated on the chips. Indeed, the peptide was phosphorylated by both kinases (Figure 8F). These data show that both SRPK4 and MAPKs can phosphorylate SCL30. However, since only MAPKs are activated by H₂O₂, we conclude that the stress-responsive PK activity observed in the peptide chip experiments is derived from MAPKs. These data suggest that SRPK4 and MAPKs can act together to mediate both constitutive and oxidative stress-induced phosphorylation of

SCL30. It remains to be determined whether SRPK4 and MAPKs phosphorylate overlapping or different residues in the splicing factor (Figure 8G).

Discussion

Site-Specific Mapping of the Intracellular *Arabidopsis* Phosphoproteome. Phosphopeptide isolation by IMAC followed by MS analysis allows mapping of numerous individual phosphosites in a single sample. Importantly, studies on *Arabidopsis* described many phosphorylation sites conserved in orthologues of other plant species suggesting that knowledge gained from this model plant can be transferred to crop species in most cases.¹⁶ Our approach of IMAC purification and sequencing of phosphopeptides by mass spectrometry revealed many novel phosphorylation sites in *Arabidopsis* kinases and substrates. The data set of more than 300 sites shows less than 20% overlap

with previous reports on the *Arabidopsis* plasma membrane phosphoproteome that collectively described more than 1000 sites.^{14,33} Some of the commonly identified sites in our data set are likely plasma membrane contaminants (receptor-like kinases, plasma membrane proton-ATPase) and highly abundant intracellular proteins (ribosomal proteins, metabolic enzymes) in theirs (Supplemental Table S1). We have found phosphorylation sites in many proteins predicted to regulate small GTPases, such as an ARF-GEF and five ARF-GAPs, including SCF/AGD3/VAN3^{61,62} and AGD7.⁷⁴ These data indicate that in plants vesicular trafficking is highly regulated by phosphorylation. Several other novel phosphoproteins are well-known regulators of developmental processes such as flowering and leaf patterning and function as chromatin remodelling factors, transcriptional regulators and RNA silencing factors. AGO1 is phosphorylated C-terminally of its PIWI domain, suggesting that phosphorylation of AGO1 might affect its slicing activity.

Jones et al.³⁰ described the use of quantitative mass spectrometry to identify pathogen-induced changes in phosphoprotein abundance. Since no phosphorylation sites were described, we compared their protein list with our data set. We found six novel phosphorylation sites for six phosphoproteins identified in their study (Supplemental Table S1). For instance, we found a conserved CK2 site in HSP90. This shows that because it is difficult to map phosphosites by pursuing a gel-based approach, a combination with IMAC-mass spectrometry is advantageous.

Identification of Upstream Kinases by Analysis of Phosphorylated Motifs. Analysis of the amino acid sequence surrounding the phosphorylation site can give valuable clues to the identity of the responsible PK(s). In our study, this analysis suggests that CK2, basophilic kinases, GSK3/shaggy-like kinases, SnRKs and proline-directed kinases collectively are responsible for most of the observed phosphorylation events. An activated form of a kinase is usually correlated with the phosphorylation state of its activation loop. In agreement with this finding, we found phosphorylation sites in the activation loops of several isoforms of AGC kinases (PKA, PKG and PKC-related basophilic kinases), SnRKs, a GSK3/shaggy-like kinase and CDKs. We further provided independent experimental evidence that the GSK3/shaggy-like kinase ASK α is phosphorylated on tyrosine 229 in its activation loop and that this phosphorylation event is indeed required for its protein kinase activity toward external substrates. The absence of phosphopeptides derived from the activation loops of the four CK2 isoforms is explained by the fact that tryptic peptides spanning the potential phosphorylation sites are too small to be detected by our mass spectrometry approach (Figure 3). Two PKs were found to be phosphorylated on a tyrosine residue in their activation loops. These residues are located at the analogous position of the tyrosine in the TxY motif of MAPKs, which is phosphorylated *in vivo* in yeast, plants and animals. Our data suggests that this is not restricted to MAPKs in plants but perhaps to members of a subgroup of PKs. Supporting this hypothesis, PK12, a PK of the LAMMER family, autophosphorylates *in vitro* on tyrosine residues in addition to serine and threonine residues.⁷⁵ However, the tyrosine site has not been determined.

A large proportion of the identified phosphorylation motifs are a combination of two kinase motifs. It has been suggested that these sites might respond to different kinases.¹² We observed in addition to the recently described dipolar motif, a

combined motif of basophilic and proline-directed kinases. These data extend the observation that phosphosites might be targeted by different types of PKs.

Phosphorylation Profiling of the Oxidative Stress Signaling Pathway Using Peptide Arrays. In addition to mass spectrometry-based approaches to study signaling pathways, peptide and protein arrays have been used for some time already for animal and yeast research, but not extensively for plant systems. Two plant protein array-based studies have suggested potential casein kinase 2 (CK2) and MAPK substrates.^{23,59,76}

Many kinases phosphorylate conserved motifs, thereby allowing mass spectrometry and peptide chip analyses to infer the kinases responsible for targeting the identified phosphorylation sites. In animals, peptide chips have been used for kinome profiling of animal cells.²⁵ With the use of nonplant peptide chips, protein kinase activities in complex plant extracts have also been successfully monitored.²⁶ Our test array containing plant peptides with *in vivo* phosphorylation sites of *Arabidopsis* proteins allowed us to examine different kinase activities toward these peptides. Currently, however, the substrate specificities of most plant kinases are unknown, and more research is needed for the high-throughput discovery of kinases–substrate links using peptide chips for kinome profiling.

Our assays showed that many peptides were phosphorylated by PKs of both cytosolic and nuclear extracts. This is in agreement with recent data suggesting that most kinases are not confined to specific subcellular locations.⁵ On the other hand, many peptides on the chip were phosphorylated exclusively by either the cytosolic or the nuclear extract. Several reasons might explain this selective phosphorylation, including the inactivation of a kinase during extraction/assaying conditions, too low kinase activity or the absence of kinase docking domains in the short peptide sequence. In any case, peptide arrays are a way to assess different kinase activities in cellular extracts that contain a complex mixture of PKs. More extensive plant peptide arrays could allow more comprehensive kinome analysis of different subcellular compartments, and changes caused by environmental cues.

To detect early changes in the kinome, we treated cells for 5 min with H₂O₂ and compared cytosolic extracts of treated and mock-treated cells. A drawback of peptide arrays is that the phosphorylation sites are not determined *in vivo* on their respective proteins. However, the fact that our peptide library was based on *in vivo* sites might suggest that the oxidative stress-induced phosphorylation of SCL30 also occurs *in vivo*. Our analysis suggests that MAPKs and not SRPKs are responsible for the oxidative stress-increased SCL30 phosphorylation, revealing a potential connection between oxidative stress and phosphorylation of SCL30 by MAPKs. This might be a more general phenomenon, since a protein array-based approach has shown that MPK3 and MPK6 target other SR proteins as well.²³ Moreover, heat stress induces dephosphorylation and inactivation of an SR protein in animal cells.^{77,78} SR proteins control both splice site selection and spliceosome assembly and interactions between SR proteins and other spliceosome components are regulated by phosphorylation.⁷⁹ Therefore, MAPKs might connect stress signals to the mRNA splicing machinery via SR protein phosphorylation, potentially leading to differential splicing of pre-mRNAs.⁸⁰

Conclusions

Our study focused on the mass spectrometry-based identification of novel PK substrates, including their potential

upstream kinases. Comparison of the identified sites with known kinase motifs suggests that many of the phosphoproteins are targets of different kinases, thereby serving as platforms for multiple signal inputs. Therefore, as stated by others,¹¹ it is clear that quantitative phosphorylation analyses require the measurement of individual phosphorylation sites. In this study, we combined mass spectrometry with a peptide-based approach, revealing a potential link between stress-induced MAPK phosphorylation and, via SCL30, the mRNA splicing machinery. Mainly in animal and yeast research, mass spectrometry-based phosphoproteomic and peptide chip analysis have been successful in providing novel insights into signaling networks.¹⁸ A combination of these large-scale approaches for plant research will likewise reveal PK specificities and allow the connection between kinases and their substrates in a high-throughput manner. This should ultimately provide a more comprehensive view of phosphorylation networks in plant signaling. Future research should also focus on the functional analysis of identified phosphorylation sites. In conclusion, approaches that combine phosphoproteome dynamics with other large-scale analyses promises to reveal the complex networks that regulate the biology of organisms.

Acknowledgment. We gratefully acknowledge Tita Ritsema (Utrecht University, Utrecht, The Netherlands) for helping us to set up the peptide chip assays. We thank Andriy Belokurov for technical assistance. The Austrian Science Foundation, the Vienna Science and Technology Fund and the European Union supported this work.

Supporting Information Available: Table S1, Excel file with all phosphopeptides described in this study; Table S2, Excel file with information about peptides on the array and their phosphorylation intensities. Figure S1, phosphorylation of metabolic enzymes. (A) Phosphorylation of phosphoenolpyruvate carboxykinase. Bold and red lettering indicates unambiguous sites. Accession numbers: AtPCK1 (At4g37870), AtPCK2 (At5g65690), LePCK (TC162799), GmPCK (TC204272), MtPCK (TC106827), OsPCK (CB675232), ZmPCK (TC299411), TaPCK (TC266102). (B) Phosphorylation of UDP-glucose 6-dehydrogenase UGD1/2/3. Although the peptide sequence is identical to At3g01010, there is no basic amino acid preceding this sequence, indicating that there is no trypsin digestion site. (C) Phosphorylation of peptide methionine sulfoxide reductase 2 (PMSR2). Accession numbers: AtPMSR1 (At5g61640), AtPMSR2 (At5g07460), AtPMSR3 (At5g07470), AtPMSR4 (At4g25130). Figure S2, phosphorylation sites grouped by kinase motif. The asterisk next to the fructose-6-phosphate 2-kinase/fructose-2,6-bisphosphatase phosphosite (partial CPK/SnRK) indicates a site that is targeted *in vitro* by CPK3.⁴¹ For the double phosphorylation motifs, the phosphopeptides with 3 amino acids spacing between the phosphosites are omitted, since this is identical to a GSK3 motif. Black and gray boxes indicate identical and homologous amino acids, respectively, if more than 50% of the sequences share this residue (except for Pro-directed and basophilic motifs, where thresholds of 20% and 30% were used, respectively). h, hydrophobic residue. Figure S3, examples of peptide fragmentation patterns. MS² and MS³ spectra of the AGO1-derived phosphopeptide FYMEPETpS-DSGSMASGSMAR and the GSK3-like kinase-derived phosphopeptide GEPNISpYICSR. Note the prominent loss of water from the threonine residue at position y14 during MS³ fragmentation. pS indicates a phosphoserine residue; S* indicates a phosphoserine that has lost its phosphate group (dehydroalanine).

Figure S4, MPK6 is maximally activated after 5 min of H₂O₂ treatment in cell culture. *In vitro* kinase assay with MPK6 immunoprecipitated from cell culture treated with H₂O₂ for indicated times (minutes). Myelin basic protein (MBP) was used as a substrate. Upper panel, autoradiogram; lower panel, the coomassie brilliant blue-stained gel checked for MBP loading. Figure S5, mass spectra of identified phosphopeptides. This figure includes MS² and, if available, MS³ spectra for each phosphopeptide, and peptides are arranged in the same order as presented in Supplemental Table S1. This material is available free of charge via the Internet at <http://pubs.acs.org>.

References

- (1) Tuskan, G. A.; Difazio, S.; Jansson, S.; Bohlmann, J.; Grigoriev, I.; Hellsten, U.; Putnam, N.; Ralph, S.; Rombauts, S.; Salamov, A.; Schein, J.; Sterck, L.; Aerts, A.; Bhalerao, R. R.; Bhalerao, R. P.; Blaudez, D.; Boerjan, W.; Brun, A.; Brunner, A.; Busov, V.; Campbell, M.; Carlson, J.; Chalot, M.; Chapman, J.; Chen, G. L.; Cooper, D.; Coutinho, P. M.; Couturier, J.; Covert, S.; Cronk, Q.; Cunningham, R.; Davis, J.; Degroove, S.; Dejardin, A.; Depamphilis, C.; Detter, J.; Dirks, B.; Dubchak, I.; Duplessis, S.; Ehlting, J.; Ellis, B.; Gendler, K.; Goodstein, D.; Gribskov, M.; Grimwood, J.; Groover, A.; Gunter, L.; Hamberger, B.; Heinze, B.; Helariutta, Y.; Henrissat, B.; Holligan, D.; Holt, R.; Huang, W.; Islam-Faridi, N.; Jones, S.; Jones-Rhoades, M.; Jorgensen, R.; Joshi, C.; Kangasjarvi, J.; Karlsson, J.; Kelleher, C.; Kirkpatrick, R.; Kirst, M.; Kohler, A.; Kalluri, U.; Larimer, F.; Leebens-Mack, J.; Leple, J. C.; Locascio, P.; Lou, Y.; Lucas, S.; Martin, F.; Montanini, B.; Napoli, C.; Nelson, D. R.; Nelson, C.; Nieminen, K.; Nilsson, O.; Pereda, V.; Peter, G.; Philippe, R.; Pilate, G.; Poliakov, A.; Razumovskaya, J.; Richardson, P.; Rinaldi, C.; Ritland, K.; Rouze, P.; Ryaboy, D.; Schmutz, J.; Schrader, J.; Segerman, B.; Shin, H.; Siddiqui, A.; Sterky, F.; Terry, A.; Tsai, C. J.; Uberbacher, E.; Unneberg, P.; Vahala, J.; Wall, K.; Wessler, S.; Yang, G.; Yin, T.; Douglas, C.; Marra, M.; Sandberg, G.; Van de Peer, Y.; Rokhsar, D. *Science* **2006**, *313*, 1596–1604.
- (2) The Arabidopsis Genome Initiative **2000**, *Nature* **408**, 796–815.
- (3) International Rice Genome Sequencing Project **2005**, *Nature* **436**, 793–800.
- (4) Ubersax, J. A.; Ferrell, J. E., Jr. *Nat. Rev. Mol. Cell. Biol.* **2007**, *8*, 530–541.
- (5) Lindling, R.; Jensen, L. J.; Ostheimer, G. J.; van Vugt, M. A.; Jorgensen, C.; Miron, I. M.; Diella, F.; Colwill, K.; Taylor, L.; Elder, K.; Metalnikov, P.; Nguyen, V.; Pasculescu, A.; Jin, J.; Park, J. G.; Samson, L. D.; Woodgett, J. R.; Russell, R. B.; Bork, P.; Yaffe, M. B.; Pawson, T. *Cell* **2007**, *129*, 1415–1426.
- (6) Deshaies, R. J.; Ferrell, J. E., Jr. *J. Cell Biol.* **2001**, *107*, 819–822.
- (7) Andersson, L.; Porath, J. *Anal. Biochem.* **1986**, *154*, 250–254.
- (8) Larsen, M. R.; Thingholm, T. E.; Jensen, O. N.; Roepstorff, P.; Jorgensen, T. J. *Mol. Cell. Proteomics* **2005**, *4*, 873–886.
- (9) Pinkse, M. W.; Uitto, P. M.; Hilhorst, M. J.; Ooms, B.; Heck, A. J. *Anal. Chem.* **2004**, *76*, 3935–3943.
- (10) Ficarro, S. B.; McClelland, M. L.; Stukenberg, P. T.; Burke, D. J.; Ross, M. M.; Shabanowitz, J.; Hunt, D. F.; White, F. M. *Nat. Biotechnol.* **2002**, *20*, 301–305.
- (11) Olsen, J. V.; Blagoev, B.; Gnäd, F.; Macek, B.; Kumar, C.; Mortensen, P.; Mann, M. *Cell* **2006**, *127*, 635–648.
- (12) Villén, J.; Beausoleil, S. A.; Gerber, S. A.; Gygi, S. P. *Proc. Natl. Acad. Sci. U.S.A.* **2007**, *104*, 1488–1493.
- (13) Bodenmiller, B.; Mueller, L. N.; Mueller, M.; Domon, B.; Aebersold, R. *Nat. Methods* **2007**, *4*, 231–237.
- (14) Benschop, J. J.; Mohammed, S.; O'Flaherty, M.; Heck, A. J.; Slijper, M.; Menke, F. L. *Mol. Cell. Proteomics* **2007**, *6*, 1198–1214.
- (15) Mukherji, M. *Expert Rev. Proteomics* **2005**, *2*, 117–128.
- (16) Peck, S. C. *J. Exp. Bot.* **2006**, *57*, 1523–1527.
- (17) Nühse, T. S.; Bottrill, A. R.; Jones, A. M.; Peck, S. C. *Plant J.* **2007**, *51*, 931–940.
- (18) Ptacek, J.; Snyder, M. *Trends Genet.* **2006**, *22*, 545–554.
- (19) Feilner, T.; Kersten, B. *Methods Mol. Biol.* **2007**, *355*, 379–390.
- (20) Beernink, H. T.; Nock, S. *Expert Rev. Proteomics* **2005**, *2*, 487–497.
- (21) Ptacek, J.; Devgan, G.; Michaud, G.; Zhu, H.; Zhu, X.; Fasolo, J.; Guo, H.; Jona, G.; Breitkreutz, A.; Sopko, R.; McCartney, R. R.; Schmidt, M. C.; Rachidi, N.; Lee, S. J.; Mah, A. S.; Meng, L.; Stark, M. J.; Stern, D. F.; De Virgilio, C.; Tyers, M.; Andrews, B.; Gerstein, M.; Schweitzer, B.; Predki, P. F.; Snyder, M. *Nature* **2005**, *438*, 679–684.
- (22) Zhu, H.; Klemic, J. F.; Chang, S.; Bertone, P.; Casamayor, A.; Klemic, K. G.; Smith, D.; Gerstein, M.; Reed, M. A.; Snyder, M. *Nat. Genet.* **2000**, *26*, 283–289.

- (23) Feilner, T.; Hultschig, C.; Lee, J.; Meyer, S.; Immink, R. G.; Koenig, A.; Possling, A.; Seitz, H.; Beveridge, A.; Scheel, D.; Cahill, D. J.; Lehrach, H.; Kreutzberger, J.; Kersten, B. *Mol. Cell. Proteomics* **2005**, *4*, 1558–1568.
- (24) Collins, M. O.; Yu, L.; Coba, M. P.; Husi, H.; Campuzano, I.; Blackstock, W. P.; Choudhary, J. S.; Grant, S. G. *J. Biol. Chem.* **2005**, *280*, 5972–5982.
- (25) Diks, S. H.; Kok, K.; O'Toole, T.; Hommes, D. W.; van Dijken, P.; Joore, J.; Peppelenbosch, M. P. *J. Biol. Chem.* **2004**, *279*, 49206–49213.
- (26) Ritsema, T.; Joore, J.; van Workum, W.; Pieterse, C. M. *Plant Methods* **2007**, *3*, 3.
- (27) Rossignol, M. *Curr. Opin. Plant Biol.* **2006**, *9*, 538–543.
- (28) Khan, M.; Takasaki, H.; Komatsu, S. *J. Proteome Res.* **2005**, *4*, 1592–1599.
- (29) Irar, S.; Oliveira, E.; Pages, M.; Goday, A. *Proteomics* **2006**, *6* (Suppl. 1), S175–185.
- (30) Jones, A. M.; Bennett, M. H.; Mansfield, J. W.; Grant, M. *Proteomics* **2006**, *6*, 4155–4165.
- (31) Agrawal, G. K.; Thelen, J. J. *Mol. Cell. Proteomics* **2006**, *5*, 2044–2059.
- (32) Laugesen, S.; Messinese, E.; Hem, S.; Pichereaux, C.; Grat, S.; Ranjeva, R.; Rossignol, M.; Bono, J. J. *Phytochemistry* **2006**, *67*, 2208–2214.
- (33) Nühse, T. S.; Stensballe, A.; Jensen, O. N.; Peck, S. C. *Plant Cell* **2004**, *16*, 2394–2405.
- (34) Heazlewood, J. L.; Durek, P.; Hummel, J.; Selbig, J.; Weckwerth, W.; Walther, D.; Schulze, W. X. *Nucleic Acid Res.* **2008**, *36* (Database issue), D1015–1021.
- (35) De la Fuente van Bentem, S.; Anrather, D.; Roitinger, E.; Djamei, A.; Hufnagl, T.; Barta, A.; Csaszar, E.; Dohnal, I.; Lecourieux, D.; Hirt, H. *Nucleic Acids Res.* **2006**, *34*, 3267–3278.
- (36) Kiegerl, S.; Cardinale, F.; Siligan, C.; Gross, A.; Baudouin, E.; Liwosz, A.; Eklof, S.; Till, S.; Bogre, L.; Hirt, H.; Meskiene, I. *Plant Cell* **2000**, *12*, 2247–2258.
- (37) Cardinale, F.; Meskiene, I.; Ouaked, F.; Hirt, H. *Plant Cell* **2002**, *14*, 703–711.
- (38) De la Fuente van Bentem, S.; Roitinger, E.; Anrather, D.; Csaszar, E.; Hirt, H. *Physiol. Plant.* **2006**, *126*, 110–119.
- (39) Wolschin, F.; Weckwerth, W. *Plant Methods* **2005**, *1*, 9.
- (40) Hardtke, C. S.; Gohda, K.; Osterlund, M. T.; Oyama, T.; Okada, K.; Deng, X. W. *EMBO J.* **2000**, *19*, 4997–5006.
- (41) Kulma, A.; Villadsen, D.; Campbell, D. G.; Meek, S. E.; Harthill, J. E.; Nielsen, T. H.; MacKintosh, C. *Plant J.* **2004**, *37*, 654–667.
- (42) Moser, K.; White, F. M. *J. Proteome Res.* **2006**, *5*, 98–104.
- (43) Boniotti, M. B.; Gutierrez, C. *Plant J.* **2001**, *28*, 341–350.
- (44) Nakagami, H.; Sekine, M.; Murakami, H.; Shinmyo, A. *Plant J.* **1999**, *18*, 243–252.
- (45) Dissmeyer, N.; Nowack, M. K.; Pusch, S.; Stals, H.; Inze, D.; Grini, P. E.; Schnittger, A. *Plant Cell* **2007**, *19*, 972–985.
- (46) Umeda, M.; Bhalerao, R. P.; Schell, J.; Uchimiya, H.; Koncz, C. *Proc. Natl. Acad. Sci. U.S.A.* **1998**, *95*, 5021–5026.
- (47) Shimotohno, A.; Ohno, R.; Bisova, K.; Sakaguchi, N.; Huang, J.; Koncz, C.; Uchimiya, H.; Umeda, M. *Plant J.* **2006**, *47*, 701–710.
- (48) Hughes, K.; Nikolakaki, E.; Plyte, S. E.; Totty, N. F.; Woodgett, J. R. *EMBO J.* **1993**, *12*, 803–808.
- (49) Rush, J.; Moritz, A.; Lee, K. A.; Guo, A.; Goss, V. L.; Spek, E. J.; Zhang, H.; Zha, X. M.; Polakiewicz, R. D.; Comb, M. J. *Nat. Biotechnol.* **2005**, *23*, 94–101.
- (50) Jonak, C.; Hirt, H. *Trends Plant Sci.* **2002**, *7*, 457–461.
- (51) Rudrabhatla, P.; Rajasekharan, R. *J. Biol. Chem.* **2003**, *278*, 17328–17335.
- (52) Kentrup, H.; Becker, W.; Heukelbach, J.; Wilmes, A.; Schurmann, A.; Huppertz, C.; Kainulainen, H.; Joost, H. G. *J. Biol. Chem.* **1996**, *271*, 3488–3495.
- (53) Goss, V. L.; Lee, K. A.; Moritz, A.; Nardone, J.; Spek, E. J.; MacNeill, J.; Rush, J.; Comb, M. J.; Polakiewicz, R. D. *Blood* **2006**, *107*, 4888–4897.
- (54) Cole, A.; Frame, S.; Cohen, P. *Biochem. J.* **2004**, *377*, 249–255.
- (55) Lochhead, P. A.; Kinstry, R.; Sibbet, G.; Rawjee, T.; Morrice, N.; Cleghon, V. *Mol. Cell* **2006**, *24*, 627–633.
- (56) Pagano, M. A.; Cesaro, L.; Meggio, F.; Pinna, L. A. *Biochem. Soc. Trans.* **2006**, *34*, 1303–1306.
- (57) Meggio, F.; Pinna, L. A. *FASEB J.* **2003**, *17*, 349–368.
- (58) Stemmer, C.; Leeming, D. J.; Franssen, L.; Grimm, R.; Grassler, K. D. *Biochemistry* **2003**, *42*, 3503–3508.
- (59) Kramer, A.; Feilner, T.; Possling, A.; Radchuk, V.; Weschke, W.; Burkle, L.; Kersten, B. *Phytochemistry* **2004**, *65*, 1777–1784.
- (60) Vernoud, V.; Horton, A. C.; Yang, Z.; Nielsen, E. *Plant Physiol.* **2003**, *131*, 1191–1208.
- (61) Koizumi, K.; Naramoto, S.; Sawa, S.; Yahara, N.; Ueda, T.; Nakano, A.; Sugiyama, M.; Fukuda, H. *Development* **2005**, *132*, 1699–1711.
- (62) Sieburth, L. E.; Muday, G. K.; King, E. J.; Benton, G.; Kim, S.; Metcalf, K. E.; Meyers, L.; Seamen, E.; Van Norman, J. M. *Plant Cell* **2006**, *18*, 1396–1411.
- (63) Fagard, M.; Boutet, S.; Morel, J. B.; Bellini, C.; Vaucheret, H. *Proc. Acad. Sci. U.S.A.* **2000**, *97*, 11650–11654.
- (64) Grigg, S. P.; Canales, C.; Hay, A.; Tsiantis, M. *Nature* **2005**, *437*, 1022–1026.
- (65) Farrona, S.; Hurtado, L.; Bowman, J. L.; Reyes, J. C. *Development* **2004**, *131*, 4965–4975.
- (66) Wagner, D.; Meyerowitz, E. M. *Curr. Biol.* **2002**, *12*, 85–94.
- (67) Bezhani, S.; Winter, C.; Hershman, S.; Wagner, J. D.; Kennedy, J. F.; Kwon, C. S.; Pfluger, J.; Su, Y.; Wagner, D. *Plant Cell* **2007**, *19*, 403–416.
- (68) Zhang, H.; van Nocker, S. *Plant J.* **2002**, *31*, 663–673.
- (69) Oh, S.; Zhang, H.; Ludwig, P.; van Nocker, S. *Plant Cell* **2004**, *16*, 2940–2953.
- (70) Kieffer, M.; Stern, Y.; Cook, H.; Clerici, E.; Maulbetsch, C.; Laux, T.; Davies, B. *Plant Cell* **2006**, *18*, 560–573.
- (71) Long, J. A.; Ohno, C.; Smith, Z. R.; Meyerowitz, E. M. *Science* **2006**, *312*, 1520–1523.
- (72) Fujii, H.; Verslues, P. E.; Zhu, J. K. *Plant Cell* **2007**, *19*, 485–494.
- (73) Nakagami, H.; Soukupova, H.; Schikora, A.; Zarsky, V.; Hirt, H. *J. Biol. Chem.* **2006**, *281*, 38697–38704.
- (74) Min, M. K.; Kim, S. J.; Miao, Y.; Shin, J.; Jiang, L.; Hwang, I. *Plant Physiol.* **2007**, *143*, 1601–1614.
- (75) Sessa, G.; Raz, V.; Savaldi, S.; Fluhr, R. *Plant Cell* **1996**, *8*, 2223–2234.
- (76) Kersten, B.; Agrawal, G. K.; Iwahashi, H.; Rakwal, R. *Proteomics* **2006**, *6*, 5517–5528.
- (77) Marin-Vinader, L.; Shin, C.; Onnekink, C.; Manley, J. L.; Lubsen, N. H. *Mol. Biol. Cell* **2006**, *17*, 886–894.
- (78) Shin, C.; Feng, Y.; Manley, J. L. *Nature* **2004**, *427*, 553–558.
- (79) Lorkovic, Z. J.; Lopato, S.; Pexa, M.; Lehner, R.; Barta, A. *J. Biol. Chem.* **2004**, *279*, 33890–33898.
- (80) Iida, K.; Seki, M.; Sakurai, T.; Satou, M.; Akiyama, K.; Toyoda, T.; Konagaya, A.; Shinozaki, K. *Nucleic Acids Res.* **2004**, *32*, 5096–5103.

PR8000173

VI. Curriculum Vitae

Personal data

Name: Alessandro Carreri
Address: Neutorgasse 5/12
A-1010 Vienna
E-Mail: carreri.alessandro@gmail.com
Date of Birth: 09.03.1979
Place of birth: Isola della Scala, Verona, Italy
Citizenship: Italian
Marital status: Unmarried

Education

1993-1999: Technical school for Microbiology and chemistry laboratory technician
1999-2005: Study of Biotechnology at the University of Verona

Employment

09/2003 – 03/2005:

Diploma thesis in plant molecular biology: “Constructs for the local and the systemic induction of the RNA silencing” c/o University of Verona, faculty of science, Dr. Angelo Spina.

Since 05–2005:

Dissertation: “Mass spectrometry-based screening for mitogen-activated protein kinase substrates” c/o Univ. Dr. Heribert Hirt’s laboratory, department of plant molecular microbiology, Dr. Bohrgasse 9, 1030 Vienna, Austria.

VII. Acknowledgments

I thank Prof. Heribert Hirt because he believed in me since the first moment we have met. He gave me a chance to live a beautiful working experience where I learnt something that I'll never forget.

I thank Sergio that was my guide during the past two years spending a lot of time in discussing experiment, results and future perspectives. Moreover, beside that a unique colleague, he is a friend that I'll never lose.

I thank Andrea who welcome me in the lab almost four years ago teaching me all the techniques we are using and for giving me the chance to work side by side with the most well prepared person I've ever met in science.

Thanks to Aladar, who helped me a lot in the past few months to carry out what is also written in this thesis, thanks also for the great discussions we have done during the smoking breaks, I'm sure I'll bring them along for all my life.

Thanks to Sarah, who shared with me a lot of happiness, sadness, troubles, depression (from your side of course), you made my lab life easier.

Thanks to Adam, I still miss you here in Vienna, but in the year we've spent together I learnt a lot from you and not only about how to work in science but especially how to live my life.

Thanks to Celine for the useful and very critic discussion about my results and for trying to teach me what does it means to be a real scientist.

Thanks to Karin who was always present when I was in some trouble, your experience and knowledge of the lab saved me.

Thanks to Andriy, your friendship and experience in the lab was fundamental for the good results in this project.

Thanks to all my “foreign” friends, Federico, Federica, Pedro, Natalia, Spyros, Juan, Florian, Lucas, Quanah, Brooke and many others, I’m sure we’ll keep in touch.

Thanks to Fabio, Luca, Nicola, Stefano, Alessandro, Marco, Francy, because every time I came back home it was like I’ve never been away.

Thanks to my parents, they supported me a lot in making good decisions when the things where not going in the proper direction and, as usual, they were right.

Thank to my sister and Damiano for coming so often to visit and spend time together, we had very nice moments all together.

And thank to Silvia, it is impossible to don’t say that what I did up to now it could not be possible without you. In these four years we pass through a lot of difficult situation but we made always the right decision: we stayed together. Thanks!